UNIVERSITY OF LIMERICK
OLLSCOIL LUIMNIGH

Measurement of strain induced responses at femoral artery bypass graft junctions

Tríona Campbell

Publication date

01-01-2015

Licence

This work is made available under the CC BY-NC-SA 1.0 licence and should only be used in accordance with that licence. For more information on the specific terms, consult the repository record for this item.

Document Version
1

Citation for this work (HarvardUL)

Campbell, T. (2015) 'Measurement of strain induced responses at femoral artery bypass graft junctions', available: https://hdl.handle.net/10344/4663 [accessed 25 Aug 2022].

This work was downloaded from the University of Limerick research repository.

For more information on this work, the University of Limerick research repository or to report an issue, you can contact the repository administrators at ir@ul.ie. If you feel that this work breaches copyright, please provide details and we will remove access to the work immediately while we investigate your claim.

MEASUREMENT OF STRAIN INDUCED RESPONSES AT FEMORAL ARTERY BYPASS GRAFT JUNCTIONS

Author

Tríona Campbell

FOR THE DEGREE OF MASTER OF ENGINEERING

DEPARTMENT OF MECHANICAL, AERONAUTICAL AND BIOMEDICAL ENGINEERING

FACULTY OF SCIENCE AND ENGINEERING, UNIVERSITY OF LIMERICK

Supervisor

Dr Reena Cole

Submitted to the University of Limerick, May 2015

The substance of this thesis is the original work of the author and due reference and acknowledgement has been made, when necessary, to the work of others. No part of this thesis has previously been accepted for any degree nor has it been submitted for any other award.

_____

Tríona Campbell Candidate

The substance of this thesis is the original work of the author and due reference and acknowledgement has been made, when necessary, to the work of others. No part of this thesis has previously been accepted for any degree nor has it been submitted for any other award.

_____

Dr Reena Cole Supervisor

This thesis was defended in Jan 2010

Examination Committee

Chairman Dr. John Jarvis, University of Limerick

External Examiner Prof. Peter Weinberg, Imperial College of London

Internal Examiner Dr. Michael Walsh, University of Limerick

Abstract

Femoral artery bypass grafts have a predilection for failure at the distal anastomosis due to restenosis, within a short period of time, the cause of which has been attributed to altered haemodynamics. This study proposes that pressure induced strain has a profound effect on the endothelium surrounding the junction leading to the onset of stenosis. It is hypothesised that the cellular response in the non-physiological distal junction of a femoral bypass graft can be predicted by measuring the strain response and that this strain response is caused primarily by the intramural pressure.

The vascular endothelium represents a highly effective fluid and solute barrier through the synchronised apposition of tight junction protein complexes between adjoining endothelial cells. As endothelial cell mediated functions and pathology are sensitive to mechanical and haemodynamic forces (cyclic strain and shear stress) the author hypothesises that the primary factor responsible for the onset of atherosclerosis surrounding femoral artery bypass grafts is blood pressure as opposed to blood flow. This theory is investigated via the direct measurement of *in vivo* deflections following elective femoral bypass surgery and the subsequent examination of the precise effects of the recorded cyclic strain versus physiological flow induced shear stress on human aortic endothelial cells (HAEC's) cultured *in vitro*, at 12, 24 and 36 hour time intervals.

Overall the findings indicate that physiological cyclic strain and shear instigate positive responses such as improved cell turnover and reduced apoptosis. These events were accompanied by a strain-dependent reduction in transendothelial permeability to FITC-dextran, an event that indicates improved barrier function. However the strain induced upon the introduction of a synthetic arterial bypass, although close to the normal physiological range, induced negative responses with subsequent consequences for barrier integrity, cell turnover and unprogrammed cell death.

To my husband and to my parents, with love xx

Acknowledgments

To my supervisor Reena, for her guidance and encouragement throughout the past few years, thank you so much.

To my husband Frank, I couldn't have done this without you. Thank you for always being there and supporting me through the good times and the bad.

To my parents, Kathy and Charlie and my siblings Lisa and Daragh you've always been there to back me up, thank you for believing in me.

Much thanks must go the the staff of the surgical department at the Mid-Western Hospital in Limerick. Professor Pierce Grace, I am indebted to you.

To Jan, you're a saviour. Thanks for all your support, not to mind the editing and proof reading!

To Mike O'Donnell I owe you, thanks!

Thanks Kev, you're some computer genius!

To Prof. Mark Davies thank you.

Thanks to the staff in DCU, Ronan, Phil, Maria, Paul, Mishan and Tony for answering all those annoying little questions and passing on your wisdom to me, what can I say, you're amazing and I look forward to working with you again.

To the postgrads and postdocs who have helped build my knowledge Julie, Angie, Heidi, Fiona, Lucy, Gra, Dave, Colin, John, and all the others who have shared the past few years with me.

To my best friends and family who have been through thick and thin with me Sophie, Fiona, Susie, Jenny, Trish, Grace and thanks Julie for keeping me fit too!!

Finally I would like to thank the Irish Research Council for Science Engineering and Technology Postgraduate Awards Scheme for their financial support.

Contents

Abstract **iii**

Acknowledgments **v**

List of Tables **x**

List of Figures **xv**

Nomenclature **xvi**

1 Introduction **1**

1.1 Cardiovascular Disease 1

1.2 Atherosclerosis 3

1.3 Treatment of Cardiovascular Blockages 5

1.4 Instigators of Vascular Disease and Graft Failure 6

1.5 Objectives 8

2 Literature Review **11**

2.1 Structure of Blood Vessels 11

2.2 Properties of Arteries 13

2.3 Endothelial Cell Functionality 15

2.4 Atherosclerosis Formation and Propagation 16

2.5 Intimal Hyperplasia 19

2.6 Surgical Intervention 19

2.7 Bypass Material Properties 20

2.8 Bypass Graft Configurations 23

2.9 Haemodynamic Hypothesis 26

2.10 Intramural Hypothesis 28

2.10.1 Endothelial Cell Responses to Pressure and Flow 32
2.10.2 Tight Junctions 34
2.11 Conclusion 35

3 Validation of Measurement Technique 36
3.1 Silicon Models 36
3.2 Finite Element Models 41
3.3 Experimental and FEA Results and Discussion 43
3.4 Summary 45

4 *In Vivo* Surgical Experiments and Finite Element Analysis 47
4.1 Procedure for Surgical Measurements 47
4.2 Modelling the artery using Finite Element Analysis 51
4.3 Surgical Results and Discussion 53
4.4 Summary 59

5 *In Vitro* Cell Culture Experiments 60
5.1 Introduction 60
5.2 Methods for the Mechanostimulus of Cells 62
5.3 Culture Conditions 63
5.3.1 Culturing Process 64
5.3.2 Cell Counts 65
5.3.3 Freezing and Thawing of Cells 65
5.4 Experimental Equipment and Methods 66
5.4.1 Shear Experiments 66
5.4.2 Strain Experiments 66
5.4.3 Immunocytochemistry 70
5.4.4 Permeability Analysis 70
5.4.5 Proliferation Analysis 71
5.4.6 Apoptosis and Necrosis Analysis 71
5.5 Results and Discussion 72
5.5.1 Immunocytochemistry 73
5.5.2 Permeability 76
5.5.3 Apoptosis 83
5.5.4 Proliferation 86

5.6 Summary 92

6 Conclusions and Recommendations for Further Work 94

6.1 Conclusions 94

6.1.1 Silicon and Finite Element Models 94

6.1.2 Surgical Measurements and Finite Element Models 95

6.1.3 Endothelial Cell Responses 95

6.2 Recommendations for Further Work 96

References 99

References 99

Appendices 114

A Publications 115

B Silicon Models 117

B.1 Wax Mould and Silicon Model Procedure 118

C Finite Element Analysis 121

D Surgical Consent Forms 125

E Cell Culturing Procedures and Assays 132

E.1 Materials 132

E.2 Media for Culturing HAEC 134

E.2.1 Freezing Media for HAEC 135

E.2.2 Function of Additives to the Media 135

E.3 Initial Culturing Process 136

E.4 Subculturing Process 136

E.5 Freezing Process 138

E.6 Permeability Assay 138

E.7 Apoptosis/Necrosis Assay 140

E.8 Proliferation Assay 141

E.9 Zonula Occluden-1 Immunocytochemistry 142

E.10 Rhodamine Phaloidin Immunocytochemistry 143

E.11 Fixing of cells 143

F FACSCalibur™ Apoptosis Analysis **144**

G Cell Experimental Results - Set 2 **147**

List of Tables

2.1 **Material Properties for Experimental Analysis** 22
2.2 **Graft Patency Rates** 25

E.1 HAEC Media 135

List of Figures

1.1 Stent Placement Angioplasty 5
1.2 A Physiological Bifurcation 8
1.3 A Non-Physiological Bifurcation 8

2.1 Structure of Blood Vessels 12
2.2 Atherosclerosis Formation 17
2.3 Schematic of Bypass Graft Junction 20
2.4 Bypass Graft Configurations 24
2.5 Pressure Induced Thickening 30

3.1 FEA Straight Section 37
3.2 FEA Bifurcation 37
3.3 45° Silicon Model 38
3.4 45° Silicon/PTFE Model 38
3.5 Laboratory Experimental Set-up 39
3.6 Measurement Technique 40
3.7 FEA Loads and Constraints 42
3.8 Radial Strain 43
3.9 FEA Displacement 44
3.10 FEA Strain at bifurcation 45

4.1 Surgical Experimental Set-up 49
4.2 Plaque Laden Artery 50
4.3 Realistic Graft Junction 52
4.4 *In Vivo* Longitudinal Strain 54
4.5 *In Vivo* Radial Strain 54
4.6 FEA Strain Outer surface Arterial model 56
4.7 FEA Strain Inner Surface of Arterial model 57

4.8 Suture Line Surface Displacements 58
4.9 Bed Surface Displacements 58

5.1 Bioflex® Plate Schematic 63
5.2 Orbital Shaker 67
5.3 6-well Bioflex® Plate Calibration 68
5.4 Flexercell® Calibration 69
5.5 Videoextensometer Biaxial Test 69
5.6 Permeability Assay 71
5.7 Rhodamine Phaloidin Stained Control Cells 74
5.8 Rhodamine Phaloidin Stained Sheared Cells 74
5.9 Rhodamine Phaloidin Stained Strained Cells 74
5.10 ZO-1 Stained Control Cells 75
5.11 ZO-1 Stained Sheared Cells 75
5.12 ZO-1 Stained Strained Cells 75
5.13 Permeability of 2-5% Strained Cells 77
5.14 Permeability of 2-5% Strained Cells 77
5.15 Permeability of 2-5% Strained Cells 77
5.16 Permeability of 8-12% Strained Cells 78
5.17 Permeability of 8-12% Strained Cells 78
5.18 Permeability of 8-12% Strained Cells 78
5.19 Permeability of 7-17% Strained Cells 79
5.20 Permeability of 7-17% Strained Cells 79
5.21 Permeability of 7-17% Strained Cells 79
5.22 Permeability of 12 Hour Low Sheared Cells 81
5.23 Permeability of 24 Hour Low Sheared Cells 81
5.24 Permeability of 36 Hour Low Sheared Cells 81
5.25 Permeability of 12 Hour Sheared Cells 82
5.26 Permeability of 24 Hour Sheared Cells 82
5.27 Permeability of 36 Hour Sheared Cells 82
5.28 Apoptotic and Necrotic reactions of endothelial cells following **12** hours of each strain range 84
5.29 Apoptotic and Necrotic reactions of endothelial cells following **24** hours of each strain range 84

5.30 Apoptotic and Necrotic reactions of endothelial cells following **36** hours of each strain range 84
5.31 Apoptotic and Necrotic reactions of endothelial cells following **12** hours of low or physiological shear 85
5.32 Apoptotic and Necrotic reactions of endothelial cells following **24** hours of low or physiological shear 85
5.33 Apoptotic and Necrotic reactions of endothelial cells following **36** hours of low or physiological shear 85
5.34 Proliferation of endothelial cells following **12** hours of 2-5% cyclic strain . 87
5.35 Proliferation of endothelial cells following **24** hours of 2-5% cyclic strain . 87
5.36 Proliferation of endothelial cells following **36** hours of 2-5% cyclic strain . 87
5.37 Proliferation of endothelial cells following **12** hours of 8-12% cyclic strain . 88
5.38 Proliferation of endothelial cells following **24** hours of 8-12% cyclic strain . 88
5.39 Proliferation of endothelial cells following **36** hours of 8-12% cyclic strain . 88
5.40 Proliferation of endothelial cells following **12** hours of 7-17% cyclic strain . 89
5.41 Proliferation of endothelial cells following **24** hours of 7-17% cyclic strain . 89
5.42 Proliferation of endothelial cells following **36** hours of 7-17% cyclic strain . 89
5.43 Proliferation of endothelial cells following **12** hours of physiological shear . 90
5.44 Proliferation of endothelial cells following **24** hours of physiological shear . 90
5.45 Proliferation of endothelial cells following **36** hours of physiological shear . 90
5.46 Proliferation of endothelial cells following **12** hours of low shear 91
5.47 Proliferation of endothelial cells following **24** hours of low shear 91
5.48 Proliferation of endothelial cells following **36** hours of low shear 91

B.1 Straight Section Mould 120
B.2 Mould for Wax Core 120

C.1 FEA Displacements at the Bifurcation 122
C.2 FEA Bulging Effect 122
C.3 FEA Displacements 123
C.4 FEA Displacements 123
C.5 FEA Results 124
C.6 FEA Results 124

D.1 Surgical Consent Form (Videoextensometer) 126

D.2 Patient Experiment Information (Videoextensometer) 127
D.3 Patient Experiment Information (Videoextensometer) 128
D.4 Surgical Consent Form (Duplex Ultrasound) 129
D.5 Patient Experiment Information (Duplex Ultrasound) 130
D.6 Patient Experiment Information (Duplex Ultrasound) 131

F.1 FACSCalibur™ system raw data for apoptotic and necrotic analysis 145
F.2 FACSCalibur™ system raw data for apoptotic and necrotic analysis 146

G.1 Trans Endothelial Exchange following 12 hours of 2-5% strain 148
G.2 Trans Endothelial Exchange following 24 hours of 2-5% strain 148
G.3 Trans Endothelial Exchange following 36 hours of 2-5% strain 148
G.4 Trans Endothelial Exchange following 12 hours of 8-12% strain 149
G.5 Trans Endothelial Exchange following 24 hours of 8-12% strain 149
G.6 Trans Endothelial Exchange following 36 hours of 8-12% strain 149
G.7 Trans Endothelial Exchange following 12 hours of 7-17% strain 150
G.8 Trans Endothelial Exchange following 24 hours of 7-17% strain 150
G.9 Trans Endothelial Exchange following 36 hours of 7-17% strain 150
G.10 Trans Endothelial Exchange following 12 hours of low shear 151
G.11 Trans Endothelial Exchange following 24 hours of low shear 151
G.12 Trans Endothelial Exchange following 36 hours of low shear 151
G.13 Trans Endothelial Exchange following 12 hours of physiological shear . . . 152
G.14 Trans Endothelial Exchange following 24 hours of physiological shear . . . 152
G.15 Trans Endothelial Exchange following 24 hours of physiological shear . . . 152
G.16 Apoptotic and Necrotic reactions of endothelial cells following 12 hours of each strain range 154
G.17 Apoptotic and Necrotic reactions of endothelial cells following 24 hours of each strain range 154
G.18 Apoptotic and Necrotic reactions of endothelial cells following 36 hours of each strain range 154
G.19 Apoptotic and Necrotic reactions of endothelial cells following 12 hours of low or physiological shear 155
G.20 Apoptotic and Necrotic reactions of endothelial cells following 24 hours of low or physiological shear 155

G.21 Apoptotic and Necrotic reactions of endothelial cells following 36 hours of low or physiological shear 155

Nomenclature

Greek

α	Radius of Rotation	cm
η	Pressure	$dynes/cm^2$
λ	% Compliance	$-$
ν	Poissons Ratio	$-$
ρ	Density	kg/L
τ	Shear Stress	N/m^2

Roman

f	No of rotations per second	rad/s
E	Modulus of Elasticity	Pa
E_p	Pressure Strain Elastic Modulus	Pa

Chapter 1

Introduction

Living tissue responds to mechanical stimuli, bones become thicker when subjected to higher loads, heart volume increases with continuous exercise and arteries change in diameter as a result of altered blood pressure. A mechanical stress can regulate the growth of a living tissue and change not only its shape, but also its chemical and cellular structures as well as altering its mechanical properties. In addition cellular response might be triggered by alterations in hormone levels, changes in diet, or direct or indirect trauma. The most commonly known example of soft tissue remodeling, due to a change of stress, is the hypertrophy of the heart caused by a rise in blood pressure (Rutherford, 2000).

1.1 Cardiovascular Disease

Cardiovascular disease (CVD) refers to the category of diseases that involve the heart and blood vessels. In excess of 8,700 people in Ireland died from heart disease in 2004 and the number of people diagnosed with the disease has increased in recent years and currently stands at 25,000 per annum (Labanyi, 2006). The statistics on stroke in Ireland are a cause for disquiet. Annually up to 8,500 people suffer from a stroke resulting in over 2,500 patients deaths (Hunter, 2009).

Many illnesses of the vascular system exist however, in this study, the two primary illnesses of interest are arteriosclerosis and intimal hyperplasia. Arteriosclerosis is characterised by abnormal thickening and hardening of the arterial walls with resulting loss of elasticity. The principal form of arteriosclerosis, atherosclerosis, is a systemic disorder characterised by localised atheromatous deposits in and fibrosis of the inner layer of the

arteries at selected sites on the arterial tree. Atherosclerosis, the primary cause of coronary artery disease (CAD), peripheral arterial disease (PAD) and stroke, is a disorder with multiple genetic and environmental contributions. Treatment for atherosclerosis can be as simple as managing the risk factors such as changing ones diet, reduction of hypertensive blood pressure, reducing a patients stress levels, quitting smoking and taking cholesterol reducing drugs. However some risk factors for developing the disease, such as gender, age, family history and ethnicity cannot be modified. If the aforemention treatments are not sufficient then surgery is often required. With the aim of ensuring oxygenated blood can be supplied to target organs and tissues, an arterial bypass is often required to circumvent the atherosclerotic area.

Haemodynamic and mechanical forces within the vascular system influence cardiovascular diseases. These forces, associated with the propagation of blood pressure through the arterial wall and the flow of blood through the vasculature, affect the initiation and progression of diseases such as atherosclerosis, hypertension and pathological vascular remodelling (Frangos et al., 2001).

Mechanical forces are significant regulators of cellular function in many tissues and are particularly important in the cardiovascular system. The physiological stimuli that impact on the endothelium include cyclic strain, caused by the transmural force acting perpendicularly to the vessel wall induced by blood pressure, and shear stress, the frictional force of blood dragging against cells. Both of these forces are essential to maintain a healthy vessel but also have a profound impact on endothelial cell metabolism and can provoke changes in endothelial gene expression leading to changes in cell fate (Patrick & McIntire, 1995; Traub & Berk, 1998; Chien et al., 1998). They have been shown to clearly influence cell structure, growth, and function. Due to its exclusive location the endothelial cells lining blood vessels are subjected to each of these mechanical forces (Fisher et al., 2001). Furthermore it has been noted that the endothelium responds quickly and with sensitivity to the mechanical conditions within its surroundings (Traub & Berk, 1998). Thus alterations created by blood flow and the cardiac cycle can have considerable local effects.

The mechanical properties of arteries are an important determinant of haemodynamics. The aorta, pulmonary artery and large distributing arteries, for example, are distended rapidly during ventricular ejections. These vessels then retract significantly during diastole (Dobrin, 1978). The tangential drag force created by blood moving across the endothelial cell surface, wall shear stress, is a function of the velocity gradient of blood close to the endothelial cell surface. When pulsatile flow in an arterial segment is smooth and undisturbed,

the probability of cardiovascular diseases such as myointimal hyperplasia, thrombosis, or atherosclerosis developing is low.

Disturbed flow, or nonuniform hemodynamics, produces both abnormally high and low arterial wall shear stresses, resulting in reciculation zones, flow separation and prolonged near-wall bllod particle residence times (Archie, 2001). Understanding the mechanical characteristics of a normal physiologically healthy arterial wall can provide a reference to compare, quantify and evaluate the performance of the arteries when affected by diseases and also possibly predict performance after surgical interventions which may lead to developing new methodologies for treatment and identifying desirable characteristics of artificial blood vessels.

1.2 Atherosclerosis

Atherosclerosis, commonly referred to as arterial plaque, is a disease characterised by the clogging, narrowing, and hardening of the body's arteries, which can lead to strokes, heart attacks, eye problems and kidney problems. It affects approximately 10.5% of the population in the first decade of their lives and 100% by the eighth decade (Boudi, 2006). Atherosclerosis is a very significant problem and the average life years lost to atherosclerosis is 7.5 years (National Cancer Institute, 2001). The consequence of atherosclerosis is a narrowing of the lumen of an artery causing ulceration and pain. It is one of the most prevalent killers in the western world being responsible for 60% of all deaths (Kaazempur-Mofrad et al., 2004; Ross et al., 1993). Within the first quarter of this century it is predicted to be the leading cause of death in the developing world.

This disease is responsible for more than 50% of the yearly mortality in the United States and costs the country more than $100 billion annually (Boudi, 2006). It has been reported that in 1999 in the UK the number of physicians visits for atherosclerosis was 734,000 (Marcovina et al., 2003) and 85% of hospital consultant episodes for atherosclerosis required hospital admission in 2002-03 with a mean hospital stay of 11.7 days (Deptartment of Health, 2004). Similarly in Ireland the occurrence of atherosclerosis is extremely widespread and although no statistics are available it is the authors belief that the percentage of sufferers requiring treatment is comparable to the UK and that it costs the country millions in treatment each year. Thus any reduction in the occurrence of the disease may not only increase an individuals state of health but also result in a huge reduction of costs to the government and general tax payer.

Once atherosclerotic deposits form, no noteworthy effects may be noticed by the patient until the disease has progressed significantly. Twenty percent of the UK population, between 65 and 75 years of age, suffer from peripheral arterial disease however only 25% of these sufferers display any symptoms (Fowkes et al., 1991). Mild occlusion and obstruction of an artery are only seen when metabolic demands are increased, either by exercise, trauma or even infection. It was shown by May et al. (1963) and Moore & Malone (1979) that until the cross sectional area of the lumen has been reduced by more than 75%, appreciable changes in pressure and flow do not occur. They along with Sydorak (1972) and VanDeBerg et al. (1964) showed that more significant drops in both flow and pressure occurred, with a less severe narrowing, in a high flow system than in a low flow system. Areas of the arterial tree, such as branched sites, and arteries which experience higher haemodynamic stresses due to pressure and blood flow are more prone to stenosis and the formation of intimal hyperplasia.

Up until recently most doctors would have described atherosclerosis as a plumbing problem. Essentially a fat laden substance builds up on the surface of the artery walls. If the deposit becomes large enough it eventually blocks the artery and prevents blood from flowing and reaching its intended tissue. In fact it is a far more complex disease involving both acute and chronic inflammatory responses, resulting from hyperlipidemia and a complex interplay of many environmental, metabolic and genetic risk factors (Liddy, 2004).

The most prominent mechanism proposed to explain the pathogenesis of atherosclerosis is the 'response to injury' hypothesis in which it is theorised that endothelial cell dysfunction is the precursor to the events leading to the formation of an atherosclerotic plaque. Endothelial cells provide a physical barrier to the penetrations of monocytes and lymphocytes and under normal physiological conditions the endothelial cell surface does not allow the adherence of platelets and leucocytes. However following impairment of their functions it may lead to pro-atherogenic and/or pro-thrombotic states characterised by adhesion of platelets and macrophages on the site of injury, the formation of lipid and cell-rich lesions or plaques on the intimal surfaces of arterial wall, and the incursion of underlying smooth muscle cells into the lumen (Clowes, 1995; Badimon et al., 1992; Blann & Lip, 1998; Gimbrone et al., 2000).

Numerous investigations have centered on the cellular activities surrounding the formation and proliferation of atherosclerotic plaque (Liddy, 2004; Clowes, 1995; Gimbrone Jr, 1995). These studies have concluded that the interaction of the living cells can alter a cells

function or turnover resulting in adaptations such as increased permeability, oxidative alteration of ingested lipids, the introduction of macrophages and the stimuli to smooth muscle proliferation. High levels of specific lipoprotein cholesterol fractions have also been implicated. These cells play a part in the development and growth of atherosclerotic deposits, which arise not on, but in the vessel walls.

1.3 Treatment of Cardiovascular Blockages

In patients suffering from atherosclerosis whose condition is not improving with risk-factor modifications such as exercise programmes and pharmacological therapy then invasive procedures may be required. Current treatments for arteriosclerosis involve invasive surgery, such as, grafting, endarterectomy, minimally invasive surgery, angioplasty, stenting, as shown in Figure 1.1, and the use of antiplatelet and antithrombotic drugs (Lemson et al., 2000). Grafting is now one of the more common and most effective surgeries available. The alternative surgeries such as endarterectomy, angioplasty and stenting can only be carried out on smaller well defined lesions.

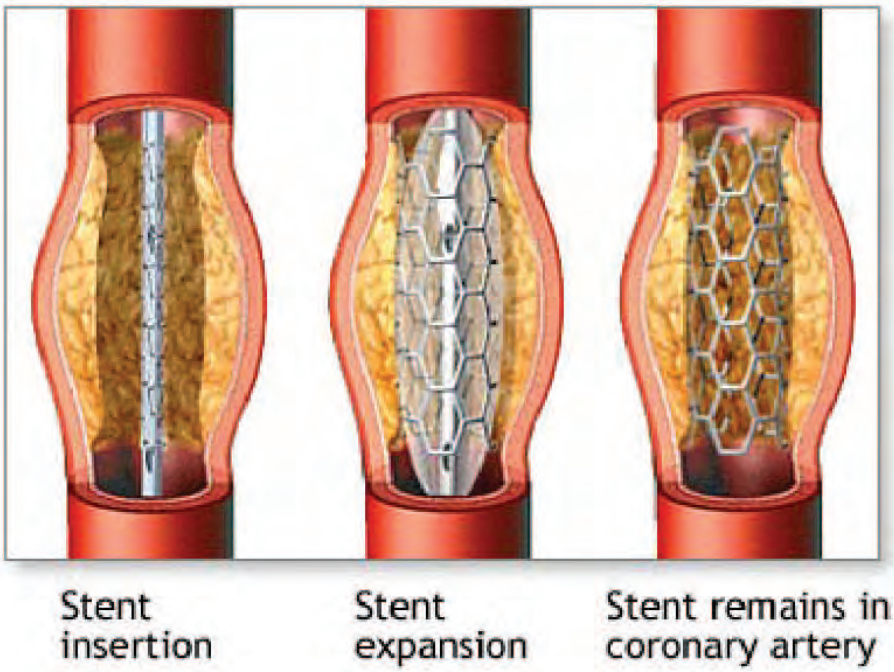

Figure 1.1: The deployment of a stent (Cardiovascular, 2009)

Examination into the concept of bypassing a blockage in the arterial system was first investigated at the beginning of the last century. Carrel & Guthrie (1905) is classified as the beginning of modern vascular grafting. This initial experimental study involved the use of

veins as arterial substitutes, however this giant step in vascular reconstruction was virtually forgotten about for over 40 years when Kunlin (1949) performed the first successful bypass of a thrombosed femoral artery using a portion of saphenous vein. The same year saw Gross et al. (1949) use a freeze dried aorta to replace a coratation of the thoracic aorta.

Since these humble beginnings many studies have investigated alternate materials for use as bypass materials. It was when Voorhees et al. (1952) proved that a porous plastic cloth tube (Vinyon-N) could be an acceptable arterial substitute, that true vascular surgery started in earnest. In 1969 a new method of extruding PTFE was discovered, by heating, stretching and extruding Teflon through a die (Gore, 1976). This created a microporous material consisting of solid nodes interconnected by fine fibrils.

Many materials have been explored for use as bypass grafts but the principal materials used to manufacture grafts are one of four basic biological derived materials; knitted or woven fabrics made from polyester, polyethyleneterephthalate (PET or Dacron), expanded polytetrafluoroethylene (ePTFE) and polyurethane. The primary graft material used in small to medium sized arteries is extruded PTFE which was first introduced in the operating theatre as a prosthesis in 1972 (Kempczinski, 2000). A number of variations on the original bypass design currently exist in the form of cuffs and patches however despite the increased patency rate of bypass grafts, post-operative failure or restenosis occurs in up to 30% of cases (Lemson et al., 2000).

1.4 Instigators of Vascular Disease and Graft Failure

Approximately one quarter of infrainguinal vein bypasses develop stenoses within one year post surgery that, if uncorrected, may progress to occlusion (Nielsen et al., 2001). Atherosclerosis and intimal hyperplasia are thought to be the primary causes of graft failure. Following intensive research over the past few years, the process of atherosclerotic plaque formation and proliferation has been defined. However despite all this research no definitive answer has been found for the instigation of atherosclerosis resulting in stenosis or restenosis of arteries.

Numerous theories have been put forward as to what is responsible for this initiation process but there are serious contradictions within this body of work principally those associated with wall shear stresses and the oscillatory shear index. Friedman et al. (1992) concluded that the intima at sites exposed to relatively high or unidirectional shears thickened initially, but with passage of time the greatest thicknesses were ultimately achieved at

sites that were exposed to lower or more oscillatory shear environments where as Nazemi et al. (1990) concluded the opposite that low wall shear stress contributes to the onset of atherosclerotic plaque formation, with high wall shear stress encouraging plaque growth. In a study performed by Benetos et al. (2002) it was stated that shear stress cannot explain the changes in intimal thickening but that the wall stress was responsible. Many theories involve a combination of multiple factors. Some such cited factors include, surgical injury, anastomotic angle, material mismatch, suture line stresses, wall shear stresses and intramural stresses.

Cheng et al. (1996) reported that the effects of blood induced shear stress on endothelial cell gene expression and biology have been intensively investigated however the effects of pressure induced strain have not received such focus and as a result are less well understood. In other words most of the recent studies, focusing on the endothelium at a bifurcation, seek correlations between variables defining the metabolism and ultrastructure of the endothelial cells with the shear stress of blood flow but few have reported a direct correlation between the responses of endothelial cells surrounding a bifurcation and pressure induced cyclic strain, even though it has been published that higher strain gradients are present, in the arterial wall, around the area of a bifurcation than in a straight section (Thubrikar et al., 1990). It is the authors belief that a combination of all factors leads to abnormal wall stresses resulting in a cascade of adverse biological events resulting in atherosclerosis. However the current study argues that the altered intramural stresses, induced by intramural pressure, are the primary initiating cause of stenosis, particularly in the restenosis of bypass grafts.

Endothelial cells are critical in the maintenance of normal vascular homeostasis, their environment constantly exposes them to mechanical forces namely blood flow-induced shear stress and pressure-induced strain. It has been suggested that steady laminar shear stress stimulates cellular responses that are necessary for endothelial cell function and are in fact atheroprotective (Traub & Berk, 1998). As indicated in previous studies (May et al., 1963; Moore & Malone, 1979; Sydorak, 1972; VanDeBerg et al., 1964) atherosclerosis preferentially occurs in areas of low flow thus the present study explores the ability of shear stress to modulate the endothelial cells responses under both low and physiological laminar shear laminar conditions.

1.5 Objectives

Physiology is defined as characteristic of, or appropriate to, an organism's healthy or normal functioning. Any deviation from this normal functioning is considered unusual or exceptional and may be classified as abnormal or non-physiological. From both a solid mechanics and a fluid mechanics point of view the distal junction associated with a femoral artery bypass graft can certainly be considered non-physiological, as no such junction exists naturally in the human arterial system. Figure 1.2 displays a physiological arterial configuration whilst Figure 1.3 represents the non-physiologcal distal junction of a bypass.

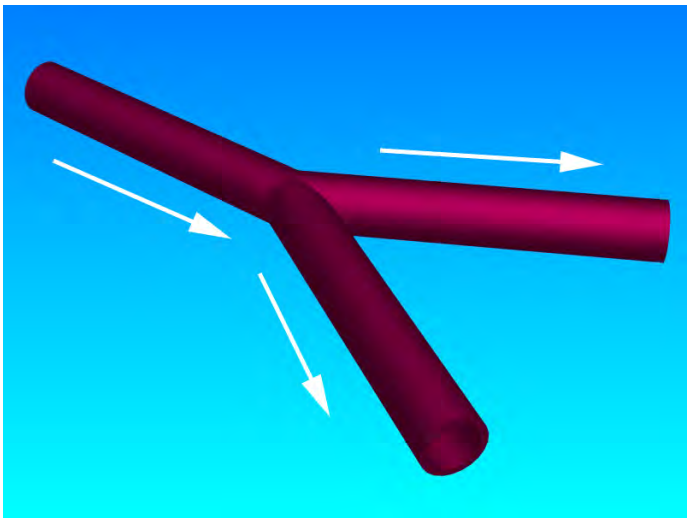

Figure 1.2: The direction of flow and structure of a physiological bifurcation

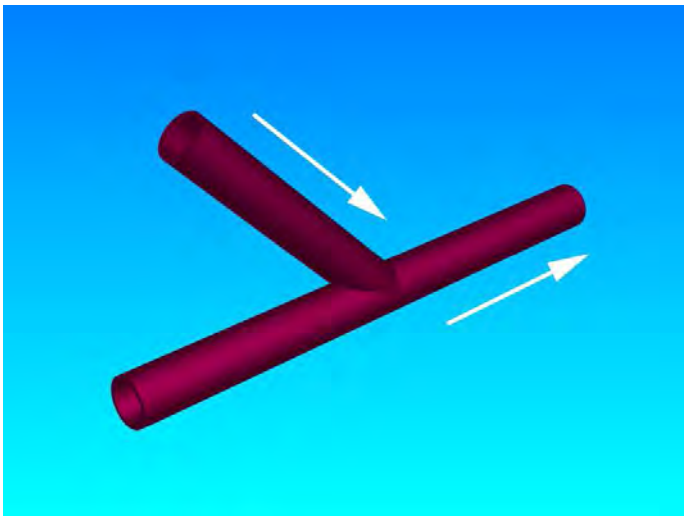

Figure 1.3: The direction of flow and structure of a non-physiological bifurcation

This study aims to focus on the effects of the pressure-induced strains at an arterial bypass graft junction. Using *in vivo* data, human aortic endothelial cells were subjected to

varying values of frequency and strain over 12, 24 and 36 hour time periods. Specifically monitoring characteristic changes of the endothelial cells. Thus gaining a greater understanding of the mechanical stimuli associated with atherosclerosis formation and restenosis surrounding bypass graft junctions.

A novel approach was employed in this study in that direct *in vivo* measurements were recorded of the deflections surrounding the area of a bypass graft and these results were used to determine the actually response of endothelial cells *in vitro*. The principle hypotheses of this work are that non-physiological strains give rise to non-physiological responses and the differences between physiological and non-physiological responses are greater than the error in the analysis.

The primary objective was to analyse the mechanical strains caused by intramural pressure and blood flow that result in injury of the endothelium in the area surrounding a bypass graft junction. This was completed by performing the following steps:

Silicon Models and Finite Element Analysis

- The production of silicon models that display similar elastic properties to that of an artery and investigation of the deflection of these models, when subjected to pressures between 10KPa and 20KPa, using a videoextensometer.
- Investigation into whether these deflections can be accurately predicted using a finite element package with identical material properties applied.

Surgical Models and Finite Element Analysis

- The measurement of deflections in the region surrounding an anastomosis during elective femoral or femoropoplitel bypass surgery following the introduction of either a vein or synthetic bypass graft.
- Using finite element analysis to predict the effect of the *in vivo* measured deflections on the inner surface of the artery, namely the endothelial cell layer.

Endothelial Cell Responses

- Examining the effect of the pressure induced strains, following insertion of a bypass graft, on endothelial cell functionality, in particular cell apoptosis, necrosis, proliferation and permeability and comparing the responses with those resulting from by blood induced shear stresses.

In chapter two the existing literature surrounding the area of bypass grafting, cardiovascular diseases and cellular responses to mechanical stimuli are examined. Although the principal interest of this study is examining the pressure induced strains in the distal anastomosis of a femoral artery bypass graft, a complete understanding of the structure and properties of the artery, the diseases associated with the cardiovascular system and the possible treatments, is required to accurately convey the environment in which grafts are utilised. The instigators of bypass graft failure are examined in detail in order to gain a greater understanding of the causes of restenosis occuring at the bypass graft location.

Chapter three outlines a validation study undertaken to examine the accuracy of a non-invasive measurement technique. This chapter details the methodologies, materials and equipment employed in the production of silicon models. The resulting deformations, when subjected to varying static pressures, are compared to finite element computer models. Finally the results inferred from the experiments performed in that section are analysed and discussed.

Chapter four details the procedures involved in recording *in vivo* deflections at the distal junction of a femoral bypass graft during surgery. A finite element investigation was completed to outline the effects of deformations on inner arterial surfaces. The results inferred are analysed and discussed.

In the penultimate chapter the methodologies associated with *in vitro* cell culture studies are presented. The procedures required for the mechanostimulus of cells are outlined and those associated with the evaluation of cellular reactions to varying stimuli. In the final section the results are summarised and discussed.

In summation Chapter six details the overall conclusions for the entire study and recommendations for further studies. Additional information is contained in the appendices on the actually step by step procedures and materials employed during the entire study.

Chapter 2

Literature Review

This chapter reviews the principal diseases of the cardiovascular system, the structure and properties of arteries, and the synthetic materials associated with the treatment of cardiovascular diseases. It examines the current literature on the surgical configurations for bypass graft attachment and investigates both the haemodynamic and intramural hypotheses as the precursor to cardiovascular disease. Finally, previous studies were examined in which endothelial cell responses following exposure to mechanical stimuli were evaluated.

2.1 Structure of Blood Vessels

An artery is a viscoelastic tube that carries blood away from the heart and whose diameter varies with a pulsating pressure. Blood vessels are composed of soft collagenous tissues, with a good deal of elastin. The wall consists of three layers: tunica intima, tunica media, and tunica adventia as shown in Figure 2.1. The materials associated with, and size of, each individual layer differentiates one artery or vein from another artery or vein. The artery wall properties are such that it will propagate pressure and flow waves.

The intima is a continuous monolayer of flat, polygonal cells, known as the endothelium, that lines the luminal surface. This endothelium performs a critical role in homeostasis and is described as a dynamic, heterogeneous organ which influences vital metabolic and immunologic functions (De Caterina & Libby, 2007). The intima is normally extremely thin with the endothelium set directly on the internal elastic lamina and it contains only a few scattered leukocytes, smooth muscle cells and connective tissue fibers. The media consists primarily of layers of smooth muscle cells, which consist of groups of similarly

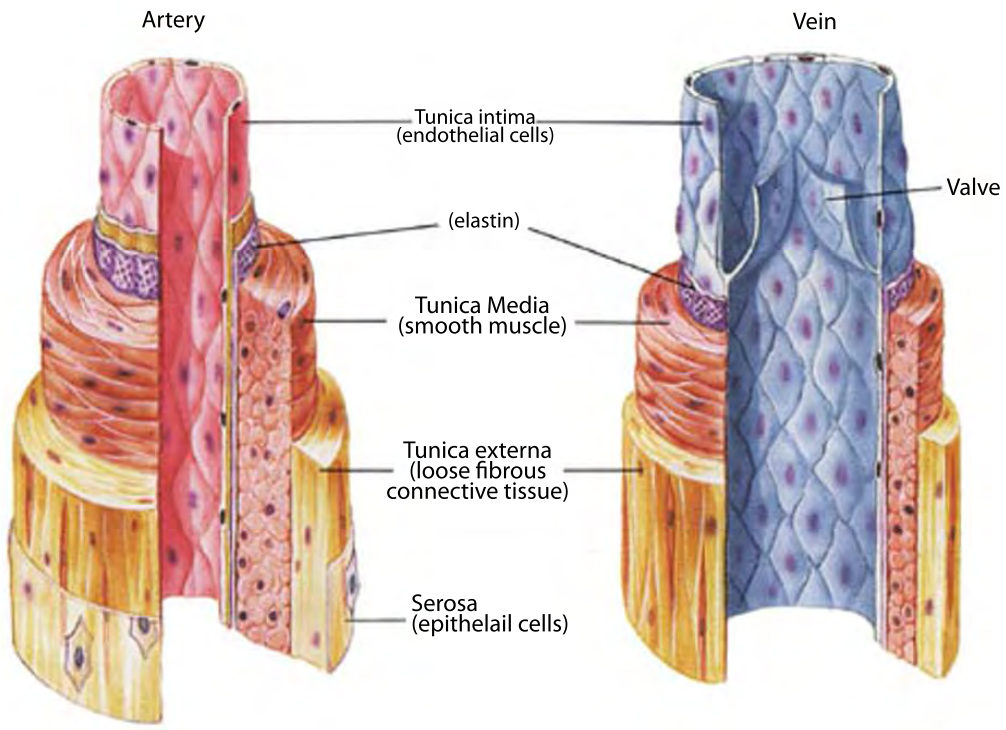

Figure 2.1: Schematic of blood vessel structure. (Fox, 1992)

orientated cells, surrounded by a basal lamina and interwoven collagen fibrils. These collagen fibrils tighten once tension is placed on the smooth muscles cell groups. Furthermore the cellular subgroups are encompassed by elastic fibers, which allow for the compliance and recoil of the artery during the cardiac cycle, and each subgroup orientates itself in the direction of applied stress (Rutherford, 2000).

The adventitia is composed of fibrocellular connective tissue as well as collagen and elastic fibers. It is a strong covering that allows the arteries and veins to stretch and prevents overexpansion due to the pressure that is exerted on the walls by blood flow. The adventitia also contains a complex system of vasa vasorum which is composed of small arteries, arterioles, capillaries and venous channels in addition to nerves that mediate smooth muscle tone and contraction.

The structure of blood vessels varies along the arterial tree. In the larger arteries the number of lamellar layers increases with wall thickness. In smaller arteries, the relative wall thickness is increased, the elastin is less prominent in the media and with increasing distance from the aorta, eventually only the inner and outer elastic laminae are clearly visible. Thus the properties of arteries vary depending on their location within the arterial

tree.

From the schematic in Fig 2.1 it can be seen that arteries have a larger media layer than veins as smooth muscle is predominantly found in the media layer it can be concluded that arteries have more of an ability to contract than veins. An important fact to consider when using a vein as an arterial bypass as if a smaller vein is employed to do the work of a larger arteries the compliance mismatch will be greater.

2.2 Properties of Arteries

Arteries are intricate biomechanical structures well suited to carrying out their metabolic and mechanical functions under a wide range of conditions. They can adapt to gradual changes in local hemodynamic stresses and to geometric alterations in order to maintain optimal diameter and mechanical characteristics and to ensure continued blood flow. The arterial tissue is inhomogenous and non-linear and undergoes significant luminal enlargement when pressure is applied. The diversity in structure of each individual layer greatly influences its response to mechanical stresses as the mechanical characteristics of blood vessels are determined by both passive and active tissue components.

The most significant passive components are the fibrous connective tissues: elastin and collagen. Collagen is found primarily in the media where it is oriented circumferentially. In a study performed by Dobrin & Canfield (1984) tests were carried out on canine carotid arteries and it was suggested that elastin bears both longitudinal and circumferential load while collagen bears only circumferential load. Other cells such as endothelial cells, nervous tissue and fibroblasts are also present although histologically it is apparent that these only represent a small percentage of the entire wall volume. The endothelium itself exhibits negligible inherent mechanical stiffness.

It is believed that the composition and thickness of arterial walls is critically linked to tangential tension and strain in the wall of the artery itself. During normal growth and development arteries are capable of regulating rises in tangential tension by increasing the number of matrix fibres in the medial lamellae thus increasing wall thickness. If the ascending aorta and pulmonary trunk are examined at birth, many common factors exist. Both arteries are equal in diameter, wall thickness and concentration of elastin and collagen fibres. As the lungs expand during the postnatal period the pressure in the pulmonary artery is found to fall but that in the ascending aorta rises, however, the volume of flow, the diameter and the number of cells remain equivalent in both vessels. The high blood pressure

experienced by the aorta results in the thickening of the arterial wall due the accrual of collagen and elastin. Thus showing the capabilities of arteries to respond to applied tensile stress (Rutherford, 2000).

It is generally thought that arteries become stiffer with age. Stiffening of the vessel results in the compromise of distensibility thus limiting stretching and expansion (Van der Heijden-Spek et al., 2000; Papageorgiou & Jones, 1988). This reduction in elasticity has been attributed to both age and increased pressure (Cox, 1977; Papageorgiou & Jones, 1988; Cockcroft & Wilkinson, 2002). In an investigation of the effect of age on the mechanical properties of tissue, Vogel (1980) deduced that the modulus of elasticity decreased in maturation but increase again in old age, at a low level of extension or strain. This indicates that the vessel stiffens with maturity but eventually losses stiffness in old age. However this conflicts with the views of Cockcroft & Wilkinson (2002) who concluded that even in extreme old age the stiffness of the artery continues to increase.

Mechanically tested specimens of abdominal aortic aneurysms show that the artery wall does not behave like a linear elastic material at higher pressures (Raghavan et al., 2006; Vallabhaneni et al., 2004; Raghavan et al., 1996). At high pressures, the arterial wall stretches and collagen fibres are gradually engaged to bear an progressively larger portion of the load. Collagen is about 1000 to 2000 times stiffer than elastin, hence arteries become stiffer at high pressures (Rutherford, 2000). Due to the orientation of elastin and collagen in the artery wall the elastic modulus various greatly depending on the applied strain. At low strains the elastin bears the load whilst the collagen fibres are randomly orientated but as the material is strained further the collagen fibres straighten out and begin to bear the load, this is termed collagen recruitment. In the human aorta this occurs at blood pressures within the normal physiological range, greater than 110mmHg (Raghavan et al., 1996).

A number of bending experiments have been performed on arteries (Yu et al., 1993). In the thoracic arteries of pigs, a modulus of 43.25 KPa was found to exist for the intima-media layer but a modulus of only 4.7 KPa for the adventia layer. When the components of each layer were examined it was found that elastin was largely responsible for the distensibility of the arterial wall. The elastic modulus of elastin has been shown experimentally to be between 1.5 and 4.1 KPa. At very large distensions much of the stiffness of arteries is attributed to collagen. Collagen is a fibrous protein possessing a helical structure with three protein chains wound around a central axis. The elastic modulus of collagen is between 0.3 and 2.5 KPa (Dobrin, 1978). The nature of both elastin-rich lamellae and of collagen is an essential determinant of vascular wall mechanics. The local tissue strains and the local

circumferential stresses are distributed across the vessel wall. When looking at the cross sections of arteries the density of elastic lamella is greatest near the intima which parallels the distribution of local circumferential strains and stresses.

2.3 Endothelial Cell Functionality

The vascular endothelium is an active cellular interface between the vessel wall and the bloodstream where it regulates the physiological effects of humoral and biomechanical stimuli. The endothelium monolayer forms the lining of the internal surface of the entire cardiovascular system. As a result it is well located to respond to, and monitor changes in, blood flow and pressure. The endothelium, is not just an inert container of blood but a vital organ whose health is essential to normal vascular physiology and whose dysfunction can be a critical factor in the pathophysiology of diseases, such as hypertension and atherosclerosis.

The endothelial cell monolayer not only provides a selective barrier for macromolecular permeability, i.e. regulates the mass transport between the blood and the body, between the blood and the vessel wall but it also serves a number of homeostatic functions. Endothelial cells can in fact (i) influence vascular remodeling via the production of growth-promoting and growth-inhibiting substances; (ii) modulate hemostasis and thrombosis through the secretions of pro-coagulant, anti-coagulant, and fibrinolytic agents; (iii) mediate inflammatory responses through the expression of chemotactic and adhesion molecules on their membrane surfaces; and (iv) regulate vascular smooth muscle cell contraction through the release of vasodilators and vasoconstrictors. Impairment of these functions may lead to pro-atherogenic and/or pro-thrombotic states and hence atherosclerosis and/or thrombosis. (Badimon et al., 1992; Blann & Lip, 1998)

Under normal physiological conditions, the vascular endothelium is a non-thrombogenic surface. Endothelial cells express several anti-coagulative factors however they can also express factors which instigate the clotting cascade, the most important being tissue factor. Disturbance of endothelial cells through vascular injury, or exposure to certain factors such as cytokines may result in a decrease of anti-coagulant mediators and an increase in expression of pro-coagulant mediators. Furthermore venous blood vessels appear more prone to thrombosis than arterial blood vessels. Endothelial dysfunction is characteristically observed early in atherogenesis, however endothelial cell disruption is not (Weinbaum & Chien, 1993). By this it is understood that in early atherosclerosis formation the endothelial

cells may not have ruptured but have had their functionality impaired, such as an increased permeability to low density lipoproteins (Hironaka et al., 1997).

A physiologically healthy endothelium displays a compact monolayer characterised by scarce intercellular spaces. Hence it acts as a barrier between the blood and tissues of the cell wall. Several elements, including but not limited to intercellular junction and cell-surface binding proteins, contribute to the regulation of endothelial integrity and thus its permeability. In an intact endothelium, the cross-wall mass transfer is mainly through active transport, i.e. it is controlled by the endothelium depending on the need of the arterial wall for different substances.

Intercellular junctions between endothelial cells exist when transmembrane proteins develop a close physical attachment to cyctoplasmic and cytoskeletal proteins of a neighbouring cell membrane resulting in a tight junction. Very close contact between cells is permitted by these tight junctions. When the endothelium is locally injured causing the release of local growth factors, enhanced monocyte deposition and/or high cell turnover, the intercellular space may be substantially widened. This makes it possible for free convection/diffusion of macromolecules and even cells through intercellular space. This inner most layer of endothelial cells will form the focus of this study, in particular the junctions that form between adjacent cells and the protective functions of the endothelium following the introduction of a bypass graft.

2.4 Atherosclerosis Formation and Propagation

Weakened endothelial cell function is an early indicator of atherosclerosis according to a study of healthy people followed from childhood to young adulthood (Juonala et al., 2004). The most widely accepted hypothesis of the first stage of atherosclerosis, as reported by Clowes (1995), is a response to injury hypothesis. This hypothesis states that an injury to the cell lining or endothelium results in cell dysfunction. Upon failing in its function as a permeability barrier the formation a series of reactions occur allowing for the formation of plaque and/or intimal hyperplasia to occur.

The development and growth of atherosclerotic plaque within the arterial wall are best described in five stages as shown in Figure 2.2 (Liddy, 2004). Initially damage to the endothelium and the exposure of subendothelial components, results in adherence of platelets to the damaged vessel wall and subsequent activation (Gimbrone Jr, 1995). Once platelets have activated, p-selectin appears in the outer membrane and this serves as a receptor site

for monocytes. The adhesion of monocytes to the lumenal surface is followed by migration across the endothelium and accumulation within the intima. Cell-surface glycoprotein's also initiate the attachment and adherence of lymphocytes to the damaged endothelial cell surface and allow them to penetrate into the tunica intima (Van de Graaff & Fox, 1995).

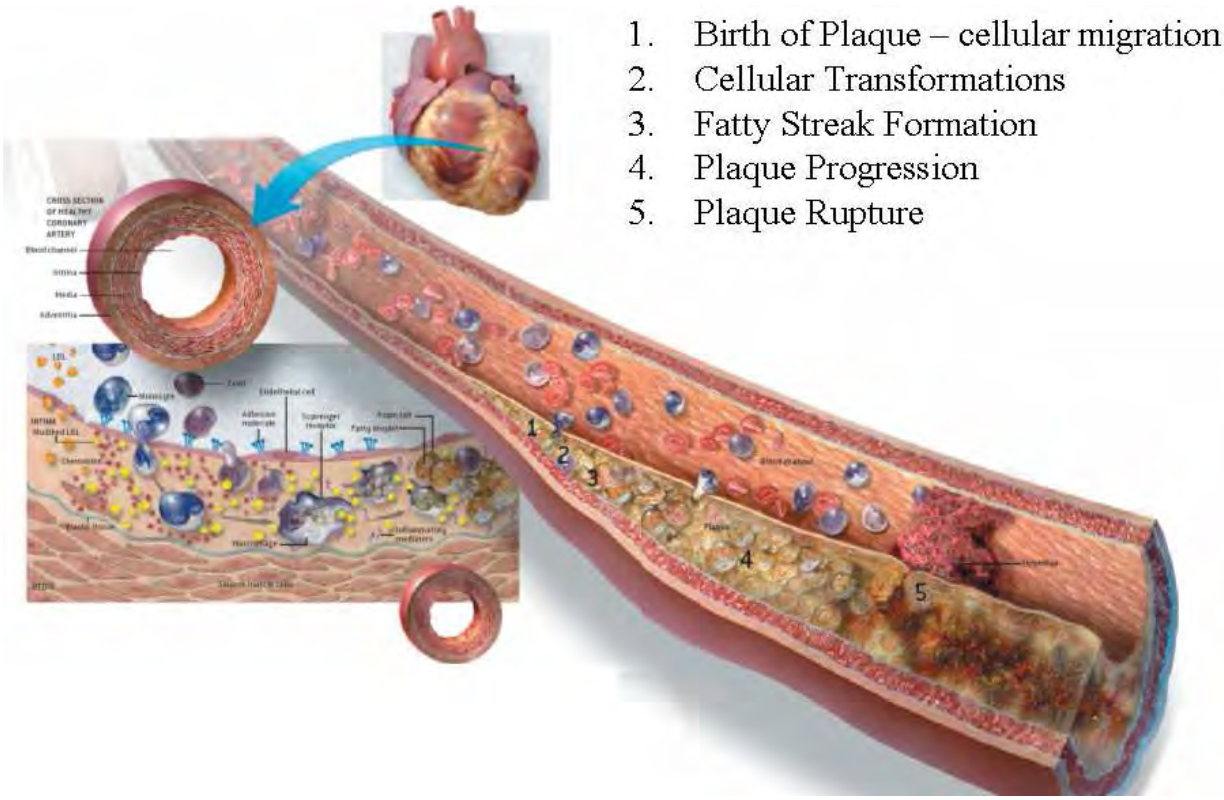

Figure 2.2: Atherosclerosis formation (Liddy, 2004)

Excess low density lipoproteins (LDL), more commonly refereed to as cholesterol, accumulates in the arterial wall (Fry, 1987; Nielsen et al., 2001). The oxidised LDL's (OxLDL) stimulate endothelial cells to display adhesion molecules, which clutch on to monocytes and T-cells in the blood. The captured cells are drawn into the intima. In the second stage cellular transformations occur in which endothelial and smooth muscle cells release chemokines and other substances, which induce the monocytes to multiply and mature into active macrophages. This second stage consists of the development of layers of macrophages which become surrounded by smooth muscles cells. The smooth muscle cells change from a contractile state to a 'synthetic' state, due to the presence of macrophages, causing them to produce and secrete connective tissue matrix proteins. The smooth muscle cells also begin to migrate from the media to the intima where they provide a protective barrier between the plaque and the blood. Platelet derived growth factor (PDGF) which is present at the site of inflammation is believed to be essential for the migration of smooth

muscle cells from the media into the intima (Cassar et al., 2005). The macrophages and T cells produce many inflammatory mediators and factors that promote further cell division.

The first recognisable change, and third stage of the disease progression, is the appearance of fatty streaks, frequently occurring at arterial branches. The unregulated macrophage uptake of cholesterol and lipids through modified forms of LDL, such as OxLDL, assists in the transformation of macrophages into foam cells. The modification not only enhances its uptake by macrophages, but also changes the natural structure of these otherwise ubiquitous molecules to generate a variety of modified lipids and proteins that represent highly immunogenic neo-determinants. The macrophages also display scavenger receptors, which help them to engulf oxidised LDLs, becoming filled with fat droplets. These frothy-looking droplets, called foam cells, and the T cells constitute the fatty streaks. Thus the fatty streaks consist primarily of oxidized LDL filled macrophages and lymphocytes. Furthermore the lymphocytes release cytokines, which amplify the inflammatory behavior further.

The penultimate stage of plaque progression refers to the continuing increase in intimal plaque volume and migrations of smooth muscle cells into the intima, which results in the narrowing of the lumen and obstruction of blood flow. Rates of progression may vary with the stage of plaque development, plaque composition, and cell population of the lesion.

Finally if the smooth muscle cell cap, which formed between the plaque and the blood, is sufficiently weakened by inflammatory matter and it ruptures it causes a thrombus to form, which if large enough can completely stop the blood from flowing through the artery. Disruption of these plaques with exposure of their lipid cores triggers the formation of a thrombus which can be up to six times larger than those generated by other components of the arterial wall (Cassar et al., 2005). This sudden thrombus formation can cause severe responses such as heart attacks, strokes, acute ischaemia of the lower limb and potentially thromboembolic episodes, depending on the location of the blockage.

Acetylsalaicylic Acid (Aspirin) or other antiplatelet and antithrombotic drugs reduce the incidence of non-fatal myocardial infarction (heart attack), non-fatal stroke or vascular death in patients at increased risk of occlusive vascular events. Thus showing that platelets have a major role in atherosclerosis and its complications in the coronary and cerebral vascular systems. However little information is known regarding what initially disrupts endothelial cell functionality in order to allow the onset of the disease.

2.5 Intimal Hyperplasia

Intimal hyperplasia is the collective response of a vessel to injury and is characterised by the thickening of the tunica intima of a blood vessel, often as a complication of a reconstruction procedure or endarterectomy. Intimal hyperplasia is believed to be an important reason of late bypass graft failure, particularly in vein and synthetic vascular grafts. Resnick et al. (2003) published a 30-50% (>30days post operation) failure rate of end to side bypass grafts due to the formation of intimal hyperplasia. They also proposed that intimal hyperplasia results from an endothelial cells response to chronic injury that leads to neutrophil, lymphocyte, platelet and macrophage adhesion and migration into the subendothelium.

2.6 Surgical Intervention

Surgical replacement or bypass surgery is the most common treatment for coronary and peripheral atherosclerotic diseases, with over 28,000 bypass cases performed each year in the United Kingdom (British Heart Foundation, 2004). Although no statistics are available for the number of Irish bypass grafts performed it is believe to be proportionate to those for the UK. In Ireland 40% of deaths are as a result of heart attacks and strokes due to atherosclerosis. Hence any research that can lead to an earlier diagnosis of atherosclerosis or that can help to improve the patency of bypass grafts thus reducing the incidence of surgery required, is of great benefit, both from an economic and health perspective. It could lead to a reduction in the number of heart attack and stroke sufferers in this country and also reduce the amount of capital that is currently spent by the state on the treatment of sufferers of the disease. Currently no non-invasive method of diagnosis exists for atherosclerosis and sufferers can often be beyond treatment by the time the disease is discovered. Despite the large number of patients suffering from atherosclerotic diseases and the vast quantities of capitol spent on treatments for the disease, no studies have been found in which direct measurements were recorded of the deflections occurring *in vivo*, post introduction of a femoral artery bypass graft.

Intimal hyperplasia and atherosclerosis have a predilection for occurrence at specific locations surrounding the distal anastomosis, specifically at the heel, toe and bed of the bifurcation shown in Figure 2.3. The toe and suture line were the primary focuses of measurement in this study as the deflections could be recorded at these locations when a CCD camera was placed immediately above the patient when in a supine position during

surgery.

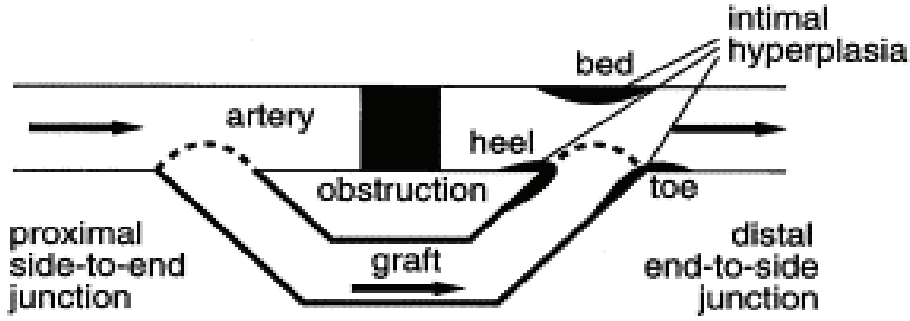

Figure 2.3: Schematic of bypass graft junctions (Ballyk et al., 1998).

2.7 Bypass Material Properties

Prior to the commencement of experiments a close examination of the various materials currently in use as vascular bypass graft materials was performed. Synthetic grafts, in particular Dacron and polytetrafluroethylene (PTFE), were examined as they are the most commonly utilised in bypass surgeries.

Dacron yarn can be woven or knitted into a graft. This weaving by its nature allows a certain looseness and the material tends to fray. To combat this the Dacron yarn is tightly woven thus making it very strong, stiff and non-porous, hence it does not leak as much blood. However a degree of porosity is beneficial as it increases the healing properties of the graft. Knitted Dacron takes longer to process but its properties are more beneficial than those of the woven yarn. Knitted Dacron can have pores and can stretch, furthermore knitting the yarn removes the possibility of fraying. These factors make knitted Dacron easier to handle and improves its mechanical compliance to the artery. However before being implanted, knitted Dacron grafts must be preclotted to prevent blood loss through its walls, this renders the inner surface less thrombogenic. Preclotting involves soaking the graft in, or repeatedly flushing it with blood that does not have the vasoactive agent heparin added to it. As an alternative to preclotting a manufacturer may coat the graft with an absorbable biodegradable material, such as bovine dermal collagen. Collagen implanted grafts involve a greater immune response than standard preclotted grafts. Although the impregnated grafts are more compliant they are also considerably more expensive than their non-coated counterparts and thus are less widely used.

Expanded PTFE (ePTFE) is a velour graft. Non-textile synthetic ePTFE can be fashioned into a tubular graft. For circumferential strength in the body a thin external layer is added. Although there are more pores in ePTFE than Dacron, bleeding does not occur as the pore size is too small and as the material is hydrophobic, thus it is also less thrombogenic than Dacron. The smooth wall of ePTFE is prone to kinking, hence a recent modification involves micro-crimping the fibrils on the tube. This leads to a more elastic graft which makes the wall even softer, more comfortable and gives excellent handling qualities as well as decreasing its tendency to kink when it crosses joints such as the knee. The surface of the graft remains relatively smooth which leads to a graft material that is easier to handle, and therefore, implant.

In the long term it has been proven that ePTFE is more effective than Dacron. In particular Dacron grafts have a disappointing performance for peripheral grafts where complications affected 13% of Dacron grafts but only 4% of ePTFE grafts (Brewster, 1995). The advantages that ePTFE grafts have over Dacron grafts include; their lack of requirement for preclotting, the fact that they do not leak or dilate, their biocompatiblity and their smooth surface is resistant to bacterial adherence and infection. The principal disadvantage of ePTFE grafts is that they are less compliant than native vein and this causes a significant problem at the distal graft artery interface. The relevant material properties can be viewed in Table 2.1. ePTFE grafts were employed as the primary synthetic grafts examined during the course of this study.

The most suitable bypass material is a homogenous vein however using a vein in the role of an artery places additional stresses on it. Mechanical stresses have long been hypothesized as important factors in regulating the structure and organization of vascular smooth muscle cells, a major load carrying element of the blood vessel. Fung (1993) detailed the sequence of reorganisation of the vascular smooth muscle cells in the neointima and media of vein grafts, and showed that the increase in pressure can induce the circumferential stress in the blood vessel wall as much as 140 times as compared with that normally experienced by the vein. In other words it is important to understand that a vein will alter its structure when used in an arterial role due to the additional stresses placed on it, despite this the vein is still the most preferred material to be used in a bypass graft.

Compliance of the artery and graft is of utmost importance. By coupling a relatively stiff graft to a compliant artery additional stresses are placed on the suture line, these additional stresses may in fact contribute to intimal hyperplasia and restenosis. Most anastomotic disruptions develop in the arterial wall with the advent of synthetic sutures. With

Table 2.1: **Material Properties for Experimental Analysis**

Material	E (MPa)	Poisons Ratio	Ep (MPa)	λ
Saphenous Vein 0 mths[1]	-	-	0.3 ± 0.06	2.2 ± 0.4
Saphenous Vein 35 mths[1]	-	-	0.49 ± 0.2	1.7 ± 1.0
Umbilical Vein 0 mths[1]	-	-	0.36 ± 0.05	1.9 ± 0.3
Infrarenal Aorta[1]	2.6 ± 1.45	-	0.98 ± 0.35	0.8 ± 0.3
Terminal Aorta[1]	3.77 ± 1.72	-	1.51 ± 0.41	0.5 ± 0.2
Common Iliac Artery[1]	2.47 ± 2.15	-	1.48 ± 1.58	0.8 ± 0.4
Common femoral artery <35 yrs[1]	-	-	0.26 ± 0.13	3.0 ± 1.0
Common femoral artery 35-60 yrs[1]	-	-	0.39 ± 0.2	2.1 ± 0.9
Common femoral artery >60 yrs[1]	-	-	0.63 ± 0.48	1.2 ± 0.9
Femoral artery[2,4]	1.35	-	0.115	-
Silicon[3]	1.17	0.47	-	-
Dacron knitted[1,2]	128	0.48	55.5	0.24 ± 0.02
Dacron woven[1]	-	-	166.6	0.08 ± 0.03
ePTFE[2]	290	0.47	-	-

[1] Sumners et al. (2000), [2] Fung (1993), [3] Morris (2004) and [4] Kawasaki et al. (1987)

application of synthetic grafts, the proper choice of the graft material can minimise compliance mismatch. Apart from surgical injury during operation, it is assumed that the occurrence of intimal hyperplasia around the suture line is caused by the tissue remodelling as a response to mechanical injury bought about by the artery-graft compliance mismatch (Trubel et al., 1994).

While investigating material mismatch, with the use of finite element analysis, Ballyk et al. (1998) found stress values along the suture line where the stiff graft interfaces with the native artery to be between 3 and 36 times higher than that of the distal host artery. When considering material mismatch, compliance of the artery and the material which it is sutured to is very important, whether it is a vein or prosthetic graft. When the compliance changed by 68% between a stiff dacron graft and a venous graft, the stress increased by 40% on the anastomosis, but overall the stress increase was only 5%. This shows the magnitude of the effect compliance mismatch of a material has on the performance of the graft (Ballyk et al., 1998).

In order to counteract this artery-graft mismatch a number of transition region configurations have been suggested throughout literature in an attempt to reduce the negative effects associated with the area surrounding the junction.

2.8 Bypass Graft Configurations

Echave et al. (1979) and LoGerfo et al. (1983) showed that in synthetic grafts significant intimal thickening develops at the anastomosis or just beyond in the distal vessels and usually appears within two years of reconstruction. To improve the patency rates of prosthetic grafts several modifications to the conventional end to side anastomosis have been proposed and implemented. Linton & Wilde (1970) employed a vein patch, sutured onto the arteriotomy and opened longidutinally, to create the anastomosis, known as the Linton patch. Miller et al. (1984) adapted this technique by introducing a vein cuff between the graft and the host artery in an attempt to improve the compliance between the relatively rigid PTFE grafts and arteries. Analysis of the Miller cuff revealed a high patency rate.

A study by Stonebridge et al. (1997) indicated that the two-year patency rates for cuffed and conventional grafts to below-knee popliteal artery were 52% and 29% respectively. The rates have been shown to drop further, to 20-30%, within 4 to 5 years (Schultz et al., 1986). Taylor et al. (1992) advocated incorporating a small segment of vein, known as a patch, at the distal anastomosis. This Taylor patch, according to their studies resulted in a reduction of intimal hyperplasia formation and an improved patency rate, particularly in peripheral bypasses. The structures of each junction configuration can be seen in Figure 2.4.

Dacron and ePTFE are high strength polymers with excellent wear properties. Bypass grafts can be used anywhere in the body but have lower patency rates in smaller conduits such as the femoral artery. Although the patency rates remain poor, the presence of vein cuffs and patches have been seen to improve the patency (Lemson et al., 2000; Ducasse et al., 2004; Heise et al., 2004). The patency rate remains low in the medium to long term because of the build up of intimal hyperplasia and the resulting stenosis. Due to the low patency rate some surgeons considered amputation in preference to bypass surgery when no autogenous vein was available (Gentile et al., 1998). Variations on the vein cuff and patches have been developed and variations continue to be made as the optimum geometry has yet to be developed. Many patency rates have been recorded but as no randomisation of results has been put in place true values cannot definitively be determined. Table 2.2 shows the patency rates recorded in literature.

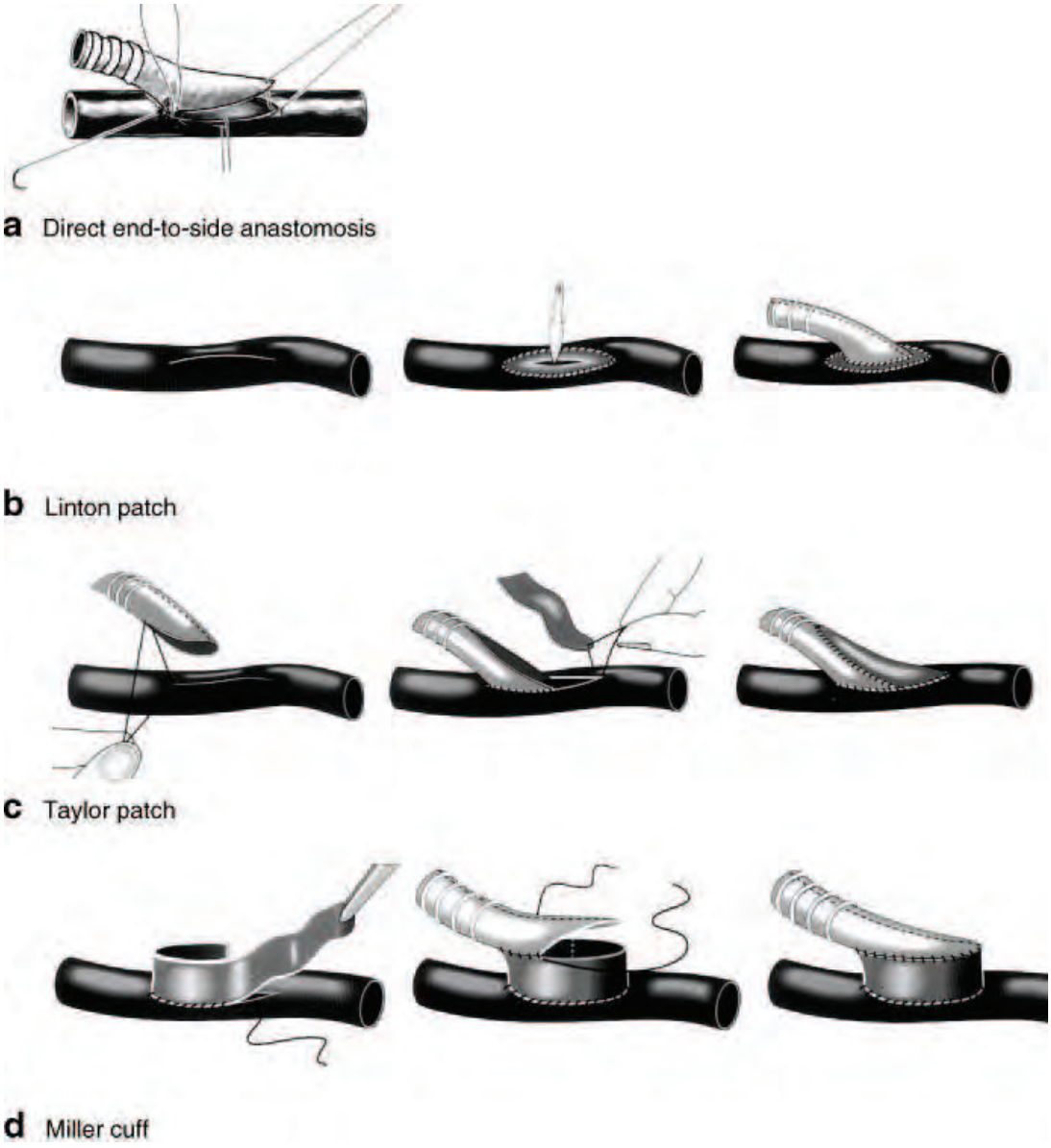

Figure 2.4: Schematic of bypass graft configurations (Trubel et al., 2004)

.

Using laser Doppler anemometry (LDA), Rowe et al. (1999) conducted flow studies on the Millar cuff model. As the flow decelerates into the Millar cuff anastomosis, a large vortex is produced that occupies most of the region of the cuff. This vortex has the effect of reducing the risk of thrombosis by mixing the fluid within the cuff, thus preventing areas of flow stasis. Furthermore, it alters the point of flow division into the proximal and distal segments of the artery and therefore redistributes the low mean shear regions. The areas of low mean shear in the Millar cuff are found within the cuff region and any intimal hyperplasia that may develop there will not significantly affect the blood flow because of the large volume of the cuff.

Cole et al. (2002b), using computational fluid dynamics (CFD), have shown that the

Table 2.2: **Graft Patency Rates**

Time	Miller Cuff	No Cuff	Linton	Taylor
30 days	96%[1]	87%[1]	-	-
1 year	78%[2]	61%[3]	74%[3]	84%[3]
	47-83%[3]	29-57%[2]	-	72-78%[4]
	49%[5]	-	-	48-53%[3]
	40%[3]	-	-	-
2 years	62%[4]	29%[4]	-	81-94%[3]
	-	-	-	65%[4]
3 years	47%[1]	48%[1]	75%[3]	76%[3]
	38%[1]	29%[4]	-	57%[4]
	29-38%[3]	7-19%[3]	-	24-35%[3]
5 years	-	-	-	0-49%[3]
	-	-	-	54-71%[3]

[1] (Kreienberg et al., 2000), [2] (Piorko et al., 2001), [3] (Lemson et al., 2000), [4] (Gentile et al., 1998) and [5] (Fisher et al., 2003)

effect of the Taylor procedure is to gradually reduce the average velocity of the blood as it approaches the distal end of the graft artery junction. The increasing cross-sectional area of the Taylor bypass prevents the sudden deceleration that the blood experiences as it enters the recipient artery in the conventional model. Their studies found that the spatial gradient of shear stress implies that endothelial cells on the distal floor experience a stretching force, which has a large magnitude during systole but which diminished during diastole. This cyclic, unnatural stretching of the endothelial cells, caused by the changing spatial gradients of the WSS may promote intimal hyperplasia development.

Using CFD Lei et al. (1996) compared the conventional anastomosis model with the Taylor patch. Their studies found that a possible explanation for the superior performance of the Taylor patch can be given by the time-averaged wall shear stress gradients (WSSG) for each graft-artery junction. Non-zero WSSG values of the Taylor patch are essentially confined to the toe and heel of the junction whereas the conventional model has distinct non-zero wall shear stress regions throughout the junction area.

Despite the positive results for both the Miller cuff and the Taylor patch compared to the conventional bypass, there is contradictory evidence of their respective patency rates that indicate that these modifications may not be advantageous and that an optimum geometry may not exist. Cole et al. (2002a) carried out a CFD investigation of an anatomosis using ePTFE shaped like Millar cuff. This study predicted that the stretching effect on the endothelial cells of the artery floor, which they believe to be caused by the WSSG, will be

more pronounced when the Millar cuff is present suggesting that aspects of the anastomotic haemodynamics are worsened when the cuff is employed. Fisher et al. (2003) investigated the effect of the Taylor patch shaped ePTFE cuff. The authors concluded that the shape of the geometry alone does not improve the patency as a vein cuff anastomosis, as the flow patterns would be identical in both geometry shapes with venous or synthetic patches thus this report further reduces the validity of the flow hypothesis as the primary cause of restenosis and leads to the more recent but less presented and less investigated argument of pressure induced intramural stress.

Much research has been performed investigating the causes of arterial blockage at the distal junction due to plaque formation and growth. Of primary interest in this study are the two theories associated with flow and pressure, the haemodynamic hypothesis and the intramural hypothesis.

2.9 Haemodynamic Hypothesis

Definite correlations between hydrodynamic stresses on the arterial wall and arterial disease were shown by Ling et al. (1968) and Fry (1968). Wall shear stresses have long since been thought of as the main cause of restenosis and many studies have been performed that concentrate on this factor. The concept of the adverse effects of fluid shearing on arterial walls was first introduced by Fry (1968) when he showed that high wall shear stresses produced histological and biochemical changes in arterial endothelial cells. The first definite correlations between hydrodynamic stresses on the arterial wall and arterial disease, under physiological conditions, came from Ling et al. (1968). Ling obtained direct measurements for the wall shear stress, due to blood flow, using a heated film probe and found them to reach values from 80 -160 dyn/cm^2. Fry (1968) studied the acute yield stress of the vascular endothelium subjected to the shearing stress of blood flow in the aorta. In this study the design of a plug inserted into a dog's thoracic aorta increased the blood flow adjacent to the endothelium. From Fry's initial analysis it appeared that the critical level of flow induced shear stress on the endothelium was not much above the values of shear stress obtained in a normal physiological situation.

Under the haemodynamic hypothesis, correlations have been made between areas of high and low shear stresses and the build up of plaque (Leuprecht et al., 2002; Heise et al., 2004). It is increasingly accepted that vascular biological processes are influenced by local haemodynamics. Rutherford (2000) stated that the adaptive responses of arteries, and the

healing response to arterial injuries, serve to maintain the structural and functional integrity of the arterial tree. Normal responses to altered biomechanical and hemodynamic conditions result in compensatory changes in artery wall thickness, lumen diameter, or both, whereas abnormal or pathologic conditions may engender alterations in wall thickness and lumen diameter that proceed to lumen stenosis, aneurysm formation, or obstructive intimal hyperplasia.

Many studies have demonstrated the abnormal flow behaviour present in graft-artery junctions (Ducasse et al., 2004; Noori et al., 1999; Leuprecht et al., 2002). The majority of studies in this area have examined the haemodynamic effects of high and low wall shear stresses. Alterations in local haemodynamic conditions result in adaptive changes in the artery wall to maintain an adequate lumen caliber for blood flow. Local non-physiological haemodynamics influence the proliferation of intimal hyperplasia in ePTFE grafts. Previous studies have proposed that intimal hyperplasia is an adaptive response of live arteries to disturbed flow conditions in an attempt to restore a wall shear stress (WSS) to within the normal range (Malek et al., 1999). However many contradicting opinions exist.

Leuprecht et al. (2002), Botnar et al. (2000) and Heise et al. (2004) believe that local hemodynamics factors play a significant part in the development of atherosclerosis following finite element studies of various anastomoses. Botnar et al. (2000) also contends that the consistency and rheology of the blood is considered to have a complimentary factor to play. Finite element fluid studies have found that blood flow in an anastomosis consists of areas of flow separation and zones of recirculation. Within zones of flow separation regions of low wall shear stress exist which are considered to contribute to the onset of the disease and once the disease has progressed to a particular stage, it will create high wall shear stress, which encourages further plaque growth (Nazemi et al., 1990). Morinaga et al. (1985) contradicted this, believing that high shear stress tends to prevent intimal thickening. According to Ducasse et al. (2004) low shear stress promotes smooth muscle cell migration and proliferation leading to intimal hyperplasia. Similarly Cole et al. (2002b) and Wentzel et al. (2003) correlate low shear stress with intimal thickening and explain it as an active response of live endothelium to retain shear stress within the physiological range. Zairns et al. (1983) found that regions with rapid laminar flow tended to inhibit lesion formation.

Further investigation has led to conflicting arguments regarding the effects of shear. Leuprecht et al. (2002) examined the region of the distal anastomosis for a conventional and Miller cuff in terms of many of the cited factors. It was found that the development and progress of distal anastomotic intimal hyperplasia seemed to be promoted by both altered

flow conditions and intramural stress distributions at the region of the artery-graft junction of vascular bypass configurations. The wall shear stress on the artery floor was found to be very low and oscillating where as the axial wall shear stress on the hood followed the pulse waveform. Steep stress gradients were observed in the artery-graft junction and the vein-graft junction whereas the artery-vein connection showed only moderate gradients. The stiff e-PTFE graft demonstrated a significant compliance mismatch to the host artery. The stiffer synthetic material also gave rise to increased maximum stresses that were about 3.5 times higher than in the vein-graft configuration. The highest stresses occurred around the suture clips on both sides of the junction. Velocity patterns and magnitude and distribution of wall shear stress did not change considerably despite rather large sidewall deformations in the anastomotic region. A number of investigations have shown that a constant vortex is created when a millar cuff is used. It is hypothesised that the vortex improved the intimal hyperplasia distribution as it increased wall shear stress at the critical areas of the heel, toe and bed and provided a constant washout of the cuff (Ulrich et al., 1999; Ducasse et al., 2004; Noori et al., 1999). However some authors who subscribe to the flow mechanics theory have concluded from their studies that it is not simply the flow pattern which increases the patency but the large buffer area of the cuff which takes longer to occlude (Leuprecht et al., 2002; Ducasse et al., 2004; Longest et al., 2003).

All the research in this area to date has not lead to any conclusive evidence to support the argument for haemodynamic factors nor has it conclusively disproved it. This can be shown from the fact that restenosis occurs not only at the heel, toe and bed of a junction but also along the suture line of the bifurcation. Flow induces low shear at the proximal lip and low shear at the distal lip of a bypass graft junction thus this suggests that the hypothesis whereby the vessel wall mechanics and the compliance mismatch of the materials seem to play the major role in the development and progress of intimal thickening in this region (Sottiurai et al., 1989). This further supports the concept that intramural pressure has a greater effect on the strain and stress at the distal anastomosis as a change in material should not have a significant effect on the flow.

2.10 Intramural Hypothesis

The opposing hypothesis to fluid mechanics is the solid mechanics hypothesis. A number of studies have examined the effects of reducing blood pressure and heart rate, on the formation of atherosclerosis. It was found that a decrease either of the mean blood pressure

or of the pulse pressure reduces atherosclerotic lesions in rabbits (Spence et al., 1984), sheep (Magarey et al., 1965) and monkeys (Lyon et al., 1987) and a decrease in the heart rate reduced the occurrence of atherosclerotic lesions in rabbits and monkeys (Ablad et al., 1988). In humans a decrease in mean blood pressure and a decrease in the heart rate is reported to reduce mortality and morbidity originating from atherosclerotic disease (Roberts, 1975; Wikstrand et al., 1988). As this reduction in atherosclerotic disease can be partially attributed to a reduction in blood pressure it can be concluded that the intramural pressure plays an important role in localised plaque formation and propagation. Thubrikar & Robicsek (1995) and Sottiurai et al. (1989) contend that it is the blood pressure induced arterial wall stress which is the principal factor in the localisation of the disease.

Dobrin (1992) found that treating monkeys with platelet-inhibiting agents after venous grafting markedly attenuates intimal hyperplasia, with less reduction in medial thickening, whilst dogs treated in the same manner attenuate intimal thickening but have no reduction in medial thickening. No significant correlation between myointimal hyperplasia and shear stress was found however there was a statistically significant correlation between myointimal hyperplasia and pressure.

High blood pressure in general is a well recognised risk factor in coronary heart disease, a phenomenon that fits well in the 'arterial wall stress hypothesis' where the stress is produced primarily by blood pressure and not shear due to blood flow. In a study performed by Raghavan et al. (2000) is was found that patients with consistently high blood pressure were more prone to abdominal aortic aneurysm (AAA) rupture and that elevated wall stress was not just an acute event near the time of rupture. It has also been found that patients suffering from aortic aneurysms and high blood pressure are more prone to rupture due to the elevated wall stress (Fillinger et al., 2003).

Upon examination of a naturally occurring physiological bifurcation Thubrikar et al. (1990) and Thubrikar & Robicsek (1995), alleged that intramural stresses, which occur throughout the thickness of the arterial wall, result from intraluminal arterial pressure and not from blood flow. The stress increase is affected only secondarily by such factors as elastic properties, thickening at the branch site, curvature around the ostium, and length of the transition zone. This study concluded that neither curvature nor length of transition region had an appreciable effect on the results and that the increase in intramural stress at the branch points occurred primarily as a result of the presence of the ostium in the main artery, and the presence of arterial pressure.

The effects of pressure on arteries were examined in detail when Fung & Liu (1991)

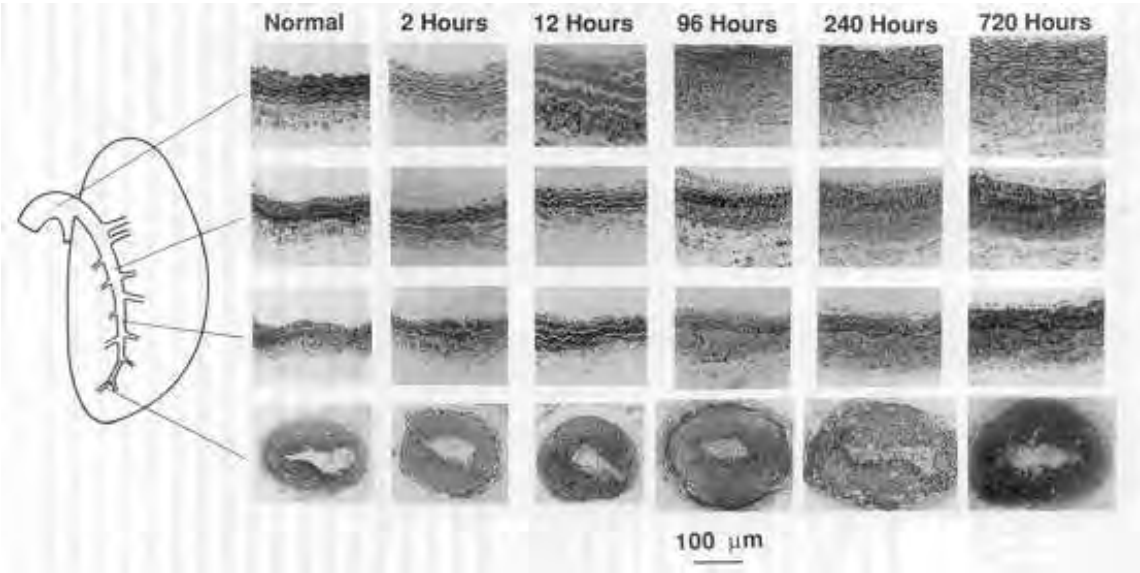

Figure 2.5: Pressure Induced Thickening of a Rats Pulmonary Artery (Fung & Liu, 1991)

performed an experiment in which rats were placed in a low oxygen chamber. Nitrogen was added so that the total pressure was the same as that at sea level. It was found that the systolic blood pressure increased from 2.0 KPa to 2.93 KPa within minutes after the rat was placed in the chamber. After one month, the pressure rose to 4.0 KPa. Significant histological changes were noticed in the tissue structure of the pulmonary artery after a few days. Even after a few hours, histological staining changes indicated a change in the total amount of elastin in the vessel. A significant thickening of the media layer in the pulmonary artery occurred after 12 hours and after 96 hours the adventitia has also experienced a significant increase in thickness as can be seen in Figure 2.5.

It was evident that early after exposure to higher pressure, the residual stress in the artery was greater than that of the controls. However, after prolonged exposure, the residual stress, as measured by the opening angle, decreased, indicating that the adaptation changes had reduced the residual stress (Fung & Liu, 1991). Hence it can be concluded that because the arteries responded quickly and significantly to changes in the overall pressure they may also respond as quickly to localised changes in pressure.

The mean blood pressure drop across normal arteries from the heart to the ankle is only a few millimeters of mercury. As the pressure wave travels distally, the systolic pressure increases, the diastolic pressure decreases, and the pulse pressure widens. Lower extremities are more prone to atherosclerosis than upper extremities, which also correlates with the pressure because lower extremities have higher absolute pressure due to the hydrostatic pressure head than do the upper extremities (Burton, 1972).

Thubrikar & Robicsek (1995) and Chaudhry et al. (1997) explain that a reduction in internal pressure and external stress leads to reduced occurrence of atherosclerosis by assuming the surrounding tissues exert a force on the artery. However Rachev & Greenwald (2003) suggest that remodelling of the artery is induced by residual stresses and report remodelling to restore wall stress distribution to normal which contradicts the explanation by Wentzel et al. (2003) that the remodelling is to restore wall shear stress.

Piorko et al. (2001) reported that enhanced stretching is shown to cause cell proliferation and matrix deposition, forming the fibrous cap associated with atherosclerosis. A correlation between the cracking sites of plaque and the areas of high wall stress show that pressure induced intramural stress plays a major role in stenosis (Lee & Xu, 2002). In this study it was found that zones of high stress and the associated stretch caused the fibrous cap to stretch and rupture. Kaazempur-Mofrad et al. (2004) oppose this correlation, stating that the strain from shear stress contradicts the wall stress hypothesis, because high mechanical strain resulting from shear stress enhance a biochemical reaction; production of MMP (metalloproteinease) which contributes to the weakening of the fibrous cap.

From their investigations Benetos et al. (2002) do not favour the correlation between low shear stress and smooth muscle cell migration. Their study shows that shear stress cannot explain the changes in intimal thickening, but that wall stress is responsible. By contrast Lemson et al. (2000) deem high shear stress as a causative factor. Under the flow hypothesis an argument can be made for the intimal hyperplasia distribution around the heel toe and bed. However the increased intimal hyperplasia in a cuff, when employed, and along the suture line cannot be explained. Under the intramural stress hypothesis the intimal hyperplasia distribution and atherosclerosis formation is explained by higher than usual wall stress at critical regions. The intramural stress theory also explains why there is a higher instance of intimal hyperplasia in patients who suffer from hypertension, and explains the intimal hyperplasia found to exist in the cuff configurations.

Tropea et al. (2000) and Lemson et al. (2000) report that hypertension has been suggested to induce changes in wall composition, including the selective barrier function of smooth muscle cells allowing the passage of atherogenic molecules, vasoactive hormones and adhesion of monocytes and leucocytes into the subendothelium layer, these changes lead to the development of intimal hyperplasia and stimulates cellular proliferation and lipid adsorption, resulting in foam cells.

The reported pattern of localisation of atherosclerotic plaques in arteries correlates with the location of highest deformations and tensile stresses. This can have a great effect on

cellular metabolism, which causes the increase of permeability to plasma constituents by increasing the stretch of the artery. Thus it appears logical that pressure-induced wall stress and not flow induced shear stress correlates with the locations of atherosclerotic lesions.

Following the review of literature available, it is the author's belief that the pressure plays a greater role than shear in altering the characteristics of the endothelial cell monolayer however both are examined within our proceeding cell culture study.

2.10.1 Endothelial Cell Responses to Pressure and Flow

It has been shown by Langille & Adamson (1981) that endothelial cell morphology and orientation in arteries *in vivo* correlate with the local hemodynamic environment. In the vasculature, the pumping action of the heart as well as containment of blood within the blood vessel lumen exposes the vascular endothelium to cyclic pressure.

When endothelial cells are subjected to shear stress resulting from blood flow they are able to convert mechanical stimuli into intracellular signals that affect cellular functions such as proliferation, apoptosis, migration, permeability and remodeling as well as gene expression. The endothelial cells are capable of using multiple sensing mechanisms in order to detect alterations in mechanical forces which lead to the activation of signaling networks. In vitro studies on cultured endothelial cells in flow channels have been conducted to investigate the molecular mechanisms by which cells convert the mechanical input into biochemical events, which eventually lead to functional responses (Li et al., 2005).

In the human circulatory system, blood flow in arteries is highly dynamic and variable. Wall shear stress generally ranges between 10 and 20 dynes/cm^2 at all levels of the arterial tree in mammals (Rutherford, 2000). As a result of these dynamic flow patterns, a complex set of mechanical forces are continuously imposed on the endothelial lining of vessels. Sato et al. (1996) showed that when endothelial cells were subjected to a shearing of 20 dyn/cm^2, after 24 hours cell elongation and increases in both cell stiffness and viscosity occurred. When subjected to chronically elevated (or decreased) flow rates, the arteries increase (or decrease) their diameters until the mean wall shear stress (MWSS) is approximately 15 dyne/cm^2. Wall shear stress consequently appears to act as a regulating signal to determine the artery lumen size, and this response relies on the presence of an intact endothelium. Atherosclerotic arteries are in addition capable of expanding in response to increases in blood flow and wall shear stress, however this process may be limited (Rutherford, 2000).

Blackman et al. (2002) performed a study in which the characteristic morphological

response of an endothelial monolayer exposed to steady flow was tested and determined the corresponding mechanical adaptations to the new flow conditions. The cultured cells were subjected to 7.5 dyn/cm^2 of steady laminar shear stress (LSS) or arterial pulsatile flow (ART) with an equivalent time averaged shear stress. They found that, after 24 hours, both the cells exposed to LSS and ART had variations in their morphology of polygonal-shaped cells, with no preferred orientation, to a well characterised morphology in which the cells were elongated and aligned in the flow of direction. It was concluded that the cell shape change was dependent on the time-average shear stress, or net direction and magnitude of the flow vector rather than the temporal gradients in shear stress.

Several studies have investigated the effects of cyclic strain on endothelial cells (Lehoux et al., 2005; Sipkema et al., 2003). It has been shown that physiological levels of cyclic strain on endothelial cells lead to increases in migration (Von Offenberg Sweeney et al., 2005) and proliferation (Iba & Sumpio, 1991; Li & Sumpio, 2005) whilst simultaneously reducing apoptosis (Haga et al., 2003; Liu et al., 2003). Cell culture studies on endothelial cells have established that cells orientate in response to cyclic stretch so that their long axis is perpendicular to the direction of stretch (Malek et al., 1999). The cells also proliferate at a higher rate and show development of stress fibres in response to stretch.

Endothelial cells react to cyclic strain both morphologically and phenotypically. The effects of cyclic strain on endothelial cells is visually evident as early as 15 minutes post-strain with the arrangement of actin stress fibres and morphological alignment of cells perpendicular to the force vector (Iba & Sumpio, 1991). This realignment is followed by phenotypic or cell fate changes, such as the expression of several classes of genes regulating such vascular functions as (i) vessel diameter - nitric oxide (NO), nitric oxide synthase (NOS) and cyclooxygenase-2 (COX-II, endothelin-1 (ET-1) (Cotter et al., 2004) (ii) Proliferation - platelet-derived growth factor (PDGF) and vascular endothelial growth factor (Sumpio et al., 1997, 1998; Zheng et al., 2001) (iii) Cell-cell communication/barrier function -, zonula occludens 1 (ZO-1) and intracellular adhesion molecule type-1 (ICAM-1) (Collins et al., 2006a; Pradhan & Sumpio, 2004; Cheng et al., 1996) and (iv) Angiogenesis - MMP-2, MMP-9 and RGD-dependent integrins (Von Offenberg Sweeney et al., 2005; Yamaguchi et al., 2002).

Shin et al. (2004) showed that the basic functions such as proliferation and apoptosis of endothelial cells are dependent on the applied cyclic pressure. In that study the modulatory role of cyclic pressure on an endothelial-specific phenotype was examined at pressures of either 60/20 mmHg or 140/100. The results demonstrated that only HUVEC exposed to

higher cyclic pressures exhibited altered barrier properties which included changes in the localization of interendothelial junctional proteins and in transendothelial permeability.

The rate of cell apoptosis has also been shown to increase significantly in a vein to artery graft, when it is subjected to mechanical stress whereas this rate does not change significantly in a vein to vein graft model (Mayr et al., 2000). Similarly Moore et al. (2001) concluded that a blood vessel is able to adapt to a change in tensile stress and strain in the wall of the blood vessel, for example hypertrophy and smooth muscle cell proliferation.

Tiwari et al. (2002) performed a study in which tissue engineering of endothelial cells and chemical engineering with anticoagulant moieties was undertaken in order to improve prosthetic graft patency and thrombogenicity. In this particular study a compliant graft was developed based on poly(carbonate-urea)urethane chemistry which had a compliance similar to the human artery. It was attempted to improve the patency of the prosthetic graft even further, by reducing the thrombogenic effects by lining the lumen with autologous endothelial cells. The graft design itself was suitable for seeding however due to the nonthrombogenic characteristic of the graft a substance was required to facilitate the attachment of the endothelial cells to it. In studies by Salacinski et al. (2001) and Tiwari et al. (2002) adhesive substances such as fibronectin, collagen and preclotting with blood and laminin were examined to improve the cell attachment. All of these substance yielded varying results. In the current study the silicone membranes were coated with pronectin to facilitate the attachment of endothelial cells to the surface of the 6 well Bioflex® plates.

2.10.2 Tight Junctions

Tight junctions, otherwise called zonula occludens, are the areas in direct contact between two cells, whose membranes bond together forming a virtually impermeable barrier to fluid. The first tight junction protein cloned was Zonula occludens (ZO-1) and it has been implicated as a significant scaffold protein. It is a member of a family of membrane-associated guanylate kinase homologues believed to be important in signal transduction at sites of cell-cell contact. Katsuno et al. (2008) showed that a deficiency in ZO-1 causes angiogenesis and apoptosis of embryonic cells thus it was decided to examine the effect of shear and strain on tight junctions as it is the authors belief that ZO-1 may be functionally important for the remodeling of endothelial cells .

2.11 Conclusion

The present study differs from all previous studies on strain in that it subjects endothelial cells to strain ranges based on *in vivo* measured values (Campbell et al., 2007) and attempts to define the ranges of strain that invoke positive proliferative responses, reduces permeability and reduces apoptosis and necrosis in endothelial cells. Upon examination the majority of the aforementioned studies performed their cyclic strain experiments from 0 to 10% strain (Cotter et al., 2004; Von Offenberg Sweeney et al., 2005; Collins et al., 2006a; Lehoux et al., 2005) or some declare an average strain of 10% but do not specify the range employed (Haga et al., 2003; Sumpio et al., 1997, 1998; Zheng et al., 2001; Li & Sumpio, 2005; Yamaguchi et al., 2002). However in the cardiovascular system the artery will never experience a strain of 0%. To the best of our knowledge this is the first study that examines actually endothelial cells responses at *in vivo* determined strain ranges.

Chapter 3

Validation of Measurement Technique

The primary goal of this study was to examine the *in vivo* environment surrounding the introduction of femoral artery bypass grafts. However prior to the performance of these experiments in surgery a comparative study was undertaken in order to examine the accuracy of the non invasive measurement technique. This initial comparative study involved the manufacture of silicon models to mimic the artery. These models were then pressurised and the deflections examined at varying static pressures using a videoextensometer. Finally all laboratory model results were compared to those predicted by finite element computer models subjected to the same conditions of pressure and identical material properties.

3.1 Silicon Models

Initial laboratory experiments involved the fabrication of various silicon models, which were idealised representations of the bypass graft anastomoses. Silicon was chosen to represent the arteries as it provided a standard by which all specimens could be assumed to be equivalent. Were, for example, pig arteries to be employed numerous unknown variables would prevent the assumption that each specimen exhibited similar material properties, thus contributing an unquantifiable error between models.

A prerequisite to the experimental procedure was to design the moulds to define the model dimensions. The dimensions used were adapted from literature (Fisher et al., 2003; Walsh et al., 2003). An important factor to consider when introducing a bypass graft is the angle at which it should be sutured to the existing artery. The angle can effect the velocity profile of the blood flow and can have a major impact on the location and intensity of induced stresses. It has been found that an angle of 45° can lead to a reduction in the

stress concentration around the suture line of the anastomosis (Lei et al., 1997; Walsh et al., 2003).

Two moulds were designed using ProEngineer Educational Edition. The lobes that are seen at the ends in Figure 3.1 and Figure 3.2, are a result of the manufacturing process and the increased wall thickness provided additional support for the models in the test rig.

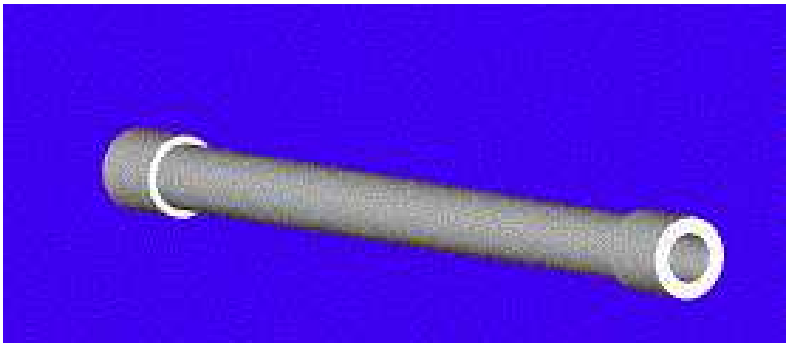

Figure 3.1: Finite element model constructed to mimic the straight tube silicon model

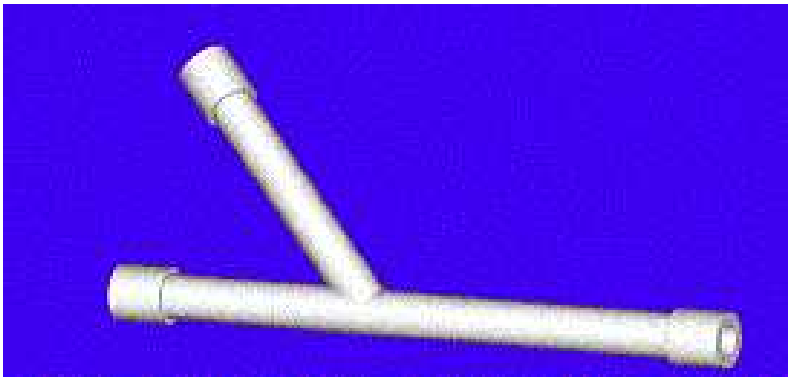

Figure 3.2: Finite element model constructed to mimic the silicon model of the graft bifurcation

Firstly a cylindrical model with homogenous material properties was manufactured followed by the modelling of a homogeneous 45° graft artery junction. Finally a model consisting of silicon and an ePTFE graft was made where by the graft section of the 45° homogenous junction was removed and replaced with ePTFE. Several approaches were tried when manufacturing the experimental silicon models before a successful process was achieved, details of which can be found in Appendix B. Silicon was employed to represent the artery due to the similar material properties it exhibits to the artery at lower pressures but more importantly silicon ensured consistent material properties between models for comparative purposes.

The dies were manufactured from flat aluminium plates with slots milled out using a

ball-nosed cutter on a vertical milling machine. Guide pins were incorporated into the design in order to facilitate quick assembly and accurate alignment.

The manufacture of the wax and silicon pieces required individual dies hence four dies were produced, two for the straight model and two for 45° bifurcation model. Texwax FG 890 (Texaco, Germany) was used for casting the wax moulds and when cooled each mould was dipped in a Wacker Schutzfilm SF 18 (DRAWIN, Germany) to prevent the silicon adhering to the wax. The inner surface of the dies were sprayed with silicon release agent (Ambersil Formula 8) and the wax moulds were then incorporated into the silicon injection dies. Using a vacuum oven any air bubbles were removed from the two part Elastosil RT 601 A and B silicon (DRAWIN, Germany). The silicon mixture was then injected into the dies. Once the silicon had cured, the wax from the interior was removed by hanging the model from a support within an oven, where the wax melted at approximately 90°C.

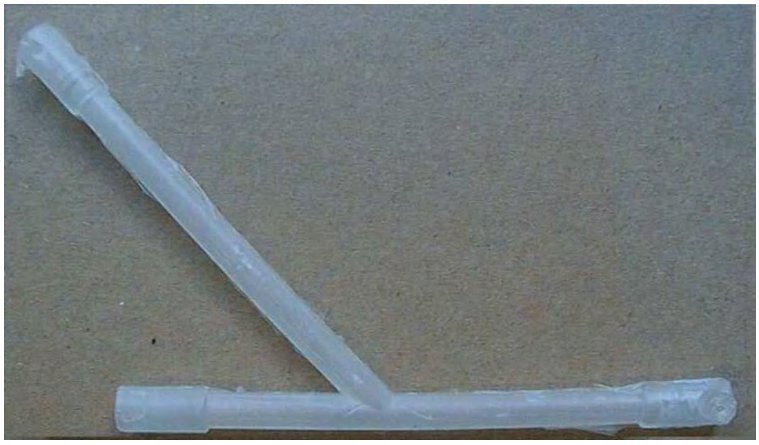

Figure 3.3: Homogenous 45° silicon bifurcation

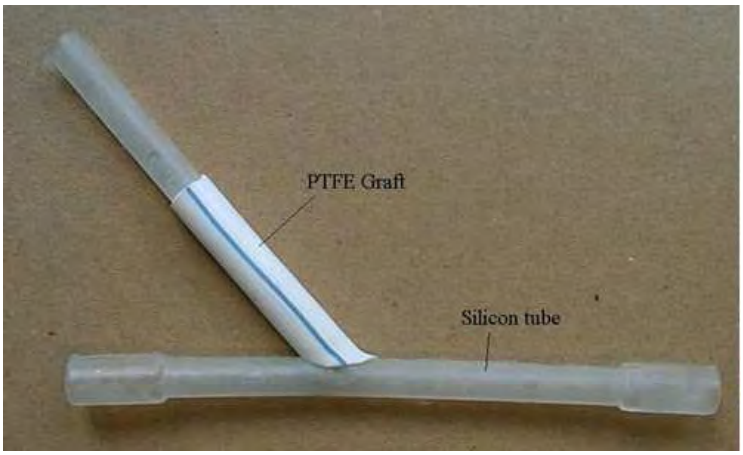

Figure 3.4: Silicon bifurcation with a ePTFE graft

Additional models were also constructed to include an artificial bypass graft material,

ePTFE. The resulting silicon models can be seen in Figure 3.3 and Figure 3.4. Furthermore in order to ensure consistency throughout experiments within this study, the same surgeon who performed all of the femoral bypass graft surgeries (Section 4.1), undertook the task of making an incision in a number of straight section silicon models and attaching the ePTFE graft to the silicon model in a similar manner as that performed in an operating theatre.

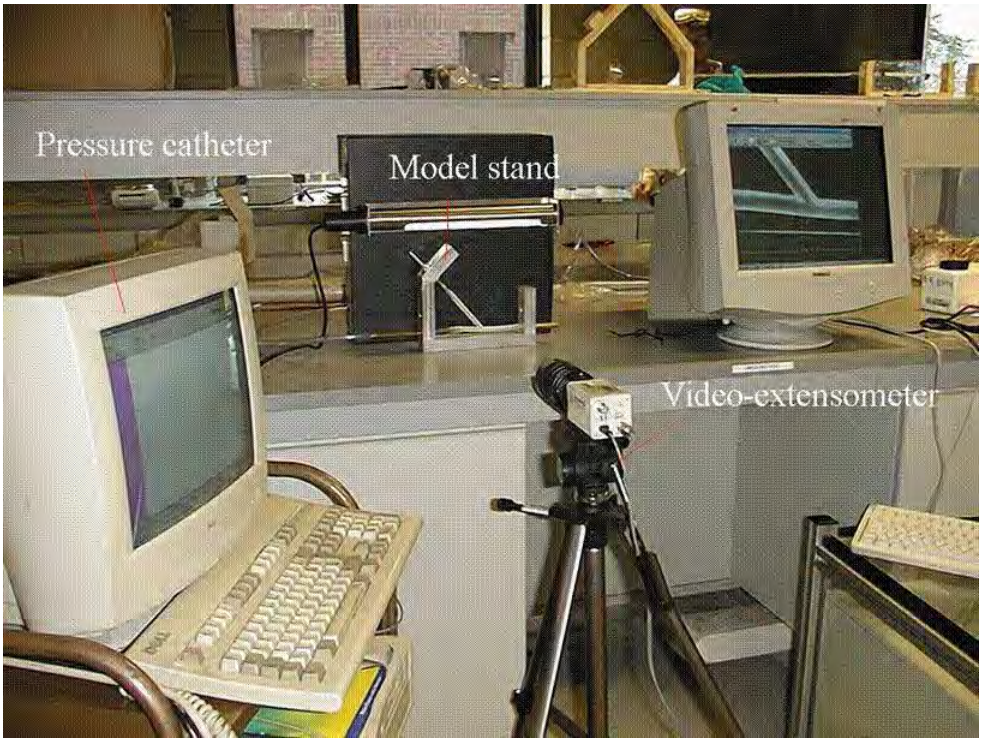

Figure 3.5: Laboratory Experimental Set-up

When determining and evaluating the reactions of the models it was essential to use accurate testing equipment and instrumentation, which could not influence the results obtained. Therefore this analysis was performed using a direct and non-contact optical measurement technique, the videoextensometer, which captured all model deformations in real-time during experiments, as can be viewed in Figure 3.5. The videoextensometer operates as a 'strain meter' by directly calculating the measured extension, by means of a change coupled device (CCD) camera, as a percentage of the original length. A bi-axial calibration was performed in order to enable actual distances between targets in two directions to be displayed and saved. In order to calibrate the videoextensometer, it was focused on a calibration ruler until a clear image was obtained and a known distance between two parameters was input. It was necessary to ensure that the focal distance then remained the same when obtaining results from the silicon models, thus assuring quantitative and qualitative accuracy.

The CCD camera was connected to a frame-grabber interface card fitted in a personal computer (PC) running on a Windows based operating platform. The camera was fixed to a tripod and focused on contrasting targets marked on the specimen. It was imperative that the distance between the camera and specimen remained constant during testing as any movement would have altered the image size which would, in turn, be erroneously interpreted by the software as a change in specimen size. Lighting had to be organised in such a manner that the specimen was illuminated at a constant level, against a dark background, during testing and this was achieved using an external light source placed immediately above the silicon model ensuring a constant level of light within the field of view.

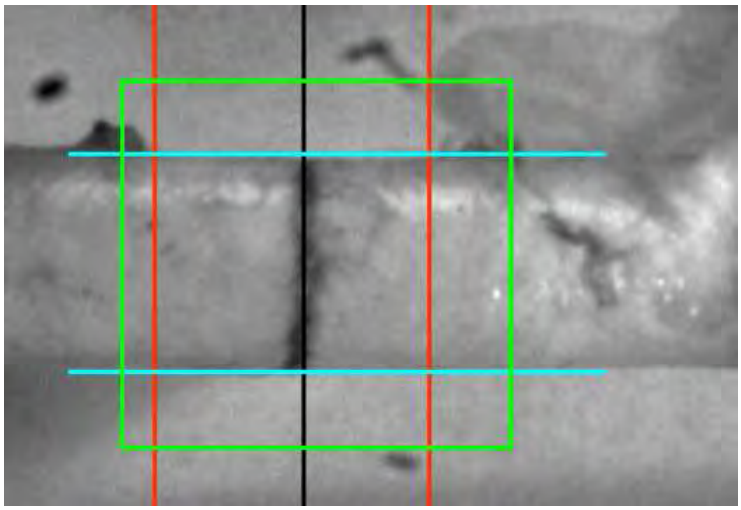

Figure 3.6: Straight section model showing viewing box (green) target lines (blue) and evaluation lines (red and black)

Straight-line targets were marked on the specimen for deflection measurements in the longitudinal direction and the specimen outline was used as specimen width targets for deflection measurements in the radial direction. These targets created the essential sharp and defined contrast difference to ensure correct automatic target recognition and tracking. Figure 3.6 shows a straight section model with the viewing box, target lines and evaluation lines clearly marked. During experiments the changes in the distances between the target lines were recorded within the area between the evaluation lines.

Experimental analysis entailed each of the aforementioned models being inflated to various static pressures between 75mmHg (10,000Pa) and 150mmHg (20,000Pa), in increments of 10mmHg, using a pneumatic supply from a mains air supply in the laboratory.

An attached air-regulating valve allowed a constant rate of air to be released thus maintaining a constant static pressure in the models at all times during testing. The pressure was recorded using a pressure catheter transducer. The catheter was an Ambulatory Oesophageal pH Recorder Type 2000-pH (Gaeltec, Scotland) and the transducer was a single sensor 6-pin gold plated Lemo insert in a light-weight machined nylon shell. Every 1/100th of a second the deflection measurements were saved automatically in an ASCII file on the attached PC. The measurements were recorded for an allotted time period at each pressure increment. In particular the area surrounding the junction of the 45° models was monitored closely.

All laboratory tests were repeated three fold, ensuring accurate and reproducible results could be consistently attained. The properties utilised for analysis of the silicon and finite element models can be viewed in Table 2.1. The material was assumed to be linear, homogeneous, isotropic and incompressible. Although Silicon is a non-linear material, at lower pressures a linear relationship can be assumed (Raghavan et al., 1996). The pressures applied in this validation study were relatively low and hence it was assumed that the linear relationship was not exceeded at pressures equivalent to low or normal blood pressures.

3.2 Finite Element Models

An integral part of this project was to compare the values of deflection measured experimentally to those predicted by finite element analysis. Hence accurate models, modelling parameters and material properties were required.

The dimensions of the models used in this study were based on the femoral artery and graft bifurcation (Fisher et al., 2003). The outside diameter of both vessels was 8mm, with a wall thickness of 1mm. The angle subtended between the artery and graft was 45° based on the angle practised by surgeons in operating theatres. The finite element models were generated in such a manner as to reflect the silicon models produced by the process detailed in the previous section.

The geometries were modelled in Pro-Engineer and then transferred directly to ProMechanica (STRUCTURE version 23.3) in order to analyse the effects of static pressure. In ProMechanica the models were immediately identified as solid models hence no further geometric changes were necessary to the homogenous arterial models. However the finite element models used for analysing ePTFE/Silicon bypass junctions required further changes. The graft section was stripped of its volume and the surface built back up in

ProMechanica. This was required as the arterial and bypass sections were assumed to be one entity by Promechanica thus preventing different material properties from being applied to the relevant sections. Applying Autogem automatically created a mesh on the solid model.

The representative solid models used the properties for silicon and ePTFE detailed in Table 2.1 to examine the effect of intramural pressure. The constraints applied to the models were dictated by the *in vivo* conditions experienced by the artery, hence the model was held rigid in all directions and a surface constraint entity was applied to the model as shown in Figure 3.7. To simulate the effects of blood pressure on the arterial walls, a face load was applied to the inner surface of the model from 75mmHg(10,000Pa) to 150mmHg(20,000Pa) in increments of 2,000Pa, i.e. uniform static pressure.

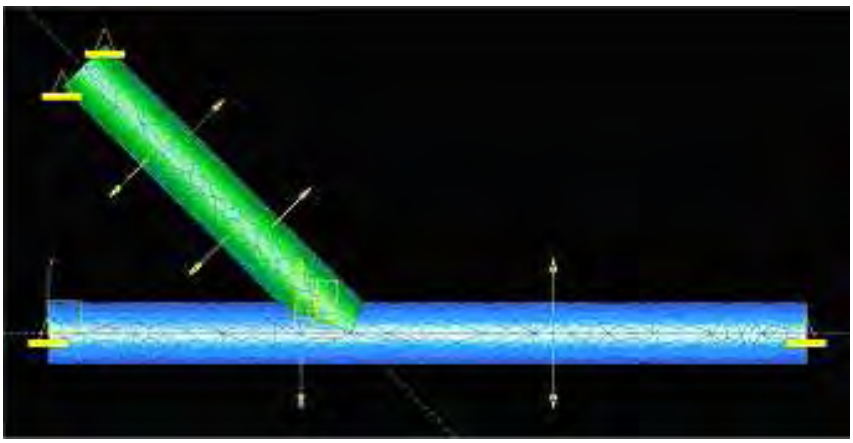

Figure 3.7: Finite element model with loads and constraints applied

The analysis used was set on a multipass, 2% convergence and polynomial order of nine. Discretisation of each model or region of interest resulted in a mesh of finite elements. The number of subdivisions depended on the accuracy required, a larger number resulted in greater accuracy but this required longer processing times and higher costs. A number of mesh densities were examined within this study in order to obtain the best balance between accuracy of results and processing time. Once the solver had complete its run, results were taken from the model using the fringe plot window and specific points of interest were queried for deflection and strain.

3.3 Experimental and FEA Results and Discussion

Deflection measurements of the laboratory models were recorded in both the longitudinal and radial directions. The changes associated with increased static pressure in the longitudinal direction were minimal, experimental models displayed a change of less than 3% strain and finite element models showed changes of less than 2.5% strain. However the radial strain in the various models ranged from 2% to 5% in the straight section models and from 4% to 18% in the 45° models depending on the presence of homologous or ePTFE graft materials. The radial strain at the toe of the distal junction, calculated from the experimental deflections, displays a similar trend and shows good numerical correlation with the finite element predictions under the same parameters of restraint and material properties. It is apparent from Figure 3.8 that the measurement technique is an accurate representation of what is occurring under varying static pressures.

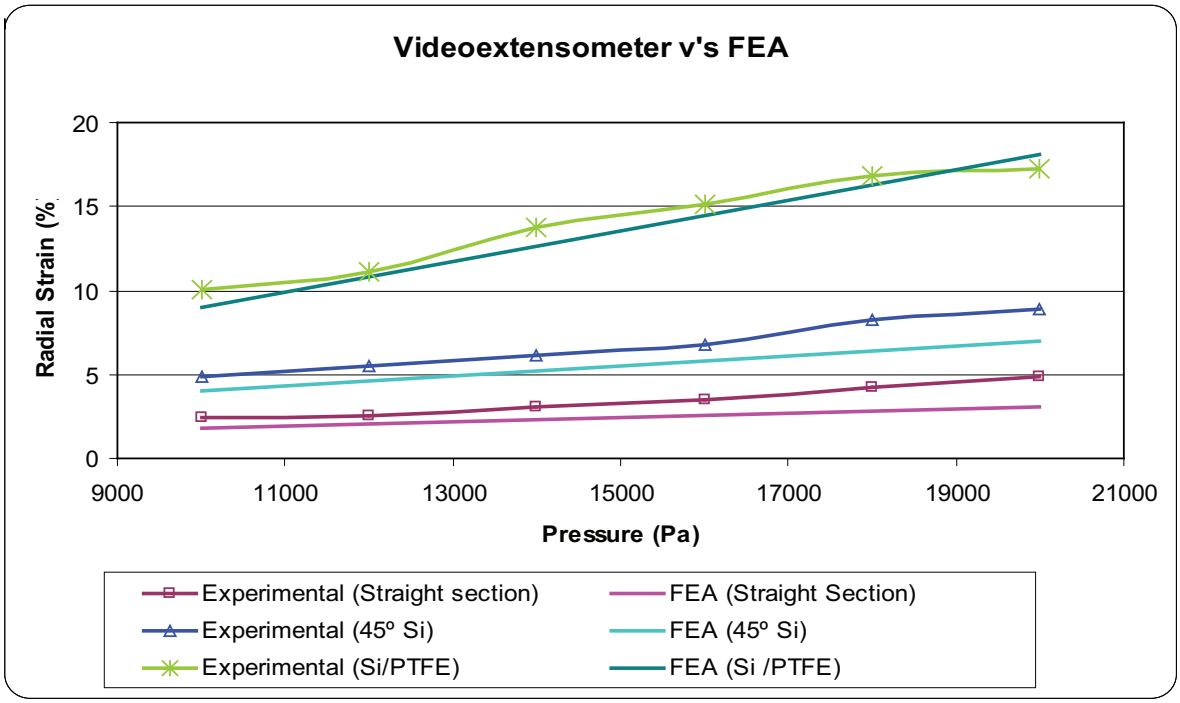

Figure 3.8: Experimental radial strain measured versus FEA predictions

Greater variations in the deflections were found to occur at higher pressures. It is believed that these variations occurred as at lower pressures silicon displays an initial linear elastic phase which mimics the elastin in arterial walls known to support arteries at pressures lower than 110mmHg (Raghavan et al., 1996) thus it is reasonable to use the silicon material as an artery tissue analogue at low or normal blood pressures. However at higher pressures the material can no longer be considered linear elastic and the strains recorded

in the radial direction, for each of the laboratory models in this study, showed increased variations and less linear behaviour at pressures above 120mmHg(16,000Pa). Furthermore at higher pressures the experimental set-up encountered problems in maintaining the seals at each of the air entry and exits of the models.

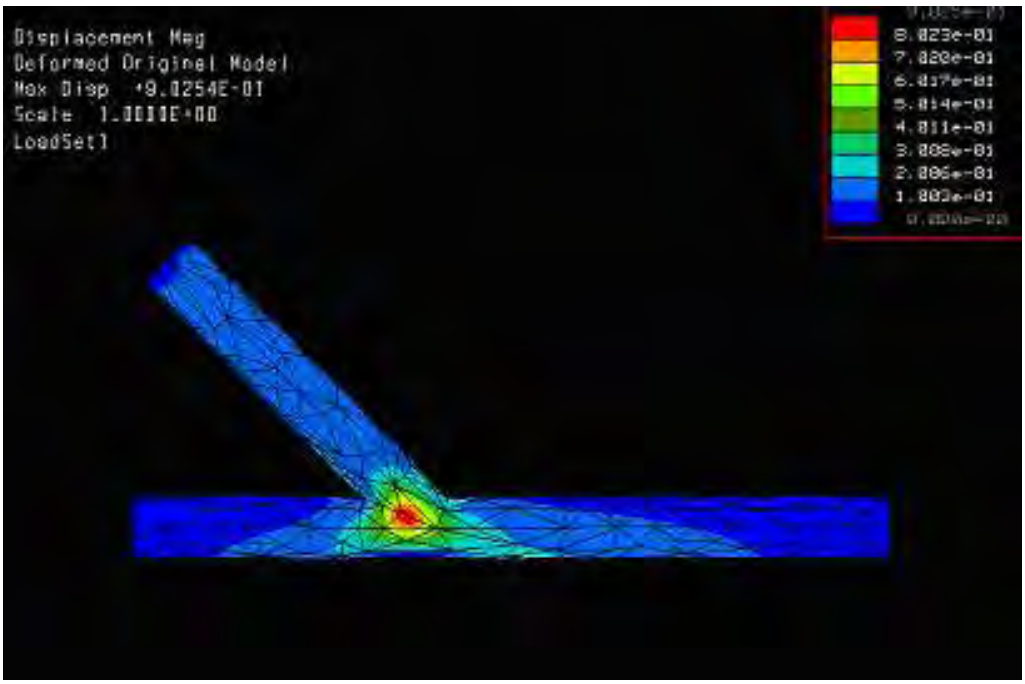

Figure 3.9: Displacement at the bifurcation subject to a pressure of 10000Pa

From the finite element models it was found that the location of greatest displacement occurred along the suture line as shown in Figure 3.9, however the greatest values of strain and stress were found to exist at the inner surface of the heel as shown in Figure 3.10, where it is believed that as the suture line bulges out under normal pressure the heel is dragged inwards. This bulging effect causes the circular cross section around the junction to become elliptical which is a greater energy configuration for the artery wall. It is believed that this shape change produces additional bending stresses in the wall and these bending stresses add to the tensile stresses on the inner surface.

The ePTFE grafted to the straight silicon tube exhibited deformation to a greater extent than the homogenous graft. In the region of the anastomosis the behaviour at the toe and heel is very similar however the deflections occurring at the heel are of slightly greater magnitude. It can be seen from the above finite element models that the intramural pressure induces the greatest strain at the suture line on the outer surface and at heel of the junction on the inner surface. The displacements at the heel, toe and bed increased with the introduction of the ePTFE compared to the homogenous silicon 45° branched model, displaying

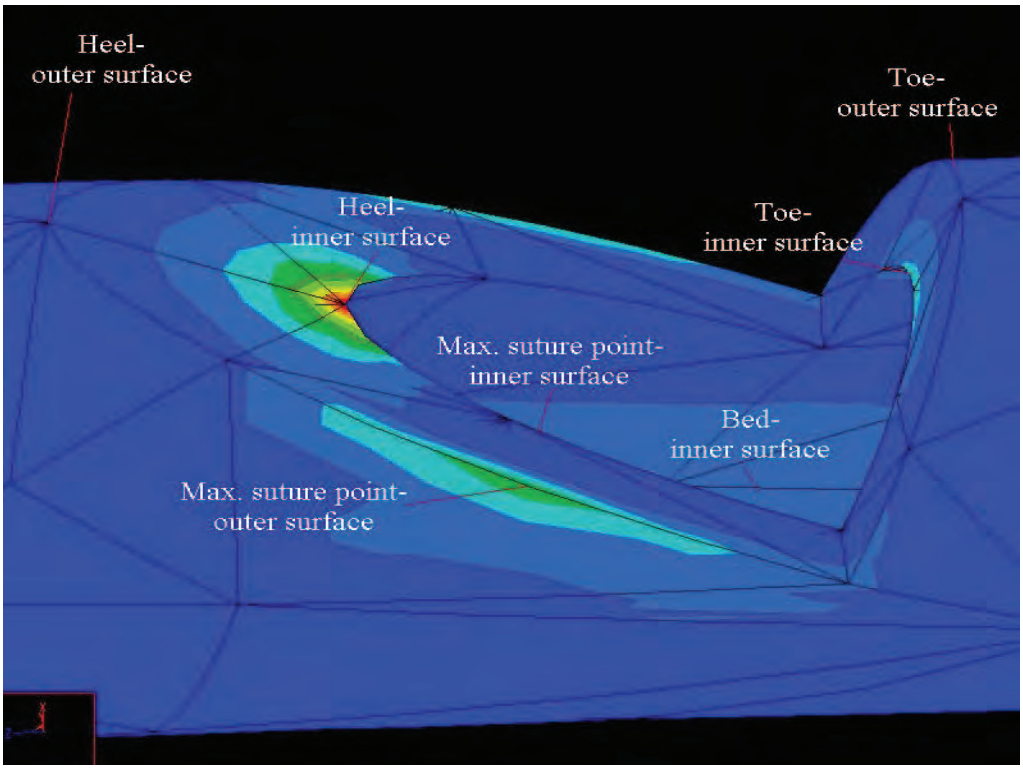

Figure 3.10: Strain at specific points surrounding the bifurcation

the phenomenon of compliance mismatch. The silicon/graft junction experienced strains up 6 times greater than that in the straight section and up to 3 times that of the homogenous 45° branched model. Furthermore a compressive, not tensile, strain was found to exist on the bed of the junction.

It can be concluded that as blood flow induces low wall shear stresses at the toe and high wall shear stresses at the heel of a bypass graft junction, whereas blood pressure induces high wall stress and increased wall deformation and strains at both of these locations, it appears logical that pressure-induced wall stress and not flow induced shear stress correlates with the locations of atherosclerotic lesions.

3.4 Summary

The above study was undertaken in order to show that the videoextensometer is an accurate measurement technique and that finite element analysis is a tool that can be employed to correctly predict the responses of arterial models subjected to internal pressures such as those experience by the human body under physiological conditions. A good correlation between the optical measurement technique and finite element analysis was found to exist at the static pressures being analysed, as shown in Figure 3.8, thus displaying the accuracy

of the optical measurement technique at varying pressures. Hence videoextensometry was selected as the measurement technique utilised for all surgical *in vivo* experiments detailed in the proceeding chapter.

Chapter 4

In Vivo Surgical Experiments and Finite Element Analysis

This chapter details the *in vivo* experiments undertaken during the course of this study. Specifically the procedures employed to carried out *in vivo* measurements of deflection following femoral bypass surgery and those associated with the production of finite element models are outlined. As many contradicting views have been reported regarding the efficacy of cuffs and patches, in the current study a conventional model was employed where by the graft material was connected directly to the host artery. Conventional models were employed as it is believed that the cuff's suggested do not sufficiently increase the patency of the graft in smaller arteries and secondly the surgeon did not employ any such cuff's or patches when bypassing smaller arteries such as the femoral artery.

4.1 Procedure for Surgical Measurements

In this section of the study the complete records of all patients undergoing femoral or femoropopliteal bypass surgery were reviewed prior to admittance into the study. Patients were regarded as suitable for the experimental measurements when no previous vascular reconstruction had been performed in the area above the femoral artery that may have had any altered haemodynamic effects on the newly introduced bypass. Four patients, aged between 51 and 72, were included in this study and had blood pressures ranging from normal, 114/73mmHg, to hypertensive, 160/67mmHg. All endovascular repairs were performed under either general or regional anaesthesia. Prior to all surgeries angiograms were taken of each patient in which the blockage could clearly be seen using a contrast

media injected into the blood stream. All surgical experiments were carried out over the period of one year and all bypass surgeries were performed by the same surgeon, under equivocal conditions at the Mid-Western Regional Hospital in Limerick, thus providing a level of consistency between all patients surgical procedures. All patients were informed of the nature of the experiments in advance of the surgery and all signed consent forms in order to take part in the study (See Appendix D). Ethical permission for the study was received from the University of Limericks Ethics Committee and the Mid-Western Regional hospital in order to perform this section of the study.

Once an artery has suffered sufficient blockage and it has been decided that a graft is required, a number of factors must be taken into considerations by the surgeon such as graft material, diameter, and anastomotic configuration. The radius of the artery is very important in determining both the viscous and inertial energy losses, hence the graft selected ought to be large enough to carry all the flow required at rest without a marked increase in pressure and it must be large enough to accommodate any increased flow likely to be required during exercise without a significant pressure drop.

The ideal material for the graft is native artery, however this is only plausible for short grafts. For longer grafts, such as is needed in the femoral artery, the ideal graft material is homogenous vein. The most commonly used vein is the saphenous vein as it is the longest vein in the body. The vein grafts have a high patency rate and the autologous vein is ideal as there is no immune response. However using a vein is a far more complex procedure as it must first be harvested and it involves three important steps when the vein/artery is outside the body in the operating theatre. Firstly a pressure must be kept on the vessel, secondly it must be kept in saline solution or blood at body temperature and finally a vasoactive agent must be added to it to protect the endothelium. However, often there is no autogenous vein available, due to it being removed in a previous procedure or being damaged or diseased. An autogenous vein is unavailable in 20-30% of first surgeries and in revision surgeries it is not available in 50-60% of cases hence prosthetic grafts must be employed (Gentile et al., 1998).

A videoextensometer was used to monitor the changes in deflections of the artery in both the radial and longitudinal directions during elective femoral or femoropopliteal surgery. A bi-axial calibration was performed, prior to each patient being monitored, in order to enable actual extension values between targets to be displayed and saved. The videoextensometer was purposely chosen for this study due to its non-invasive method of measurement, as can be seen in the surgical set up displayed in Figure 4.1, thus no possible

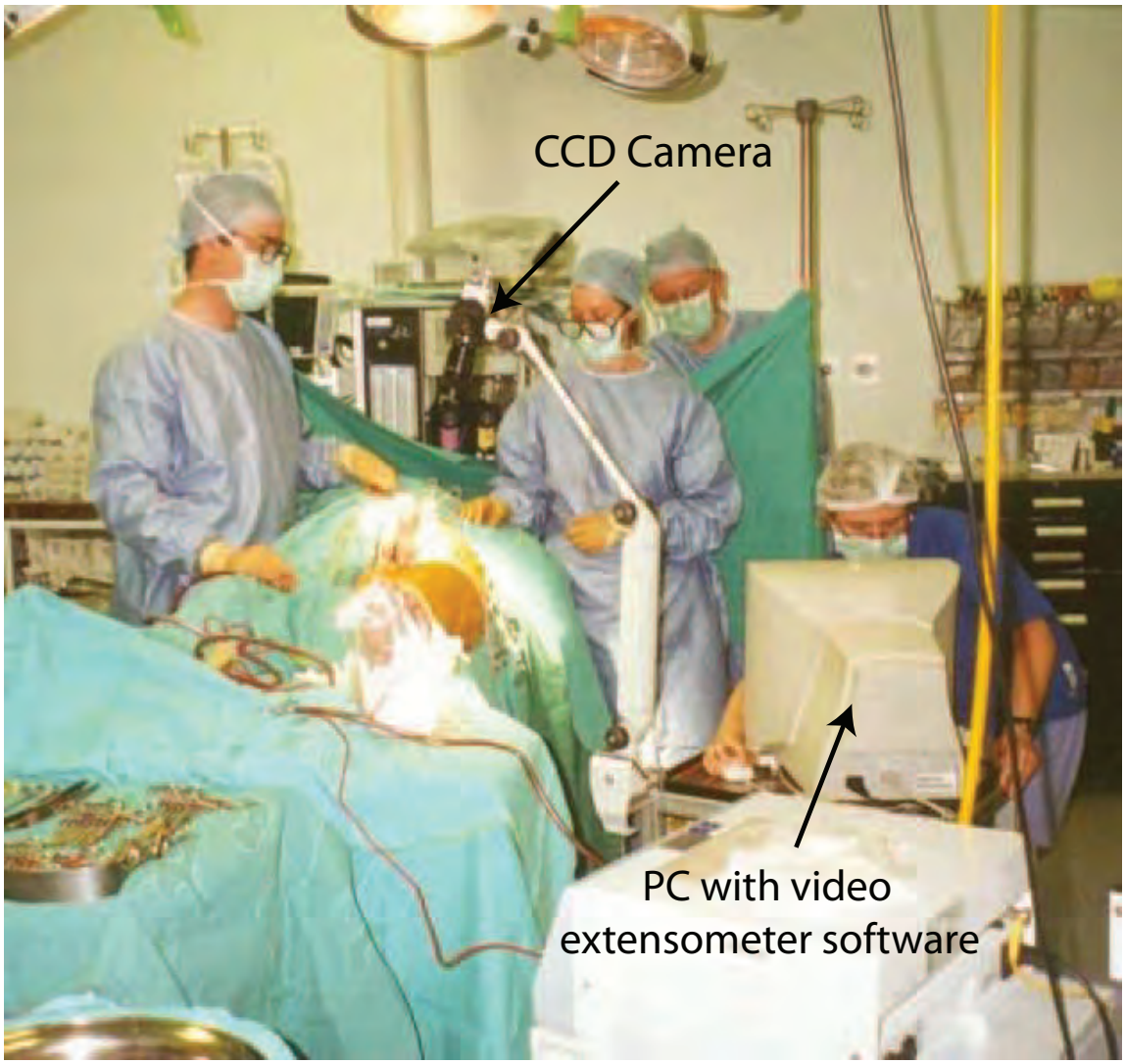

Figure 4.1: *In vivo* measurement set-up showing the CCD camera over the area of interest and the PC recording real time deformations.

adverse reactions could be experienced by the patient. Physical contact with the patient only occurred when the surgeon used a surgical pen to mark the artery thus enabling the CCD camera to pick up a colour change in order to measure deflections in a longitudinal direction. In the radial direction the artery outline was used as the target for deflection measurements, however difficulties arose as the colour of the artery and surrounding tissue were similar, as can be seen in Figure 4.2. In a number of patients this was overcome by placing a single white surgical swab at the side of the artery in order to facilitate a temporary colour change. Deflection measurements were taken at the toe of the distal junctions post surgery. The toe of the junction was selected for monitoring as this was the location most visually accessible and could be easily analysed for each patient thus allowing direct comparison between patients. The patients blood pressure was also periodically monitored

during surgery.

Figure 4.2: Plaque and clot blocked femoral artery

A number of the patients monitored had an ePTFE graft inserted whilst others had a vein harvested for use as the bypass material. The criteria for the surgeon selecting a synthetic or autologous material to use for the bypass depended solely on the availability of a suitable vein, the patients age and the patients present state of health. If the surgeon deemed that the patient could not effectively undergo two surgeries, one procedure to harvest the vein and a second to attach the bypass, then an ePTFE graft was selected. However if the patient was younger, in relatively stable health and did not suffer from any other illnesses, and surgery for harvesting a vein was possible, this option was the chosen due to its increased patency.

It must be noted that when measurements were taken using the videoextensometer, the external diameter of the artery was measured and the goal of this analysis was to examine the effect of bypass grafts on the endothelial cell lining on the inner arterial surface. However detailed in the following finite element analysis it is shown that the measurements of deflections of the outer surface can be related to those occurring on the inner surface.

Furthermore the *in vivo* conditions were slightly altered, namely the exposure of arteries eliminated the constraint imparted on it by surrounding tissues. Hence the arteries may have been capable of distending themselves to a greater extent than under normal physiological conditions. Thus attempts were also made to monitor deflections of the artery post surgery using Duplex ultrasound.

4.2 Modelling the artery using Finite Element Analysis

A number of assumptions were employed within this analysis. As the arterial wall is a macroscopically inhomogeneous material, therefore it is an uncertain assumption that the material is isotropic, however much experimental evidence indicates that under in vivo conditions this is approximately true (Nichols & O'Rourke, 1998). Arteries subjected to pressure experience both circumferential and longitudinal distention with almost no twisting of the vessel so that the shearing strains are minimal. Hence in the arterial models it can be assumed all net strains are oriented along the longitudinal, circumferential and radial directions. Arterial motion *in vivo* occurs primarily in the circumferential direction with very small movements in the longitudinal direction. Thus the vessel walls were considered both incompressible and isotropic. These conditions dictate that the vessel remains at constant axial length on pressurisation. The forces in a system of solid objects were analysed under the presumption that the solid objects themselves are rigid bodies with no particular properties of their own. There was no distinction between the properties associated with the tunican intima, media and adventitia.

Table 2.1 illustrates the properties that are known for the required analysis. However as can be clearly seen a number of vital properties are still required, such as those for diseased arteries, as a result of intimal hyperplasia or atherosclerosis, and the specific properties relating to each layer within the artery.

All models were created in ProEngineer and subsequently imported into MSC Marc. The models although idealised contained a more realistic geometry than those used in the validation study. The junction associated with the 45° models were created such a manner that in the region of the ostia the artery was opened up and a cylindrical bypass attached. Similar to surgical procedures no portion of the artery is removed it is simply opened up and a bypass sutured to it. This resulted in the arterial junction shown in Figure 4.3. Reflective symmetry was used as the geometry and boundary conditions were equivalent across the mid-plane.

The element type chosen for the straight section was element type 21, a hexagonal element with 20 nodes. This element type gives accurate results for the material type used in this analysis as it allowed for an accurate representation of the strain fields in elastic analyses. There were 2040 elements in the final mesh for the straight tube model. A number of adjustments were made to the model before meshing was possible. It was checked for surface loops and one division was applied to each curve. The curve divisions

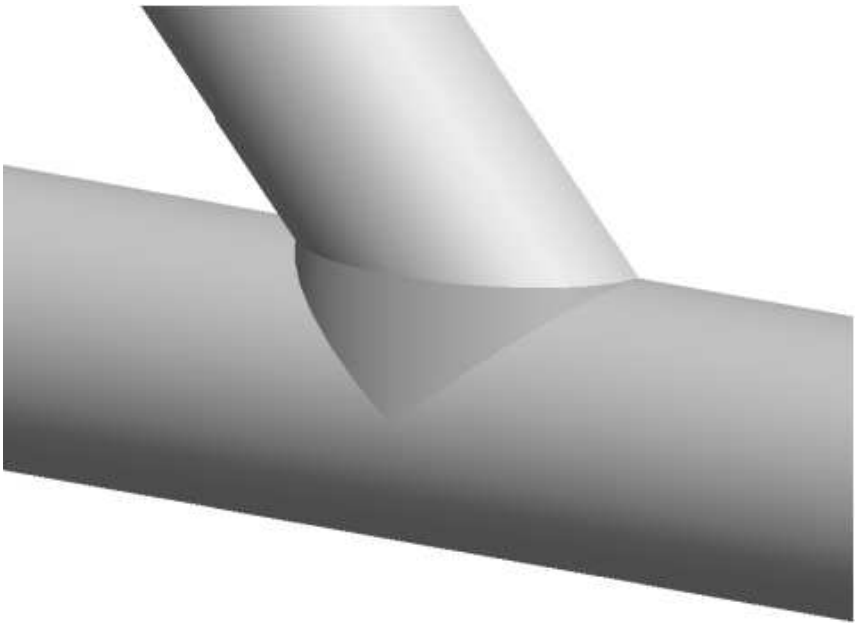

Figure 4.3: FEA modelled graft junction

were assigned a tolerance of 0.005.

A 2D planar automesh was used, beginning with a surface mesh followed by the addition of a solid meshing. This involved three basic steps: cleaning the geometry, applying the surface mesh, applying the solid mesh. The geometry was cleaned to ensure there were no open surfaces or curves, hence the model would be fully and accurately meshed. The surface mesh incorporated applying curve divisions along selected edges of the model, denoting a fixed length and matching the curves divisions to each other. As MSC Marc uses h element types for analysis, to improve the accuracy of the results the mesh was manually refined around the area of interest. This was performed by reapplying the curve divisions, giving a fixed length of 0.1 to the edges surrounding the anastomosis resulting in a model with 85527 elements. The model was then solid meshed. The 'tri-mesh' generator was chosen. This created triangular elements on the surface, thus when the 3D mesh was applied a 'tet-mesh' option was taken. The element type used in the meshing of the standard 45° model was element type 136 with 10 nodes. This element is particularly accurate for strain in elastic analysis and this element had the capacity to work with the updated Lagrangian procedure. The updated Lagrangian procedure was chosen due to its accuracy of strain analysis. To simulate the effects of blood pressure on the arterial models a face load was applied to the faces on the inner surfaces. The performance of the models were examined in MARC under deformation and total strain.

Although it is believed that the sutures and resulting surgical injury may cause endothelial cell damage and/or proliferation, for this study it is assumed that the effects of these cease in advance of restenosis occurring at the junction hence they were disregarded in this analysis.

4.3 Surgical Results and Discussion

A total of four patients were chosen for inclusion in this study. Although a greater number of patients were monitored during surgery, it was discovered upon commencement of the procedure that an additional stent had to be placed in the illiac arteries thus altering the haemodynamic conditions above the area of interest that could not be quantified. Of the four patients included two patients had a ePTFE graft inserted and two had a vein harvested for use as the bypass.

Upon removal of the clamps post attachment of the grafts, it was observed that the ePTFE grafts, which are perfectly circular stiff tubes when homogenously pressurised, attained a slight elliptic component following implantation. This indicated to the author that the material mismatch between the graft and host artery altered the distribution of the pressure induced strain such a change was not apparent in the patients in which a vein was employed.

The deflections of the distal junction of the arteries were all examined at identical locations. Following introduction of the femoral bypass graft, deformations were measured in the longitudinal direction at the toe of the junction and in the radial direction at the midpoint of the ostia. The deflections were converted to strains and the resulting ranges of *in vivo* longitudinal and radial strains recorded on the outer surface for each of the patients can be seen in Figure 4.4 and Figure 4.5. In both graphs the patients with ePTFE bypass grafts are referenced as patients 1 and 3 (blue lines). Patients 2 and 4 (red lines) had autologous veins harvested, namely the saphenous vein, for use as a bypass.

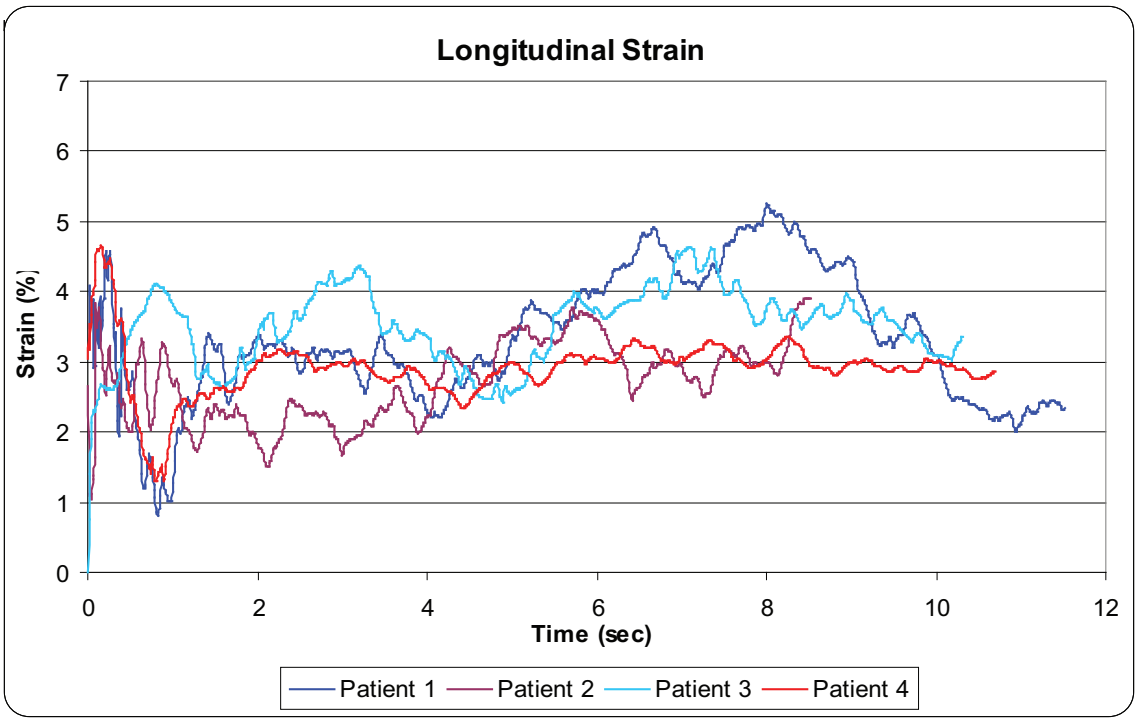

Figure 4.4: Longitudinal strain experienced by each patient

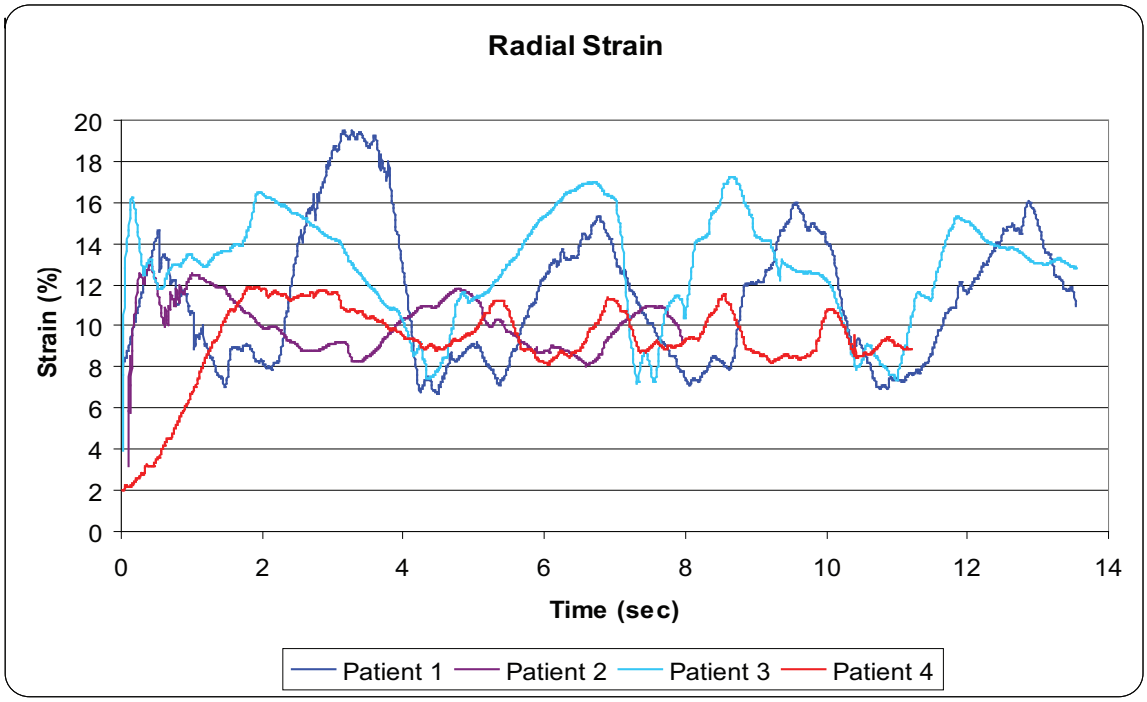

Figure 4.5: Radial strain experienced by each patient

Although only four patients were analysed for this section of the study a clear trend is evident in Figure 4.4 and Figure 4.5. When a vein was employed as the bypass material not only was there a marked decrease in the magnitude of deflection but also the amplitude of deflection in both the radial and longitudinal directions were greatly reduced. The reduced strain experienced by the vein grafts should lead to increased patency however the cost to the patient is an extended recovery period due to the intricate surgery required to harvest the vein.

In Figure 4.4 it can be seen that the pressure induced strain in the longitudinal direction varies only slightly depending on the material used in the bypass configuration. Furthermore it can be observed that when a vein is utilised a pulsation of approximately 70 beats per minute is evident, however this is not apparent when ePTFE is employed and the pulsation of the artery appears to be far more random.

In the radial direction, Figure 4.5, both the magnitude and amplitude of deflections at the toe is greatly increased upon the use of ePTFE. Another outcome of note is that the arteries no longer appear to contract radially with the same frequency as the heart is pumping.

Attempts were also made to monitor patients post surgery using Duplex Ultrasound to measure the outer diameter of the artery. Patients were monitored immediately post surgery and at 12, 24 and 36 months however the use of duplex ultrasound encountered problems due to patient suitability. One of the contributing factors to atherosclerosis is weight and the majority of patients who partook in this study were clinically overweight or obese. This resulted in a difficulty in obtaining verifiable results of either a qualitative or quantitative nature due to thick layers of fat and muscle between the location of the ultrasound wand on the skin and the artery of interest. Similarly Sorensen et al. (2003) found that the effect of structured, postoperative surveillance programs with conventional ultrasound sonography is controversial since it is not clear whether ultrasound technology is helpful to reliably detect failing femoropopliteal prosthetic grafts.

Furthermore the physical properties of the most widely used grafts in this position, ePTFE prostheses, make if difficult to obtain adequate acoustic penetration of the initially air filled interstices in the microporous node-fibril structure of the ePTFE material. The compliance of the PTFE grafts is very small (around 1.2% per mmHg x 10^{-2}, Sorensen et al. (2003)) hence differential detections of position changes under the various heart cycle phases were not demonstrable. Due to the lack of appropriate non-invasive techniques, the biomechanical and haemodymanic properties of these grafts after implantation are poorly

developed.

In this study finite element models analysed in MSC Marc and based on the properties indicated in Table 2.1, had various pressures were applied from 75mmHg to 160mmHg in which all materials were considered homogeneous, isotropic and incompressible.

It was found that the finite element models did not give the same values of deflection as those recorded in surgery for the same values of pressure experienced by each patient. It is believed that this variation is due to the fact that the FEA models were idealised and exact properties of each diseased artery and the autologous graft materials were not known. However although the models do not supply quantitative data for comparison purposes they do provide valuable qualitative data regarding the locations of greatest strain and the strain gradient occurring through the artery wall itself. The locations of maximum strain were consistent regardless of the pressure applied of up to 160 mmHg (21,333Pa). The greatest strain was found to occur at the suture line, heel, toe and bed as can be seen in Figure 4.6 and Figure 4.7.

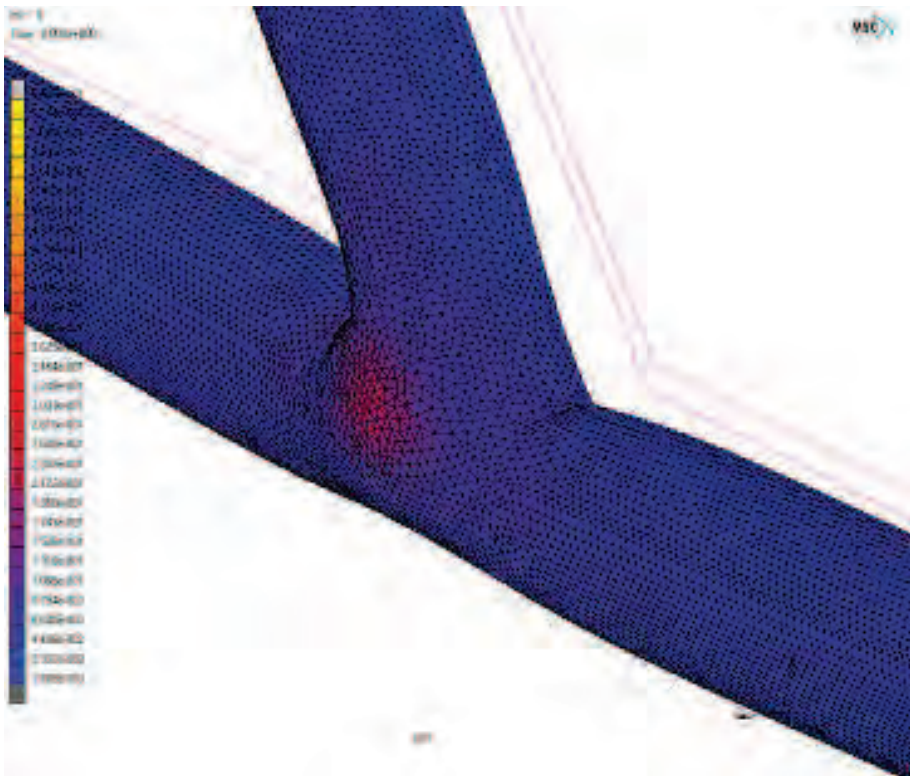

Figure 4.6: Strain on the outer surface of the arterial model

The yellow and red areas relate to zones of the highest strain and the blue indicates low strain. Models with an artificial graft experience higher strains in both directions, as was also found in surgery. The results from the finite element models concluded that the

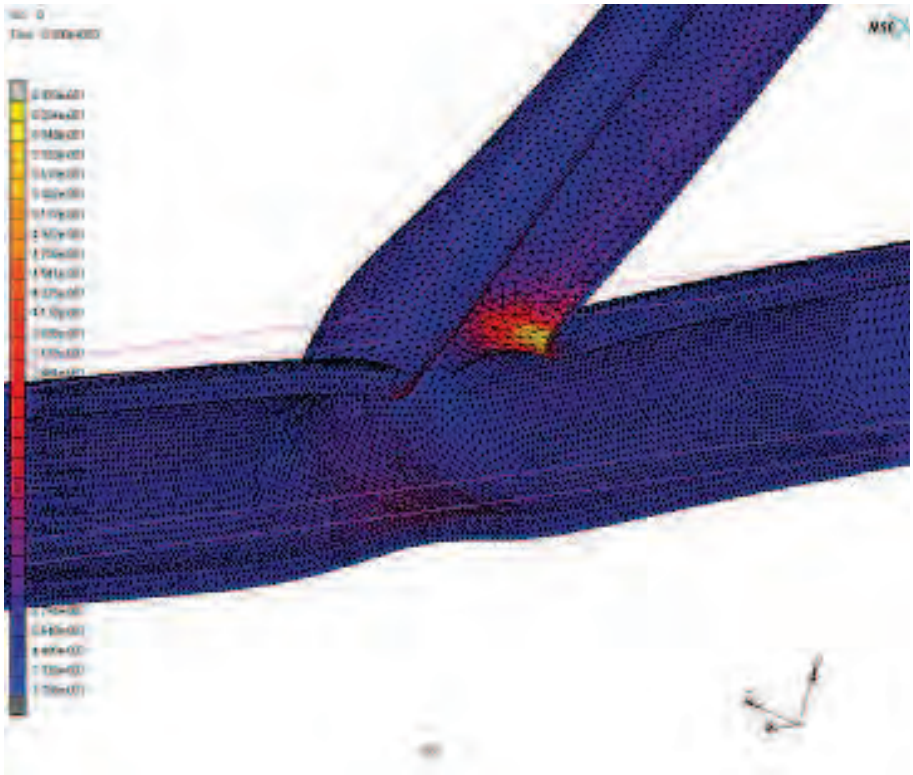

Figure 4.7: Strain on the inner surface of the arterial model

introduction of a bypass graft produced strains of up to 7 times greater than those usually experienced by the artery under the same conditions of pressure.

The primary goal of the finite element models was to predict the strains experienced by the endothelial cells on the inner surface of the artery when the strains on the outer surface were known. In order to find the strain/deflection gradient between the inner and outer surfaces a node path was created along the length of the inner artery wall and another was created along the length of the outer artery wall at specific areas of interest, namely the bed and suture line (incorporating the heel and toe) of the anastomosis. At each node the deflections in the x, y and z directions were recorded. The results can be viewed in Figures 4.8 and 4.9.

As illustrated in these plots there is a large gradient around the area of the anastomosis however there is not a substantial quantitative difference in the relative values between the inner and outer surfaces at a specific location. The maximum difference in deflection between the inner and outer surfaces at any point was 0.14mm. Thus with almost negligent differences in the magnitude of deformations existing between the inner and outer surfaces of the arterial models it was concluded that the optical measurements of deflection recorded *in vivo* for the outer surface of the artery were an accurate indication of the deformations

experienced by the inner endothelial cell surface of the artery.

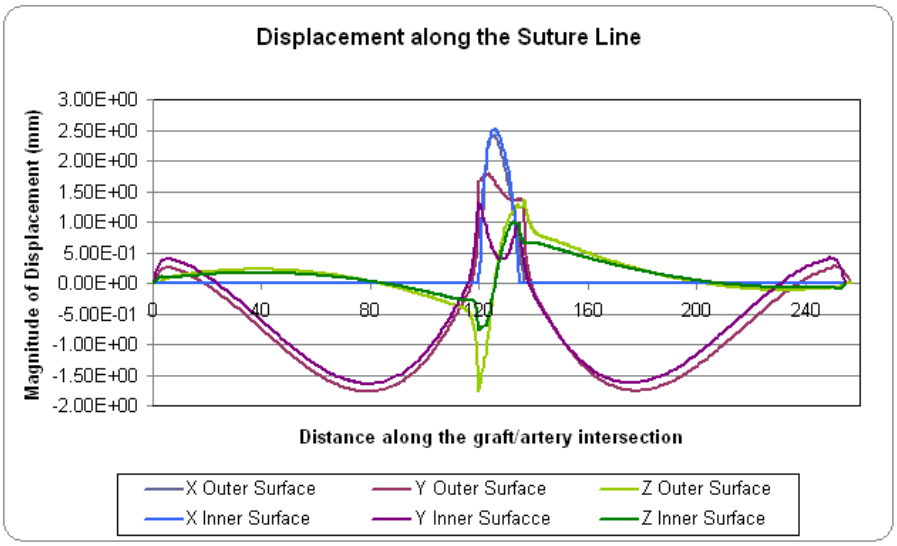

Figure 4.8: Displacement at the suture line subject to a pressure of 140mmHg

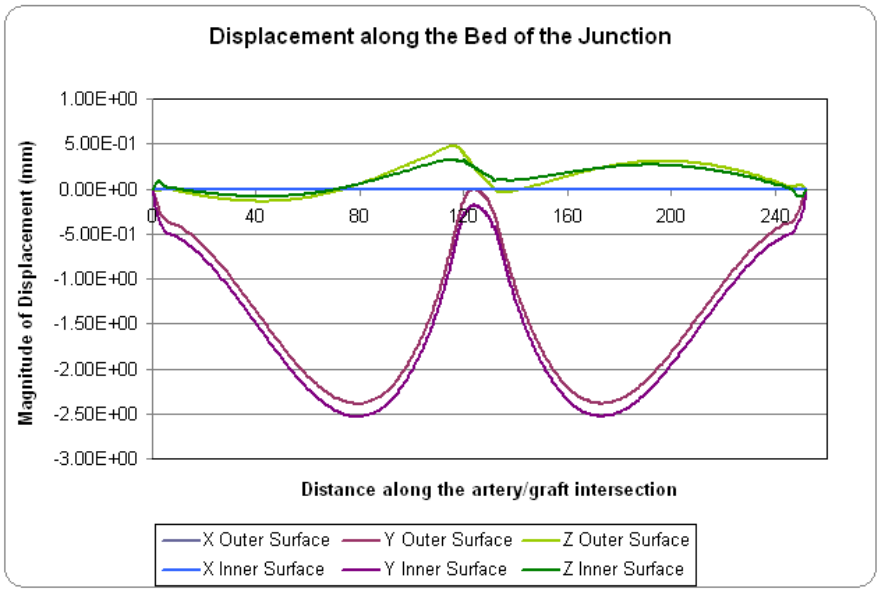

Figure 4.9: Displacement at the bed of the bifurcation subject to a pressure of 140mmHg

Although the strain was higher on the sutures at the heel than at the toe of a standard anastomosis, as can be seen in Figure 4.7, caution must be taken in correlating these differences. In the analysis carried out for this study the difference may be due to concentrations caused by the sharp geometries used in the generation of idealised models. It is possible that this acute angle at the heel of the junction caused a stress concentration point, it can be assumed that if this edge were more rounded the there would be a reduction in the stress concentration but that the strain would still increase along the wall but the peak would be lower.

It can clearly be seen from Figure 4.6 and Figure 4.7 that the intramural pressure induces the greatest strain at the heel of the junction. This is also a common region of intimal hyperplasia. In fact the regions of higher strain due to pressure co-locate with the known sites of cardiovascular disease formation. Increased pressure induces stretching of the arterial walls which in turn increases strain experienced by the endothelium. It is proposed that these strains give rise to responses such as LDL accumulation and changes in proliferation, apoptosis and tight junction configurations thus contributing to atherosclerosis and leading to the growth of intimal hyperplasia.

4.4 Summary

Patients with an artificial graft experience higher strain in both radial and longitudinal directions. Finite element analysis predicted that the introduction of a bypass graft produced strains of up to seven times greater than those usually experienced by the artery. Surgical measurements showed similar increases, as presented in Figures 4.4 and 4.5. From the analysis to date it can be concluded that the post surgery locations of high stress values correspond to the areas that have a preference for the pathogenesis of atherosclerosis. It is this correlation between the location of atherosclerotic lesions in the artery and the stress concentrations induced by intramural pressure that indicates the role of mechanical stress to the disease. Furthermore the *in vivo* experiments provide valuable qualitative and quantitative strain ranges occurring post introduction of a bypass graft in the femoral artery. Hence these ranges were employed to accurately monitor the reactions of endothelial cells *in vitro*, which it is believed that when damaged may be the precursor for the onset of atherosclerosis and restenosis of bypass grafts.

Chapter 5

In Vitro Cell Culture Experiments

This section of the study examines the responses of endothelial cells to the strains that were found to exist following femoral bypass surgery. For thoroughness and comparative purposes cells were not only examined under the specified conditions of strain but also under laminar and low shear conditions. All tests were carried out *in vitro* in a sterile environment. All assays used were initially optimised and details of the procedures, following optimisation, can be found in Appendix E.

5.1 Introduction

Cell culture studies were initiated in order to examine the response of human aortic endothelial cells to increased intramural pressure and the effects of blood flow. Given the importance of mechanical forces in regulating vascular haemostasis, the ability of cyclic strain to alter the permeability of endothelial cells was investigated as well as analysing alterations in cell apoptosis, necrosis and proliferation in human aortic endothelial cells when subjected to the strains found to exist during earlier *in vivo* experiments. This chapter also examines the effect of cyclic strain and flow on, the tight junction protein, ZO-1 and actin realignment.

In a study performed by Crawford & Blankenhorn (1991) it was suggested that insufficient oxygen could act as a trigger for atherogenesis. A sign of early atherosclerosis is the accumulation of high molecular weight lipoproteins within that arterial intima. This abnormal accumulation implies that mass transport between the blood and the artery wall plays a role in the development of atherosclerotic lesions/plaque. It is not clear however, if mass transport abnormalities are themselves atherogenic or whether lipoprotein accumulation is

secondary to other primary atherogenic processes (Ethier, 2002).

Vascular pathologies associated with altered vessel haemodynamic loading frequently correlate with compromised endothelial barrier integrity (Harhaj & Antonetti, 2004; van Nieuw Amerongen & van Hinsbergh, 2002; Tinsley et al., 2004) the present study hypothesises a direct link between pressure induced strain and endothelial cell permeability.

Barrier function is preserved by the regulation of tight junctions, composed of transmembrane proteins occludin, ZO-1 and a complex network of additional proteins, in addition to adherens protein complexes, between adjacent endothelial cells. The goal of all endothelial cell responses is to keep the integrity of intercellular junctions and prevent endothelial cells from hydrodynamic injury and/or detachment (Weinbaum & Chien, 1993). In a recent study by Katsuno et al. (2008) zonula occludens were knockout in mice leading to apotptosis of embryonic cells. It was concluded that ZO-1 may be functionally important for cell remodeling and tissue organization in both the embryonic and extraembryonic regions.

ZO-1 is an important component found in the tight junctions of all endothelial cells. It has binding sites for many cellular proteins via multiple protein-binding domains. Of utmost importance is the fact that ZO-1 co-sediments with F-actin thus an association between endothelial permeability and haemodynamic stimuli is established, as tight junction components are closely coupled to the haemodynamically responsive actin cytoskeleton (Fanning et al., 1998; McCue et al., 2004). It is plausible therefore that force-dependent modulation of tight junction assembly is a highly likely process, thus the link between barrier function and hemodynamic and mechanical forces is investigated in the present study due to the evidence of compromised barrier function in many disease states.

Actin filaments are composed of two intertwined actin chains of approximately 6nm in diameter. They are responsible for resisting tension and maintaining cellular shape. Thus when endothelial cells are stained actin provides clear images of cell shape changes following exposure to mechanostimuli. Fluorescent derivatives of phalloidin are used for investigating the distribution of F-actin in cells. Rhodamine phalloidin is the most commonly used F-actin stain. The red fluorescent probe binds to F-actin with nanomolar affinity. It is highly photostable thus allowing the visualising of actin filaments in fixed cells following in vitro studies.

It is believed that both flow and pressure effect the functionality of cells however it is the authors belief that pressure has a greater effect than flow on altered endothelial cell functionality. The following section details the methods employed to subject endothelial

cells to various conditions of flow and pressure.

5.2 Methods for the Mechanostimulus of Cells

Numerous apparatuses have been devised for the purpose of the mechanostimulus of cells. Of primary interest in this study are the methods employed to apply flow induced shear or pressure induced strain to adherent cells.

A number of configurations have been employed in previous studies in order to induce shear on cell surfaces. Firstly there is the cone-and-plate system (Dewey Jr, 1984; Hermann et al., 1997). In this system a rotation is imposed about the axis of a cone which is oriented perpendicular to the surface of a flat plate. This system is capable of achieving homogeneous fluid shear on both the cone and plate surfaces.

The second principal configuration is the parallel plate flow chamber. In this system a pressure differential is created between two openings at opposite ends of a chamber, thus inducing uniform laminar flow to develop across the surface of the cultured cells. The pressure differential has been created by both gravity heads and active pumps. (Levesque & Nerem, 1985; Tseng et al., 1995; Kuijper et al., 1996).

Other more specialised flow configurations have been developed capable of imparting shear stress transients of up to 800 dynes/cm^2 (LaPlaca & Thibault, 1997). A further quantified approach has been the use of orbital shakers (Pearce et al., 1996) for which a dimensionally based estimate of maximum shear stress can be calculated depending on the rotational speed of the orbital shaker. Orbital shakers were employed for the current study due to their ease of use and availability.

The first flexible-bottomed circular cell culture plates designed for mechanostimulus work were developed by Banes et al. (1985). The initial design stretched the substrate downwards using a vacuum system hence imparting a strain onto the cultured cells. Due to this systems programmability and its ease of set-up and operation, it lent itself to a broad range of mechanostimulus applications. However flaws became apparent in that the substrate in the center distended to a greater extent than that at the edges.

A number of engineering studies were completed in order to characterise the performance of this new vacuum controlled Flexercell® system (Brown, 2000). Finite Element Analysis of the substrate anisotropy, heterogeneity, hyperelasticity and inhomogeneity were performed (Gilbert et al., 1994; Brown et al., 1998). As a result of these studies

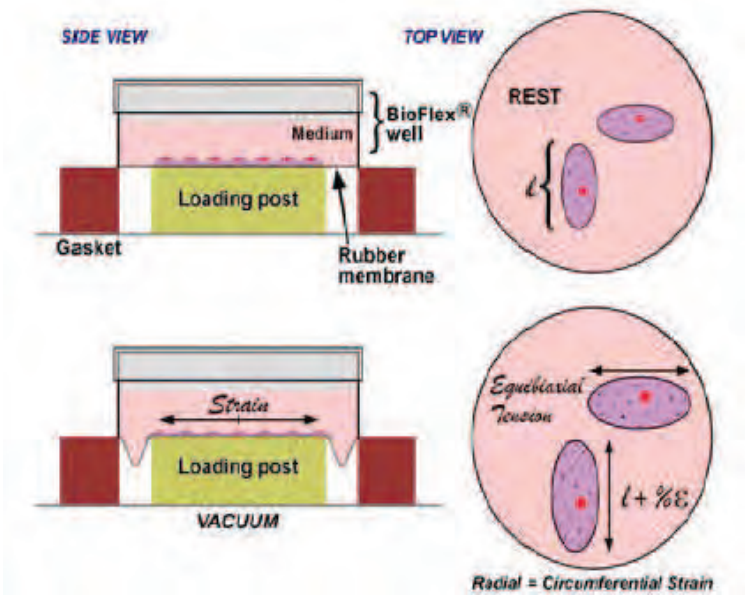

Figure 5.1: Schematic of the Bioflex® plate (Dunn Labortechnik, 2009).

modifications to the system were made which reduced the thickness and increased the diameter of the substrate. Furthermore a loading post was introduced in the centre of the substrate in order to ensure constant radial strain was applied across the substrate as can be seen in Figure 5.1. The Flexercell® system was employed for all strain experiments in the current study as the operator could control the vacuum magnitude, input waveform and frequency. Furthermore the system provides radial strain homogeneity and can be calibrated using the aforementioned videoextensometer prior to the commencement of all tests.

5.3 Culture Conditions

All tissue culture manipulations were carried out under clean, sterile conditions using a laminar flow hood (Holden Laminar Flow Unit - class 2 downflow recirculating, with UV light). Anything introduced into the culture vessels was either autoclaved or filter (0.2 μm) sterilised. All cells were maintained in a humidified incubator at 37$^{\circ}C$ with 95% air and 5% CO_2 which was controlled by a gas analyser. In order to prevent contamination of the cultured endothelial cells, it was essential that any surface in contact with them or the cell culture medium be sterile. Ethanol was used for this purpose. Cells were monitored daily and cell morphology change was assessed using an Olympus CKX31 inverted phase contrast microscope.

The principal advantage of employing cell culture studies is the consistency and reproducibility of results which can be obtained from a specific type of cell of a homogenous population. Additionally, cell culture techniques contribute to a greater understanding of the effects of a particular compound on a specific cell type and routine tests are far less expensive in cell culture than in whole animals. However, the primary disadvantage of cell culture is that, after a period of continuous growth, cell characteristics can change and may be significantly different from those that are highly differentiated *in vivo* where growth has ceased. Thus all tests were performed at low passage numbers during the course of this study.

5.3.1 Culturing Process

Cryopreserved passage 2 differentiated human aortic endothelial cells (HAEC's) were obtained from Cambrex BioScience UK. HAECs are a strongly adherent cell line forming a confluent contact-inhibited monolayer with a distinct cobblestone morphology. The media was supplemented with 2% FBS (foetal bovine serum) and an isotonic solution of nutrients including amino acids, carbohydrate energy sources, vitamins, salts and bicarbonate for buffering (hydrocortisone, hFGF-B, VEGF, R3-IGF-1, ascorbic acid, heparin, hEGF and GA-1000). All types of medium provide serum, which should be applied heat-inactivated to avoid the possibility of complement-mediated lysis of cultured cells. The media was also supplemented with 5ml penicillin-streptomycin to discourage the growth of microorganisms.

The endothelial cells were grown to 80% confluence in tissue culture grade flasks (T75), growth was ensured by replenishing media every other day. As endothelial cells are adherent cells, trypsinisation was required for their subculture. In brief the cells were subcultured by aspirating the spent medium, leaving the cells adhered to the bottom of a flask. The cells were subcultured by initially rinsing them with Hanks Balanced Salt Solution (HBSS), as the medium contains complex proteins that neutralise the trypsin. The cells were then covered with trypsin/ethylenediamene tetracetic acid (trypsin/EDTA) solution and incubated at $37°C$ for 5 minutes. The cells were examined microscopically until they were rounded up, but not fully detached. The flask was gently tapped to remove the cells from the growth surface and trypsin neutralizing solution was added. Finally the flasks were again rinsed with HBSS to collect residual cells and the detached cells were centrifuged at 1000 x g for 5 minutes to pellet the cells (Centrifuge EBA8, Hettich, Germany). The pellets of cells was

were resuspended in growth media or freeze media, and either split at a 1:3 ratio for experiments or cryopreserved. A step by step description of the culturing process is available in Appendix E.3.

5.3.2 Cell Counts

Following trypsinisation the number of trypsinated adherent cells were estimated using a brightline haemocytometer. Cell counts were made using a trans-illuminated microscope thus ensuring uniform suspension and volume dispensed into new culture vessels. To distinguish between viable and non-viable cells on the haemocytometer, trypan blue staining was employed. Live cells can exclude the trypan blue stain, leaving them with a normal appearance under the microscope. Dead cells however take up the stain making them appear blue. 20 ml of trypan blue was added to 100 ml of cell suspension and incubated at room temperature for 2 min. Following this 20 μl of the suspension was added to the counting chamber of the haemocytometer and visualized under phase contrast microscopy. The number of viable cells was calculated according to the equation:

Average cell no. x 1.2 (dilution factor) x 1x10^4 *(area under coverslip) = Viable cells/ml*

Equation 1

5.3.3 Freezing and Thawing of Cells

Cells were frozen and stored in liquid nitrogen. Medium, containing serum and dimethylsuphoxide (DMSO) was employed during the freeing process hence the formation of ice crystals was prevented, which would otherwise cause cellular damage. The cells themselves were cooled at a rate of $1°C$ per minute in a Nalgene temperature controlled freezing container. However for the recovery of the cell culture samples for testing cryovials were heated rapidly in a $37°C$ water bath and immediately mixed with pre-warmed media and centrifuged as the DMSO needed to be diluted as it is cytotoxic to the cells. The remaining pellet of cells was then added to a T75cm^2 flask containing 15ml of growth media. After 24 hours, the media was removed, the cells were washed in HBSS and fresh growth media was added.

5.4 Experimental Equipment and Methods

Endothelial cells were grown on 6 well plates (Sigma Aldrich, Dublin, Ireland) in order to perform shear tests *in vitro*. For all strain experiments endothelial cells were grown in 6 well Bioflex® culture plates (Dunn Labortechnik GmBH, Asbach, Germany). Apoptosis and necrosis assays were performed using Alexa Flour 488 annexin V and propidium iodide and proliferation was examined using carboxyfluorescein diacetate, succinimidyl ester. Permeability assays were completed using Transwell®-Clear tissue culture treated polyester membrane filter inserts in the 6 well format with 0.4 mm pore size and 24 mm filter diameter and fluorescein isothiocyanate labelled dextran . All experiments were carried out on cells between passage 7-9. All reagents used in this study were of the highest purity and unless otherwise stated were obtained from Sigma-Aldrich (Dublin, Ireland) or Cambrex BioScience Wokingham Ltd (Wokingham, UK).

5.4.1 Shear Experiments

For laminar shear and low shear stress studies, HAEC's were seeded at 5 x 10^5 cells/cm^2 in 6 well plates and allowed to come to confluency over 48 hours. The cells were starved of FBS for 24 hours and following this, media was removed and replaced with 4 ml of fresh growth media. Cells were then sheared at either 5 or 10 dyne/cm^2 for 12, 24 and 36 hours on an orbital shaker (Stuart Scientific Mini Orbital Shaker OS) as shown in Figure 5.2 set to the appropriate rotational speed as determined by the following equation (Hendrickson et al., 1999; Pearce et al., 1996).

$$\tau = \alpha\sqrt{\rho\eta(2f\pi)^3}$$

Equation 2

After completion of the experimental time-course, cells were harvested by washing with HBSS and removing the remaining cells by treatment with trypsin-EDTA. The harvested endothelial cells were monitored for (i) early and late stage apoptosis; (ii) necrosis; (iii) transendothelial permeability; (iv) or fixed in situ for immunocytochemical analysis.

5.4.2 Strain Experiments

For cyclic strain studies, HAEC's were seeded into 6-well Bioflex® culture plates which have a flexible, pronectin bonded growth surface. HAEC's were seeded at a density of

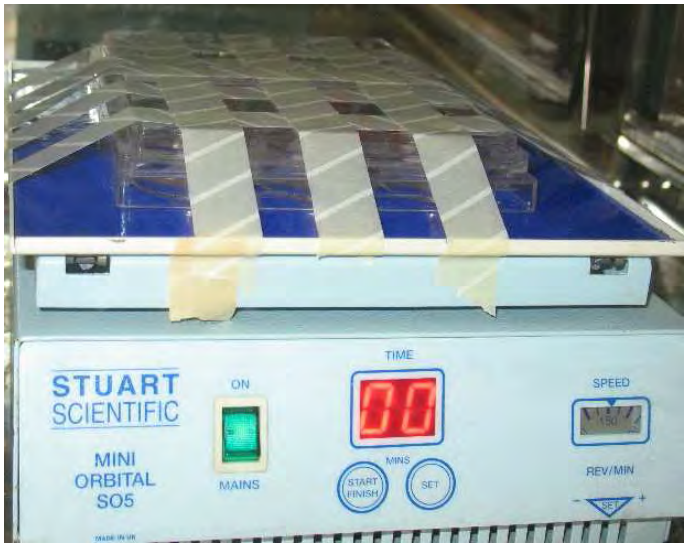

Figure 5.2: *In vitro* shear test set-up.

approximately 5x10^5 cells/well. The cells were permitted to come to confluency and then starved of FBS for a 24 hour period. One day post-confluency a Flexercell® Tension Plus™ FX-4000T™ system (Flexcell International Corp. - Hillsborough, NC, USA) was employed to apply the previously recorded *in vivo* levels of physiological, equibiaxial cyclic strain to each plate. The Flexercell® system enables precise stretching of cultured cells by microprocessor-controlled vacuum (Banes et al., 1985). The radial substrate distension in the Flexercell® system is induced by an undersurface vacuum. This vacuum pulls down on the outer segment of the circular substrate in each of the 6 wells. The area of the substrate supported by the loading post then experiences in-plane distention. This allows the cells to be subjected to defined levels of cyclic strain in a variety of wave patterns. In this way it is possible to monitor the effect of various levels of cyclic strain on the endothelial cells.

A biaxial calibration of the equipment was performed prior to each testing sequence. In order to do this the videoextensometer was again employed to monitor the deflections of the Bioflex® plate. Each 6 well plate was marked at known distances as shown in Figure 5.3 and the plates were then subjected to varying strains. The camera was set up at a known distance from the Bioflex® plate as can be seen in Figure 5.4. The value of strain input by the Flexercell® Tension Plus™ was then compared to the specific values recorded by the videoextensometer, thus ensuring the accuracy of the experimental set-up. A biaxial test viewed by the videoextensometer can be seen in Figure 5.5

Following calibration the 6-well Bioflex® culture plates were subsequently placed in

Figure 5.3: 6-well Bioflex® plates marked for calibration of the Flexercell® system.

the loading platform with a small amount of silicon gel (Loctite® 8104™ Henkel Technologies, Dublin, Ireland) placed between the loading posts and the bioflex membrane. It is assumed that upon application of the silicon gel there is frictionless sliding of the substrate over the edge of the loading posts. Two separate platforms were employed during each experiment hence two different levels of physiological strains were run consecutively making a comparison of results possible. Two individual but identical pumps (TRIVAC D8B, ProVac, Wexford, Ireland) provided the vacuum for each platform by means of one control system. Control plates with static endothelial cell cultures were placed in the same incubator.

Longitudinal *in-vivo* strains of 1% to 5%, with a sinusoidal input waveform and 60 cycles/min, were analysed at 12, 24 and 36 hours. Similarly *in-vivo* measurements of physiological radial strain at the bypass junction with a autologous, 8% to 12% strain, and synthetic bypass material, 7% to 17% strain, were analysed at 12, 24 and 36 hours again with 60 cycles/min and a sinusoidal input waveform. All tests were performed twice to ensure repeatability. Following each test the conditioned media was removed from each well and centrifuged at 1,000g for 5 minutes at 40°C to gather any cell debris. Thus ensuring apoptotic cells were accurately monitored.

Following each test cells were harvested for measurement of (i) early and late stage apoptosis; (ii) necrosis; (iii) proliferation; (iv) transendothelial permeability; (v) or fixed in

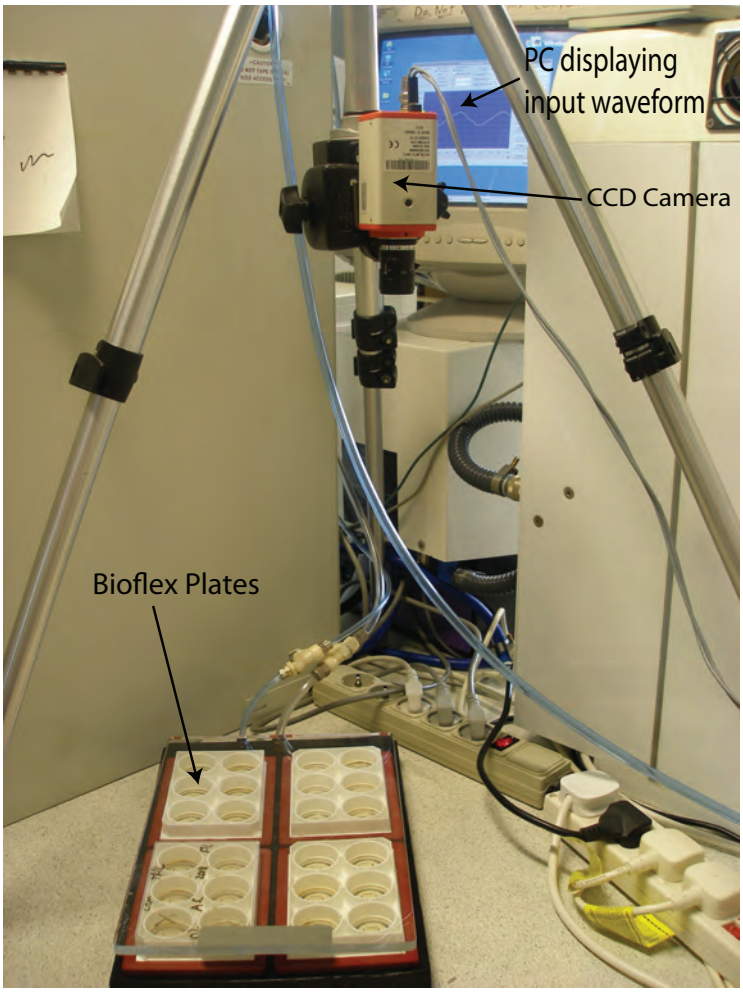

Figure 5.4: Laboratory calibration set-up.

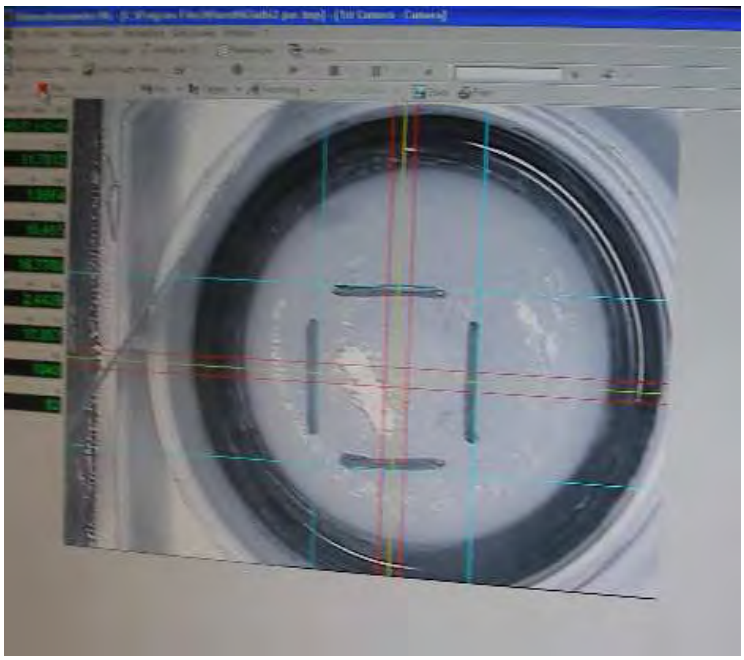

Figure 5.5: Biaxial calibration test of the Flexercell® system.

situ for immunocytochemical analysis.

5.4.3 Immunocytochemistry

In order to visually monitor the subcellular localization of proteins, cells were prepared for immunocytochemical analysis as previously described (Groarke et al., 2001) with minor modifications. Cells were washed twice in phosphate buffered saline (PBS) and fixed with 3% formaldehyde for 15 minutes. Cells were subsequently washed, permeabilised for 15 minutes with 0.2% Triton X-100 and blocked for 30 minutes in 5% BSA solution. Following blocking, cells were incubated with the appropriate primary antibody or stain, Zonula Occluden-1 (ZO-1) or Rhodamine Phallodin, followed by 1 hour incubation with 1:400 dilution of either Alexa Fluor 488 anti-mouse or anti-rabbit fluorescent secondary antibody. Nuclear DAPI staining was routinely performed by incubating cells with 0.5 x 10^{-6} mg/ml DAPI for 3 minutes. Cells were sealed with coverslips using DAKO mounting media (DAKO Cytomation, Cambridgeshire UK) and visualised by standard fluorescent microscopy (Olympus BX50). Specific procedural details can be found in appendices E.9 and E.10.

5.4.4 Permeability Analysis

As transendothelial permeability could not be directly monitored following shear stress studies in 6-well plates and strain studies in Bioflex® culture plates, cells were trypsinised and replated into Transwell®-Clear Polyester (PET) Membrane inserts which were placed above Transwell®-Clear plates at 2.5 x 10^5 cells/cm^2 as can be seen in Figure 5.6. After 24 hours when cells were confluent, transendothelial permeability was measured as previously described (Collins et al., 2006b). Fluorescein isothiocyanate (FITC)-labelled dextran (40 kDa, Sigma-Aldrich) was added to the abluminal chamber (to give a final concentration of 250 g/mL) and diffusion of dextran across the monolayer was allowed to proceed at 37°C for 3 hours. Media samples (28 μl) were collected every 30 minutes, over the period of 180 minutes, from the subluminal compartment and monitored in triplicate (7 μl sample + 93 μl media) for FITC-dextran fluorescence at excitation and emission wavelengths of 490 and 520 nm, respectively (Perkin-Elmer Luminescence Spectrometer LS50B with microplate reader attachment). Results are expressed as total subluminal flouresence at a given time point (from 0 to 180 minutes) which is expressed as a percentage of total subluminal flouresence at t = 0 minutes, i.e % of Trans Endothelial Exchange (%TEE). For a

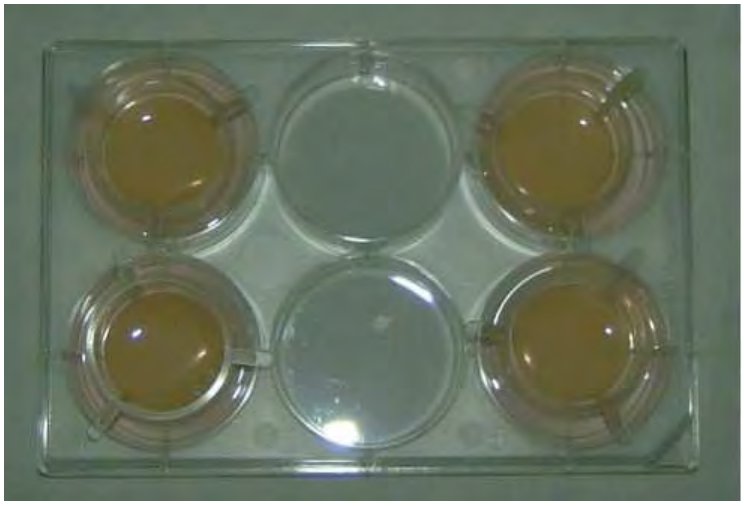

Figure 5.6: Transwell®-Clear Polyester (PET) Membrane inserts placed above Transwell®-Clear plates.

detailed description of the process see appendix E.6.

5.4.5 Proliferation Analysis

24 hours prior to the commencement of each experiment 1ml of carboxyfluorescein diacetate, succinimidyl ester (CFDA-SE) cell tracer (12.5μl in 25ml HBSS) was placed in each well for proliferation analysis. Subsequent to the shear stress studies in 6-well plates and strain studies in Bioflex® culture plates, cells were trypsinised and spun to pellet the cells. The cells were washed in PBS and spun twice in 1.5ml eppendorfs and transferred a falcon tube for Fluorescent-activated cell sorting (FACs) (Becton Dickinson FACSCaliber™ BD Bio Sciences Ltd, Dun Laoghaire, Ireland) for analysis. Full details are given in appendix E.7. All samples were subsequently assessed in duplicate and the results are expressed as an uptake of fluorochrome (FL1) relative to the number of cells present.

5.4.6 Apoptosis and Necrosis Analysis

Following shear stress studies in 6-well plates and strain studies in Bioflex® culture plates, cells were trypsinised and washed in HBSS. The cells were washed and spun twice. Annexin binding buffer (ABB) 200μl, Alexa Flour 488 annexin V 1μl and propidium iodide (PI) 0.4μl were added to the cells and transferred a falcon tube for Fluorescent-activated cell sorting (FACs) for analysis. Full details are available in appendix E.8. Measurement of programmed cell death by using annexin V may be considerably affected by a number of factors namely; calcium concentration, the time of incubation on ice and the type of

medium. Furthermore the binding buffer should be a simple balanced salt solution, HEPES-based buffers should be used rather than phosphate buffers (Trahtemberg et al., 2007). Thus HBSS was used for all experiments involving annexin V during the course of this study. All samples were subsequently assessed and the results expressed as a percentage uptake of Annexin V and PI indicating (i) healthy; (ii) early apoptotic; (iii) late apoptotic; and (iv) necrotic cells. The flowcytometer output clearly displaying each aforementioned group of cells can be viewed in Appendix F.

5.5 Results and Discussion

The endothelial lining of arteries is exposed to a complex mechanical environment. In addition to the wall shear stress induced by blood flow, pulsatile pressure generates a cyclic circumferential strain or hoop stretch over the entire arterial wall, which is enhanced at branched regions and points of extreme curvature within the arterial system. Factors varying from physical exertion to psychological stress can result in a transient rise in blood pressure and a consequent temporary increase in cyclic strain. The *in vitro* cellular responses to these mechanical forces include both functional and morphological adaptations. Helmlinger et al. (1991) proposed that cell orientation is an adaptive process of endothelial cells to reduce the local mechanical load in order to protect the cells from hydrodynamic injury.

Morphologically, confluent cultures and all control samples displayed the cobblestone pattern typical for endothelial cells in static culture in which the cells have no alignment pattern and have a slightly polygonal shape. It was found that laminar shear stress induced endothelial cells to elongate and flatten, giving the characteristic teardrop configuration. The cells aligned parallel to the direction of flow and the adaptive response was time dependent. Following exposure to the various levels of strain a similar change in cell shape occurred in which the HAEC's oriented transversely to the direction of stretch and became more elongated. However the teardrop configuration was not apparent as with flow. The results for the morphology of sheared cells parallel those observed previously by Zhao et al. (1995). A goal of the present study was to produce duplicate sets of experimental results in which shear stress values of 5 and 10 dynes/cm^2 were compared with cyclic strains of 3.5% $\pm$1.5% , 10%, $\pm$2% and 12% $\pm$5% as recorded during the *in vivo* studies. one set is presented here and a second can be viewed in Appendix G.

5.5.1 Immunocytochemistry

It was found that both shear stress and strain induced the formation of stress fibres that were aligned with long axes of the cell. The mechanical stimuli of shear and strain resulted in the remodelling of intracellular F-actin structures.

The continuous cyclic stretch applied to the HAEC's resulted in the elongating and aligning transversely, of cells, to the direction of stretch. This also induced a rearrangement of the actin microfilaments into stress fibers that are favoured alignment with the long axis of the cells. In the control samples the small short filaments cross the cytoplasm as a network exhibiting no particular preferential orientation. However following exposure to cyclic strain the cytoplasmic filaments both thickened and aligned with the long axes of the cells. The subcellular arrangement of actin monitored by immunocytochemistry, in which Alexia Phalloidin was used to counterstrain F-actin filaments, show the actin arrangement of control, sheared and strain endothelial cells Figure 5.7 to Figure 5.9. Control cells expressed actin in an unorganised fashion, however subsequent to the exposure of endothelial cells to cyclic strain or shear, actin localised at areas of cell-cell contacts and actin cortical ring formation around the cell periphery was observed.

Okano & Yoshida (1994) showed that the number of tight junctions increases in cultured endothelial cells following exposure to laminar shear stress. Although the specific levels of ZO-1 were not examined during this study, the cells were monitored visually for ZO-1 to show the changes in the configuration of contact between endothelial cell membranes following exposure to strain and shear. A clear change in the contact points can be seen between all the samples tested, Figures 5.10 through 5.12. ZO-1 exhibits a discontinuous and jagged localisation pattern at the cell to cell border in unstrained cells and becomes considerably more continuous and well defined following strain and shear experiments. This report proposes that tight junctions, which protect the endothelium against haemodynamic forces, are disrupted due to the changes in localised strain thus these tight junction allow the passage of foreign molecules into the arterial wall.

At a site of inflammation leukocytes bind to and roll on the endothelial cell surface. Eventually the leukocytes emigrate between the endothelial cells to reach underlying tissues. This process is not completely understood but it may require disruption of cadherins (transmembrane proteins) at endothelial tight junctions. The alterations within the tight junctions that can be seen following exposure to strain, Figure 5.12, display a membrane that is not in constant contact unlike the membrane following shear tests, Figure 5.11.

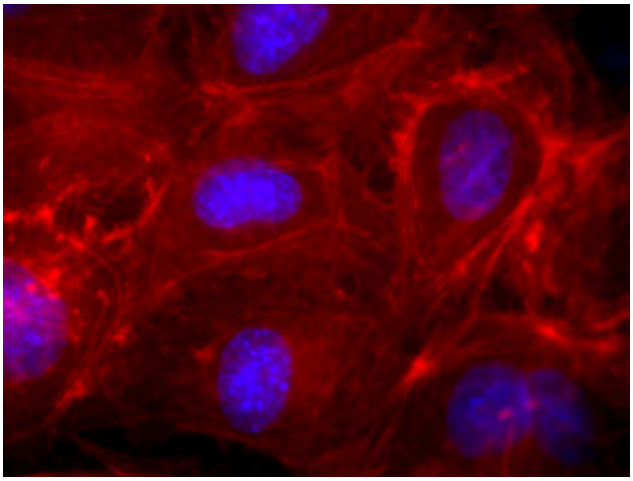

Figure 5.7: Rhodamine Phaloidin Stained Control Cells

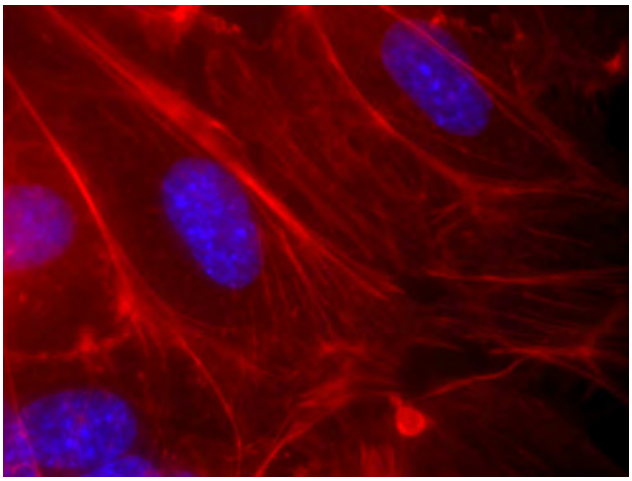

Figure 5.8: Rhodamine Phaloidin Stained Sheared Cells

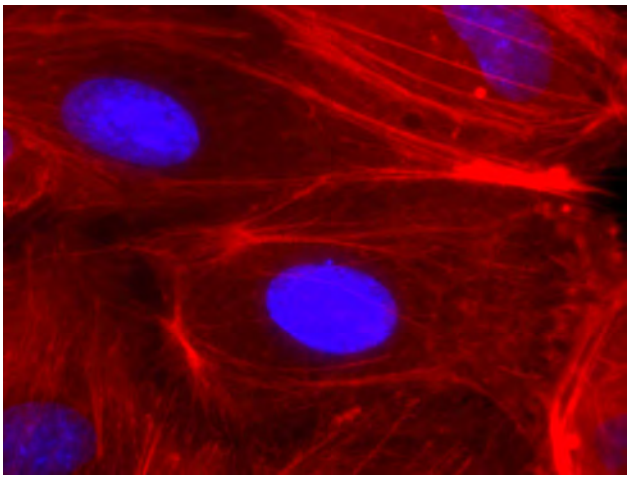

Figure 5.9: Rhodamine Phaloidin Stained Strained Cells

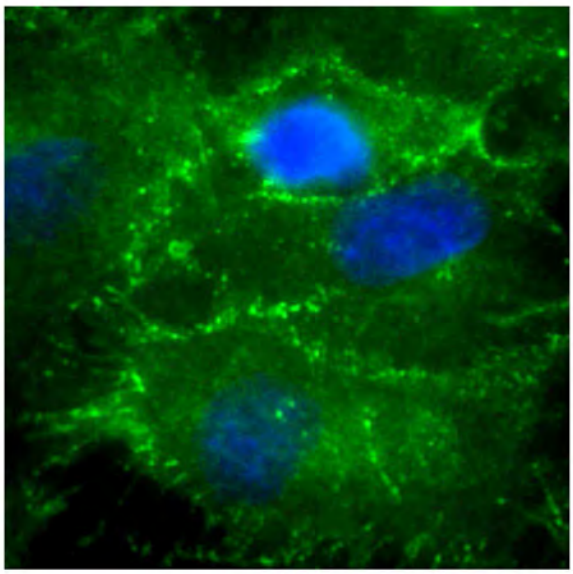

Figure 5.10: ZO-1 Stained Control Cells

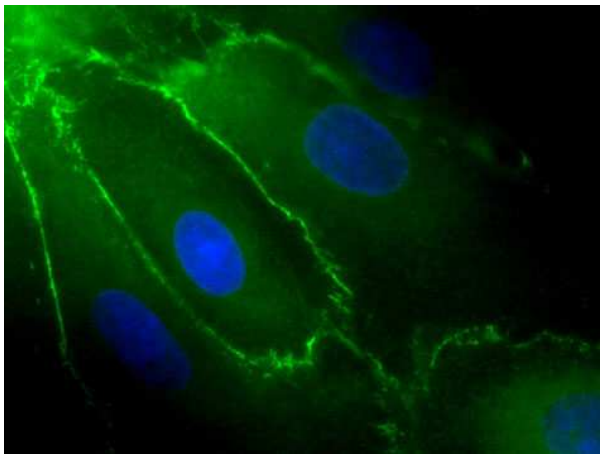

Figure 5.11: ZO-1 Stained Sheared Cells

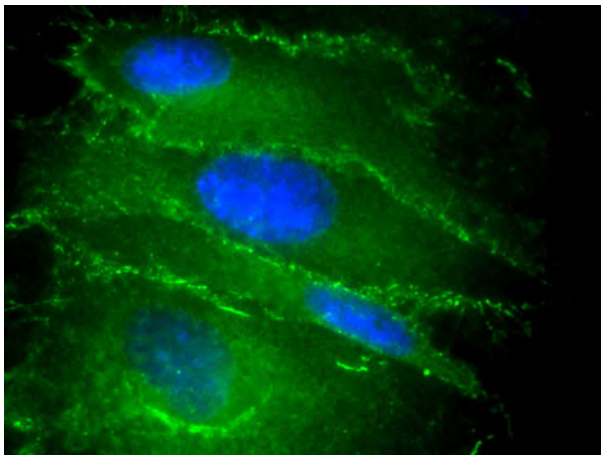

Figure 5.12: ZO-1 Stained Strained Cells

This implies that strain might have the catastrophic effect of reducing tight junction contact and thus increasing the interstitial space allowing the passage of molecules through the endothelium. These results lead the author to assume that the endothelium is rendered dysfunctional by the aberrant levels of mechanical stimuli surrounding the distal junction following the introduction of an ePTFE graft, leading to increased permeability and the build up of atherogenic particles in the intima.

Changes in permeability results in altered rates of macromolecular diffusion or transport through endothelial cell junctions. If inflammatory mediators such as thrombin are attracted to the site then a further increase in endothelial permeability occurs as thrombin can modulate the phospohorylation of proteins involved in the organisation of endothelial junctions resulting in a cascading effect and the protective barrier of the endothelium ultimately breaking down.

5.5.2 Permeability

Endothelial cells provide a critical interface between blood and arterial walls. Free diffusion of substances across the endothelium is prevented in part by the aforementioned tight junctions, the permeability of which varies depending on its environment. Endothelial cells, following subjection to the magnitudes of strain that were found to exist at a femoral artery bypass graft junction, were analysed for any alterations in transendothelial cell permeability. The three variations of strain were assessed at 12, 24 and 36 hours.

The changes in ZO-1 and actin realignment discussed so far indicated that cyclic strain induces barrier properties in endothelial cells. However it is the transendothelial permeability assay that provides the most compelling evidence. Shear and physiological levels of cyclic strain significantly reduces endothelial cell transendothelial permeability to FITC-dextran (a measurable index of barrier function).

Each line on the permeability graph represents the results from one well on the Bioflex® culture plate. To ensure accuracy a second sample was analysed for each of the control and strained or sheared cells. Each point on the graph is the average of three readings taken at that time point. Figures 5.13 to 5.15 represent the transendothelial permeability at various time points when subjected to a strain of 2% to 5%. It can be seen that the small magnitude and low amplitude of strain appears to slightly decrease the permeability of endothelial cells.

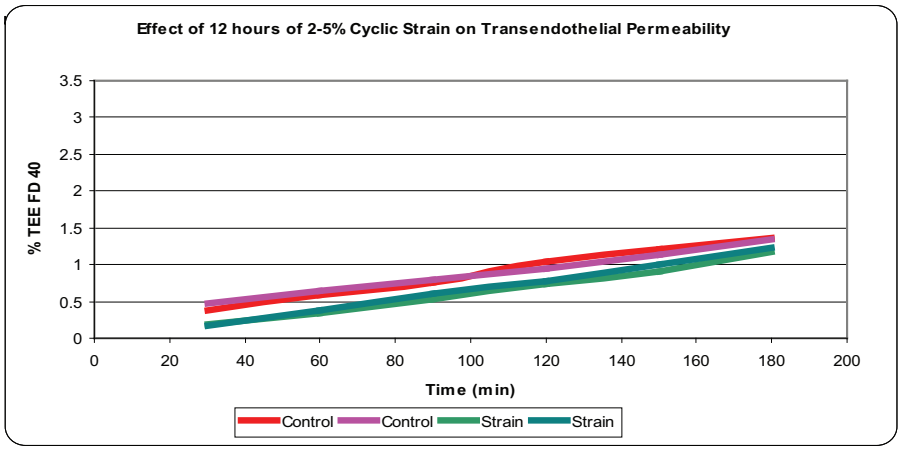

Figure 5.13: Trans Endothelial Exchange following **12** hours of 2-5% strain

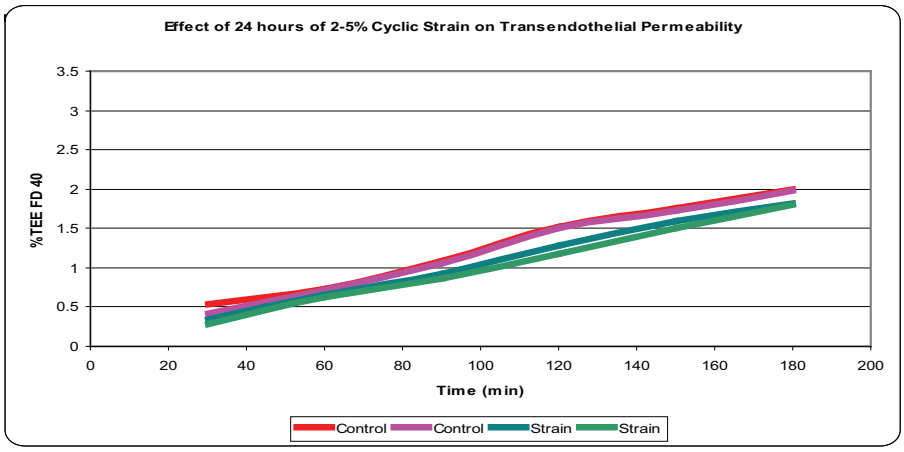

Figure 5.14: Trans Endothelial Exchange following **24** hours of 2-5% strain

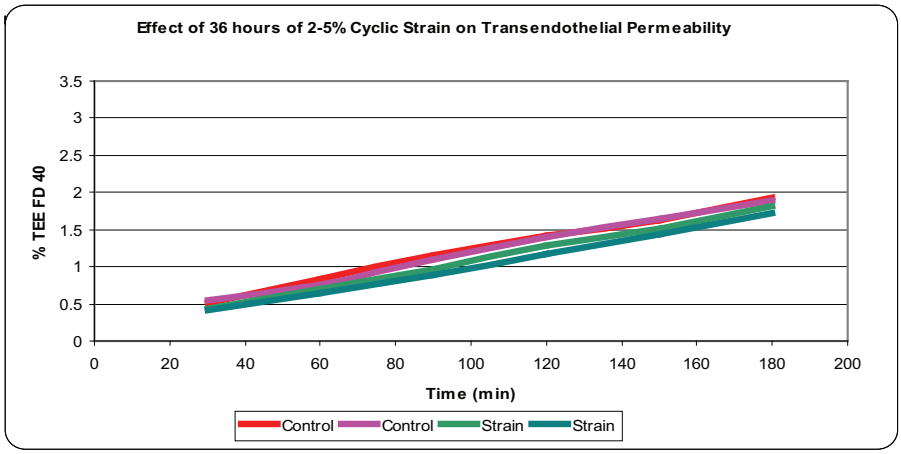

Figure 5.15: Trans Endothelial Exchange following **36** hours of 2-5% strain

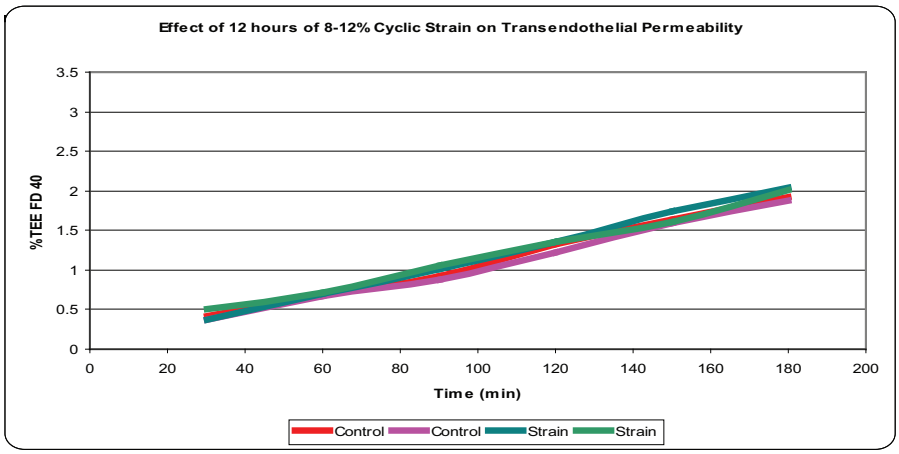

Figure 5.16: Trans Endothelial Exchange following **12** hours of 8-12% strain

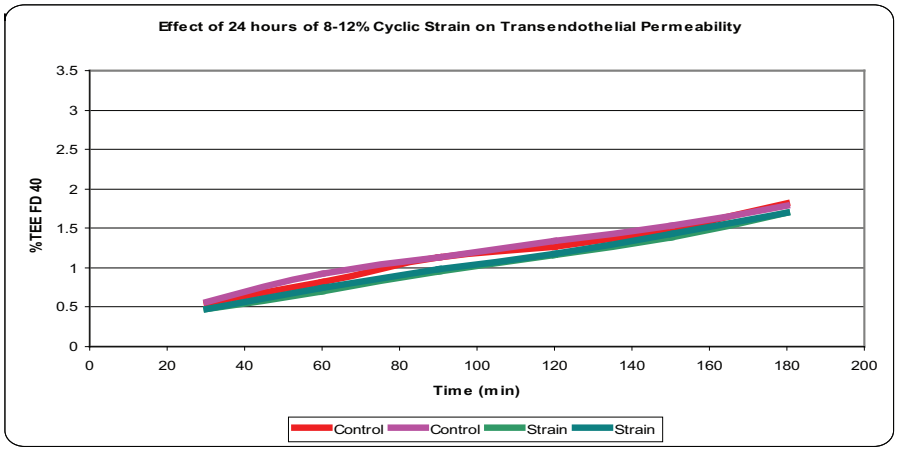

Figure 5.17: Trans Endothelial Exchange following **24** hours of 8-12% strain

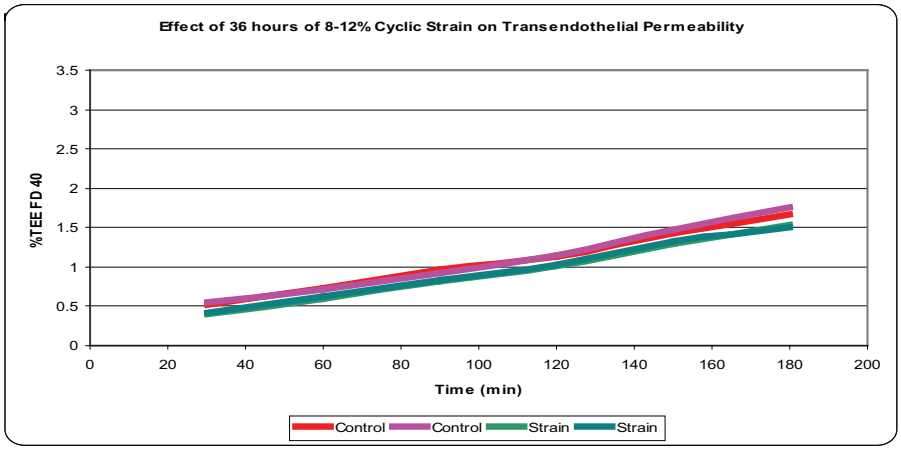

Figure 5.18: Trans Endothelial Exchange following **36** hours of 8-12% strain

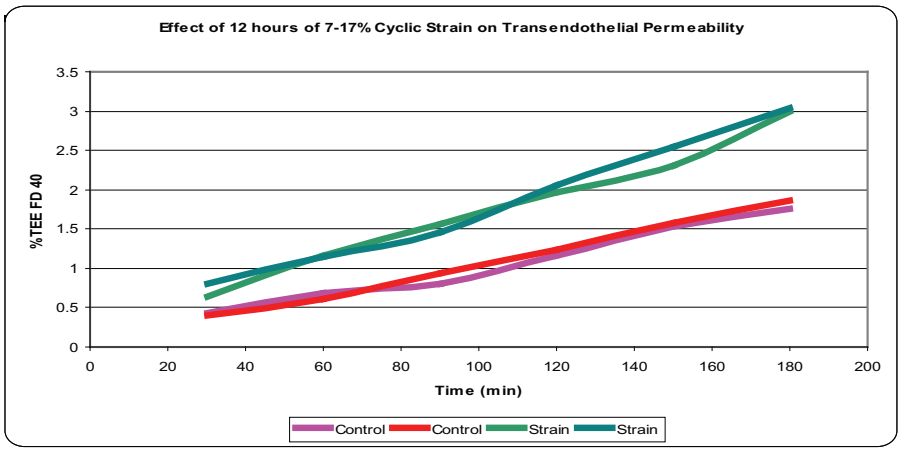

Figure 5.19: Trans Endothelial Exchange following **12** hours of 7-17% strain

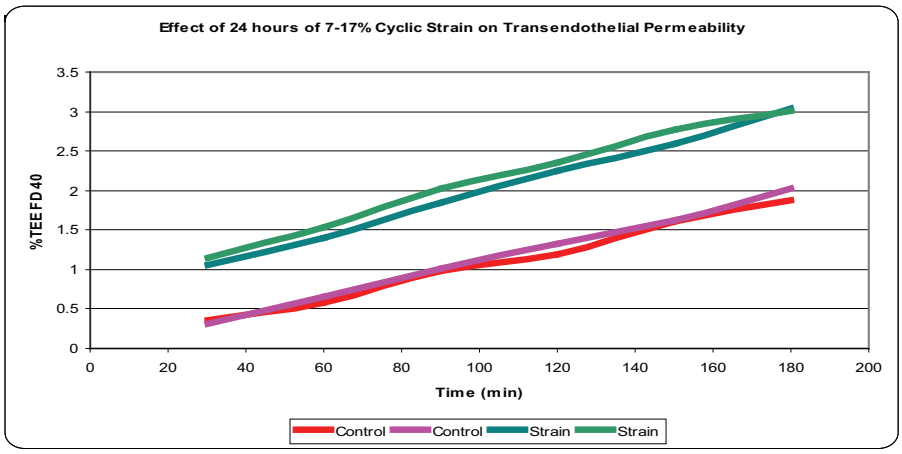

Figure 5.20: Trans Endothelial Exchange following **24** hours of 7-17% strain

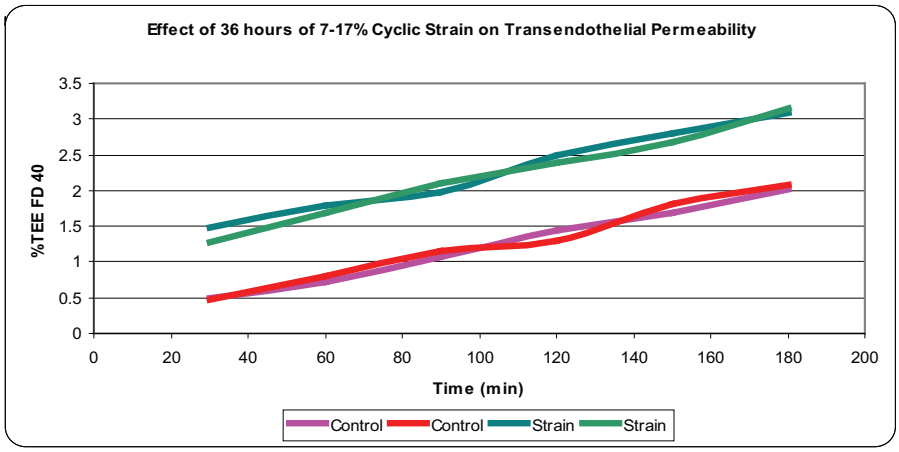

Figure 5.21: Trans Endothelial Exchange following **36** hours of 7-17% strain

When comparing the cells that were strained at a range of 2% to 5% and 8% to 12% (Figure 5.13 to Figure 5.18) only small variations in the transendothelial cell permeability occurred. It is the authors belief that the cells adjust quickly to the magnitude of the strain and after the first few hours the cells respond primarily to the constant changes in amplitude of the cyclic strain. The average strain in each of these instances is 3.5% and 10% but the variations in the amplitude were only $\pm 1.5\%$ and $\pm 2\%$ respectively. Consistent with this conclusion, a recent study by Shin et al. (2004) demonstrated reduced transendothelial permeability to albumin following exposure of HUVECs to an average of 10% cyclic strain.

However when the amplitude of strain is increased to 12% in the strain range from 7% to 17% a completely different response is seen. Instead of the strain inducing a positive response and reducing the transendothelial permeability a negative response is encouraged and the permeability of the endothelial cells is greatly enhanced, as presented in Figures 5.19 to Figure 5.21. This change in the functionality of the endothelial cells may allow the passage of molecules such as LDL and monocytes and other factors associated with the build up of plaque to pass through the arterial wall and allow for the onset of atherosclerosis.

Locally nonuniform haemodynamics trigger abnormal biological responses. Lei et al. (1995) have postulated that significant and sustained values of wall shear stress gradient (WSSG) play a key role in endothelial cell turnover and leaky junctions and/or individual bond rupture of the endothelial cells. Atherosclerotic plaques preferentially form in regions of low or disturbed shear stress at vessel branch points, bifurcations and regions of high curvature. In contrast to this high laminar shear stress is considered to be atheroprotective (Tzima et al., 2005). Endothelial cells experiencing variations in blood flow, outside of the physiological range, can abrogate the protective effects of laminar shear. Thus the endothelial cells, in this study, were subjected to a low shear stress of 5 dynes/cm^2 and a physiological shear stress of 10 dynes/cm^2.

Following 12, 24 and 36 hours continuous exposure to steady shear stress, the cells was analysed for transendothelial permeability. Little difference was found to exit between the control samples and samples sheared at 5 dynes/cm^2 as can be viewed in Figures 5.22 to Figure 5.24. When a physiological shear stress of 10 dynes/cm^2 was applied a reduction in the transendothelial cell permeability occurred, as shown in Figures 5.25 to 5.27.

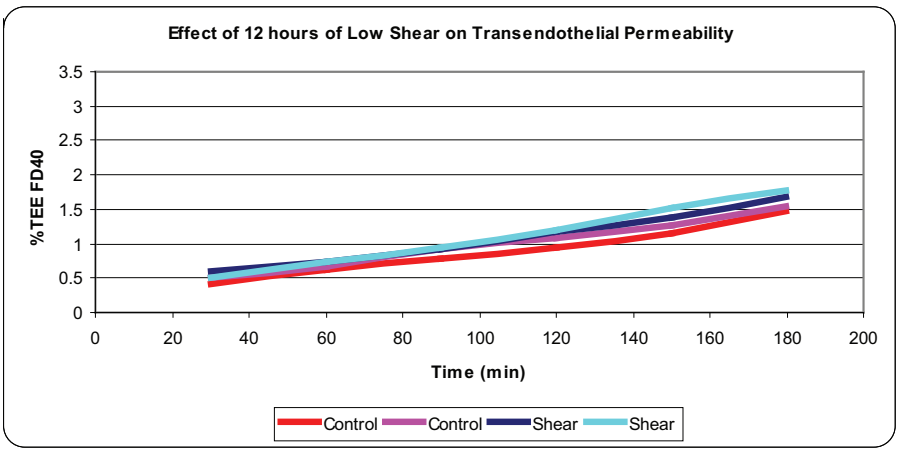

Figure 5.22: Trans Endothelial Exchange following **12** hours of low shear

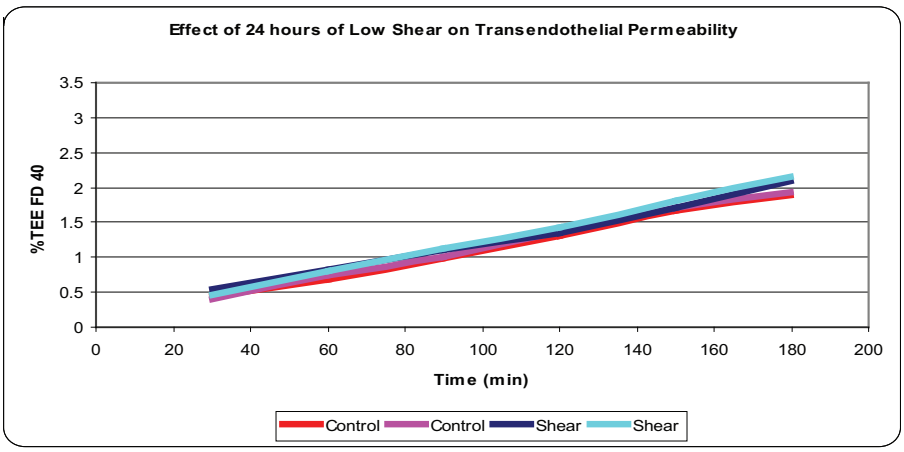

Figure 5.23: Trans Endothelial Exchange following **24** hours of low shear

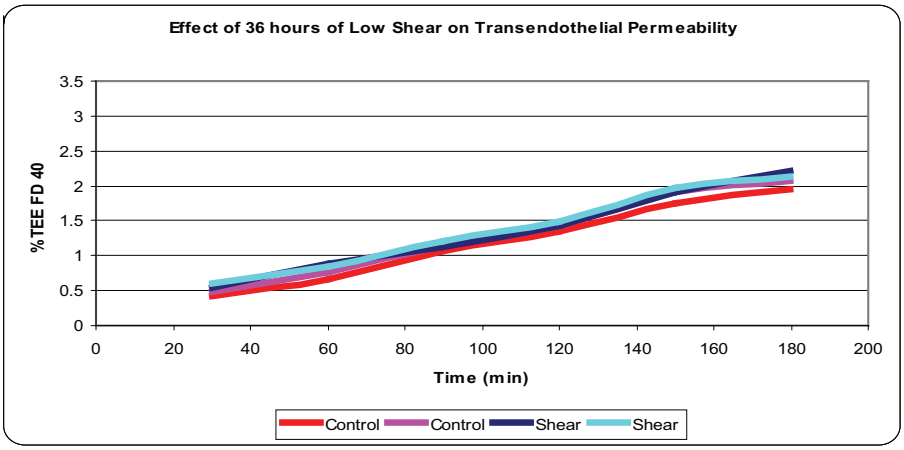

Figure 5.24: Trans Endothelial Exchange following **36** hours of low shear

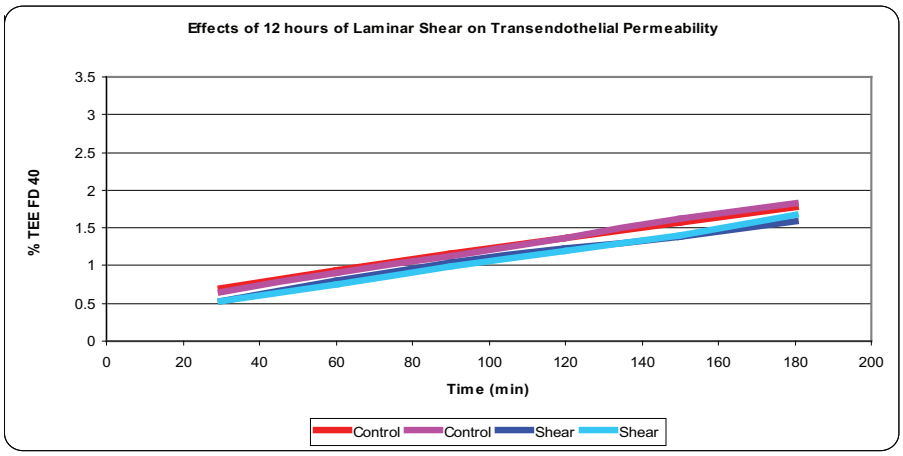

Figure 5.25: Trans Endothelial Exchange following **12** hours of physiological shear

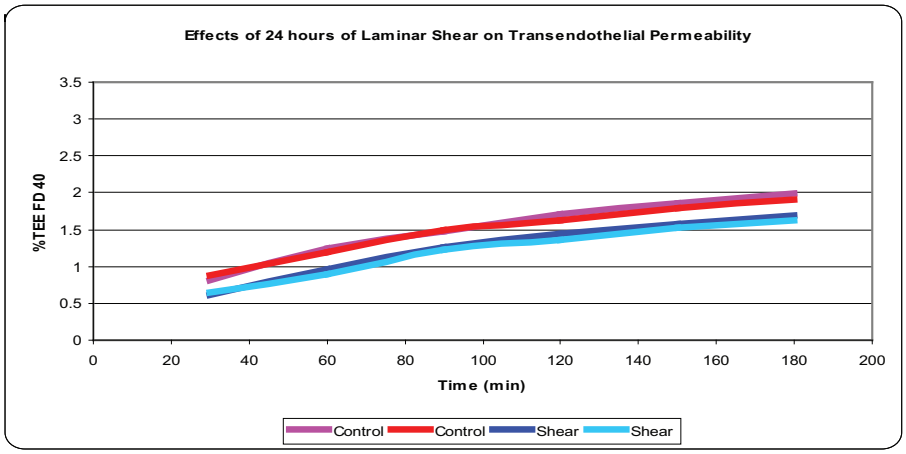

Figure 5.26: Trans Endothelial Exchange following **24** hours of physiological shear

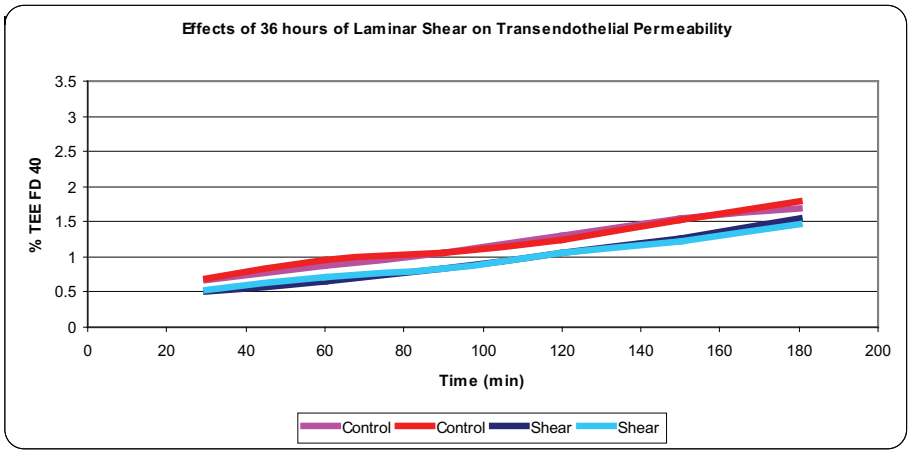

Figure 5.27: Trans Endothelial Exchange following **36** hours of physiological shear

From this it is clear that cells function best under physiological conditions and any alteration in these conditions induce negative responses. It is the authors belief that low shear exists at lesion prone sites and endothelial permeability to macromolecules is enhanced.

5.5.3 Apoptosis

A balance between cell proliferation and cell death ensures homeostasis is preserved in multicellular organisms. Several categories of cell death have been classified: apoptosis (type I), cell death associated with autophagy (type II) and necrosis or oncosis (type III). The destiny of almost any dying or dead cells regardless of death type is engulfment by phagocytes (Kroemer et al., 2005). The apoptotic and necrotic cells analysed by the flowcytometer were grouped into one of the aforementioned categories (see appendix F for raw data). Apoptosis has been characterised by several biochemical criteria, such as different kinetics of phosphatidylserine (PS) exposure on the outer leaflet of the plasma membrane and changes in the mitochondrial membrane permeability (Denecker et al., 2001). In healthy viable cells, PS is to be found on the cytoplasmic surface of the cell membrane. However in apoptotic cells PS is translocated from the inner surface to the outer leaflet of the plasma membrane, when on the outer leaflet it can be detected by annexin V conjugates.

In contrast to this, necrosis is characterised by rapid cytoplasmic swelling and thus is often called oncosis. It is believed that necrosis is a consequence of extreme physiochemical stress, such as heat and freezing to mechanical stress. When exposed to such physiochemical stress cell death occurs quickly hence this process is described as accidental and uncontrolled. Due to the unnatural physiological behaviour of necrosis it is of particular interest in this study. The generation of apoptosis and necrosis as a result of applying the various levels of cyclic strain and shear can be viewed in Figures 5.28 to 5.31.

It is immediately apparent that the rate of necrosis increases significantly as the cyclic strain rate increases to non-physiological levels. The highest level of cyclic strain has a dramatic effect inducing over 20% necrotic cells. Furthermore the necrosis increased over the various time points from 12 hours to 36 hours showing that the cells did not appear to reach an equilibrial state within that time frame.

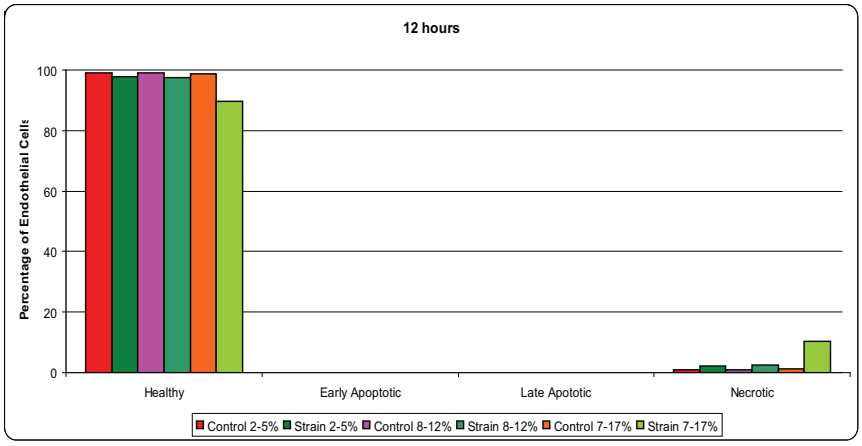

Figure 5.28: Apoptotic and Necrotic reactions of endothelial cells following **12** hours of each strain range

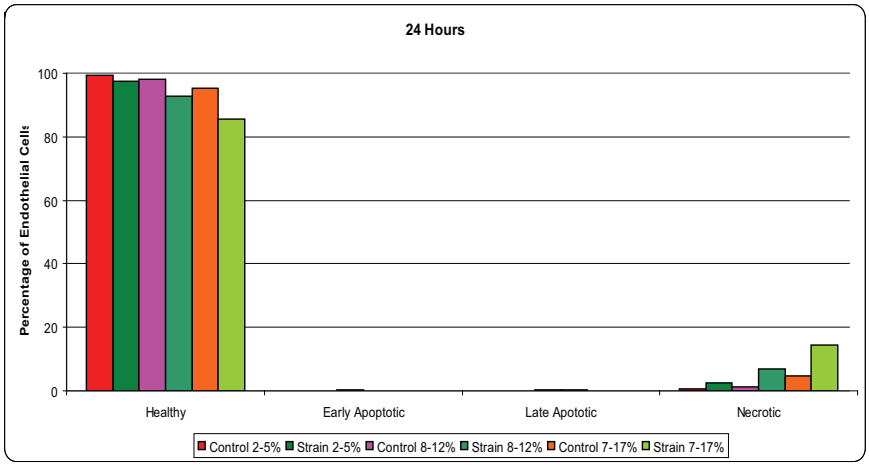

Figure 5.29: Apoptotic and Necrotic reactions of endothelial cells following **24** hours of each strain range

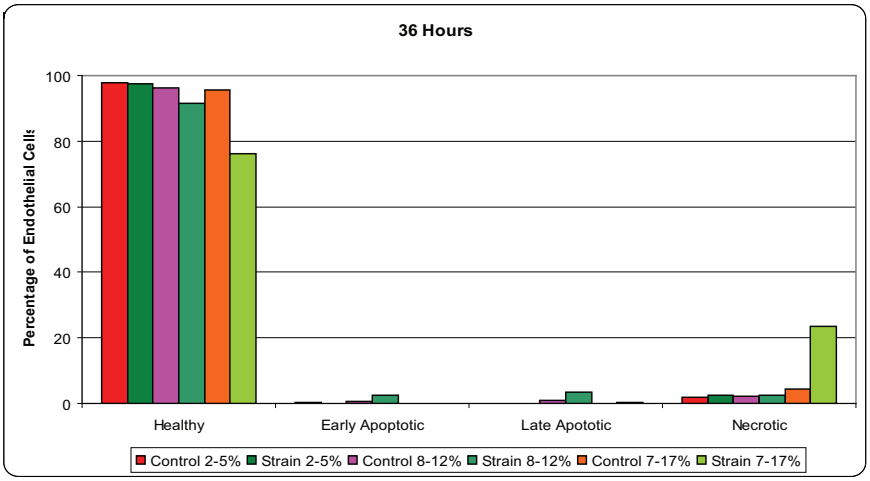

Figure 5.30: Apoptotic and Necrotic reactions of endothelial cells following **36** hours of each strain range

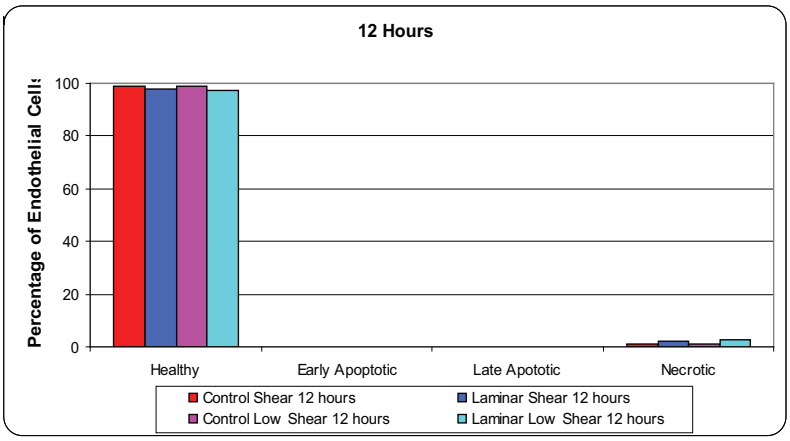

Figure 5.31: Apoptotic and Necrotic reactions of endothelial cells following **12** hours of low or physiological shear

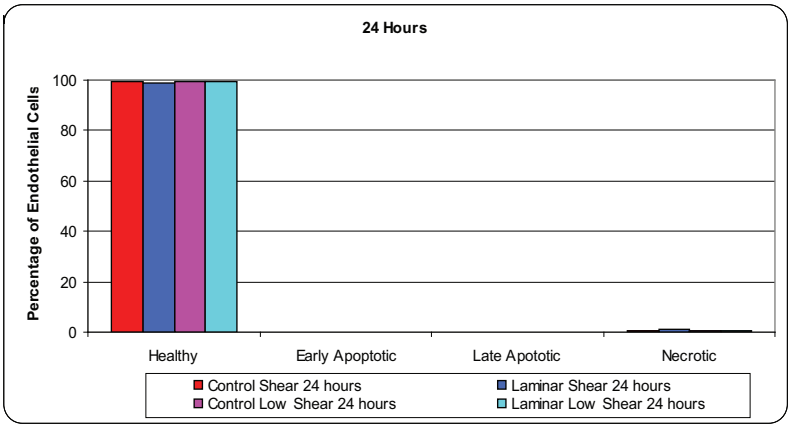

Figure 5.32: Apoptotic and Necrotic reactions of endothelial cells following **24** hours of low or physiological shear

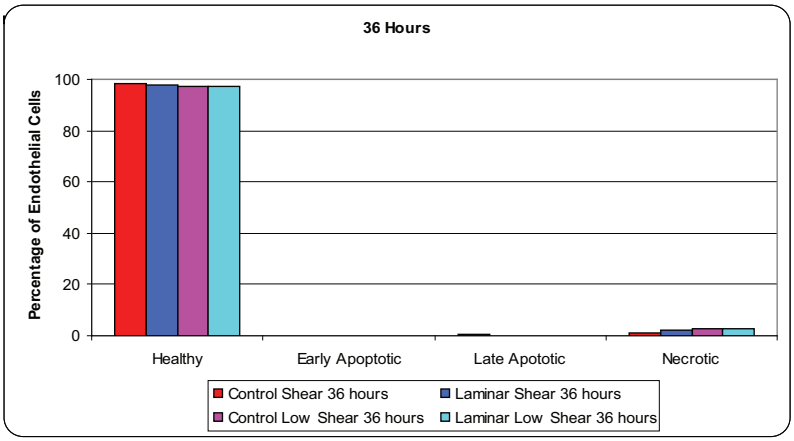

Figure 5.33: Apoptotic and Necrotic reactions of endothelial cells following **36** hours of low or physiological shear

Apoptosis only becomes apparent after 36 hours which is to be expected as all cells were initially starved of FBS and hence each tests commenced at G0. The G zero phase is a time in the cell cycle in which the cell exist in a quiescent or inactive state, i.e. the cell is neither dividing nor preparing to divide. With a cell doubling time of over 24 hours, apoptosis would only be expected to appear in tests run for longer than that period. The physiological strain rate of 2-5% had negligible adverse effects on cell death. A maximum of 7% necrosis was induced in cells subjected to the 8-12% cyclic strain range. These findings establish cyclic stretch as a novel regulator of programmed and unprogrammed cell death.

Liu et al. (2003) performed a study on the inhibition of apoptosis in the vascular endothelium. It was found that cyclis stretch of 6-10% inhibited apoptosis however high potential pathologic levels of stretch 6-20% stimulated apoptosis. To the authors knowledge, this is the only other existing study reporting on the putative role of the pulsatile force ranges required to induce varying levels of apoptosis in endothelial cells.

Following physiological shear tests, Figures 5.31 to 5.33, the occurrance of apoptosis and necrosis was found to be negligible. Similarly the shearing of endothelial cells at 5 dynes/cm^2 resulted in miniscule increases in necrosis. An insignificant difference existed between sheared cell samples for comparison purposes. This infers that both physiological and low shear have little influence on either programmed or unprogrammed cell death over the time periods analysed.

5.5.4 Proliferation

Following exposure to flow and strain, the cells were analysed for CFDA-SE concentrations. In the results shown in Figures 5.34 to 5.48, a shift to the left implies an increase in proliferation. As the cell divides the amount of fluorescent die is shared between the newly divided cells thus the less fluorescent the cell the more it has proliferated. The same number of cells were analysed by the flow-cytometer for each test and the graphed results all portray control samples in red, strain in green and shear in blue.

In Figures 5.34 to 5.36 longitudinal physiological strain (2-5%) is shown to encourage cell proliferation. Similarly in Figures 5.37 to 5.39 it can be seen that cell proliferation was promoted when the endothelial cells experienced a higher average strain rate (8-12%) with a similar variation in amplitude.

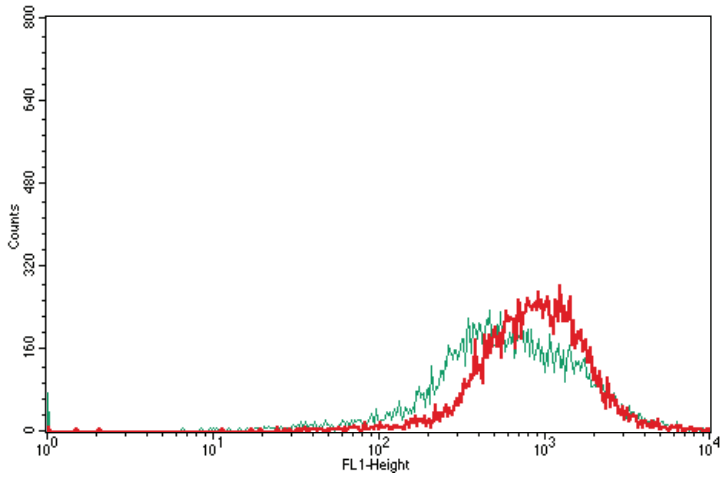

Figure 5.34: Proliferation of endothelial cells following **12** hours of 2-5% cyclic strain

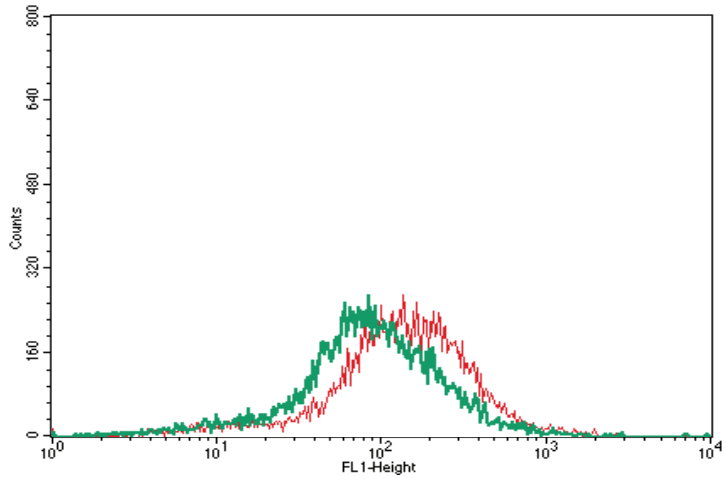

Figure 5.35: Proliferation of endothelial cells following **24** hours of 2-5% cyclic strain

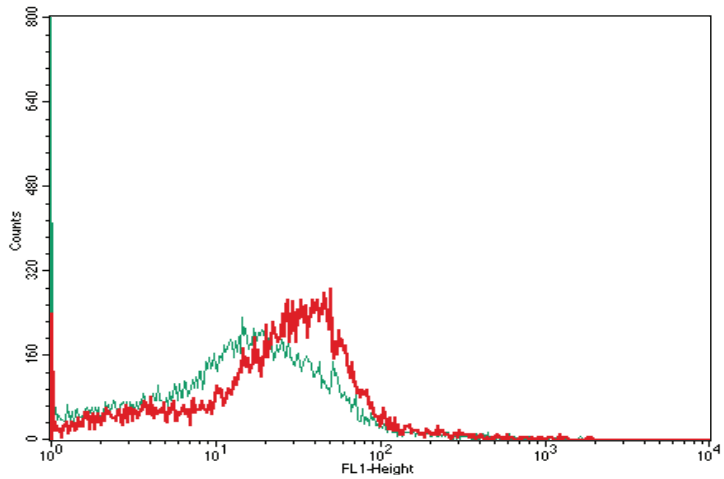

Figure 5.36: Proliferation of endothelial cells following **36** hours of 2-5% cyclic strain

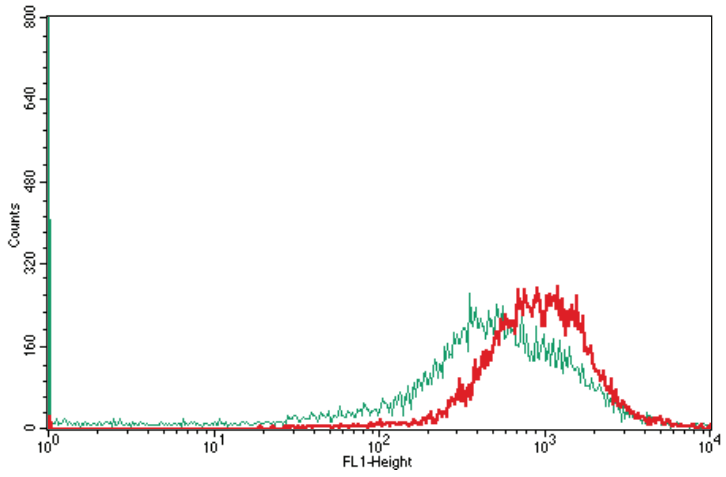

Figure 5.37: Proliferation of endothelial cells following **12** hours of 8-12% cyclic strain

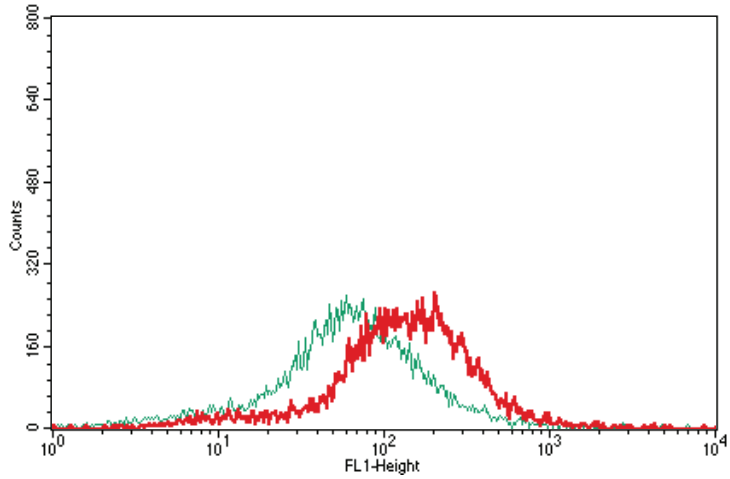

Figure 5.38: Proliferation of endothelial cells following **24** hours of 8-12% cyclic strain

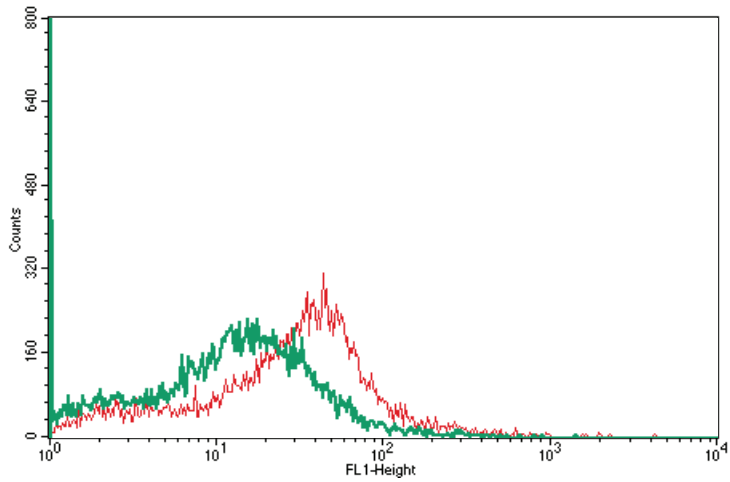

Figure 5.39: Proliferation of endothelial cells following **36** hours of 8-12% cyclic strain

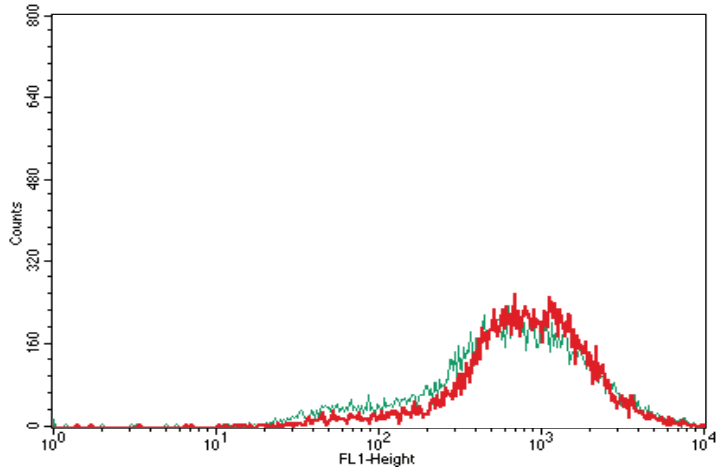

Figure 5.40: Proliferation of endothelial cells following **12** hours of 7-17% cyclic strain

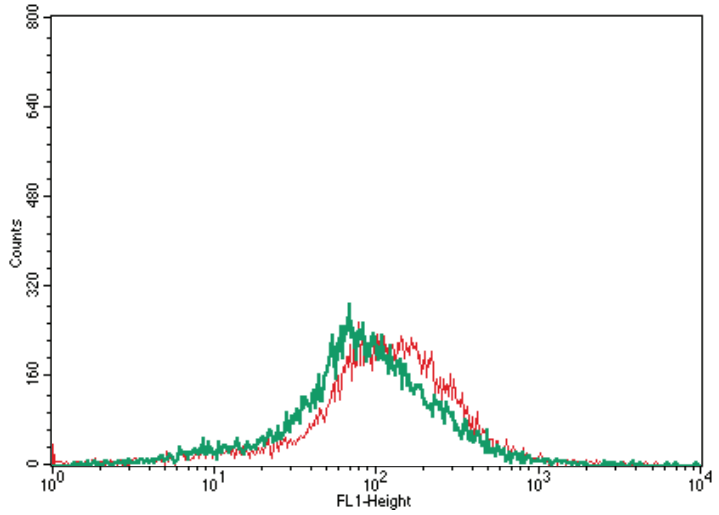

Figure 5.41: Proliferation of endothelial cells following **24** hours of 7-17% cyclic strain

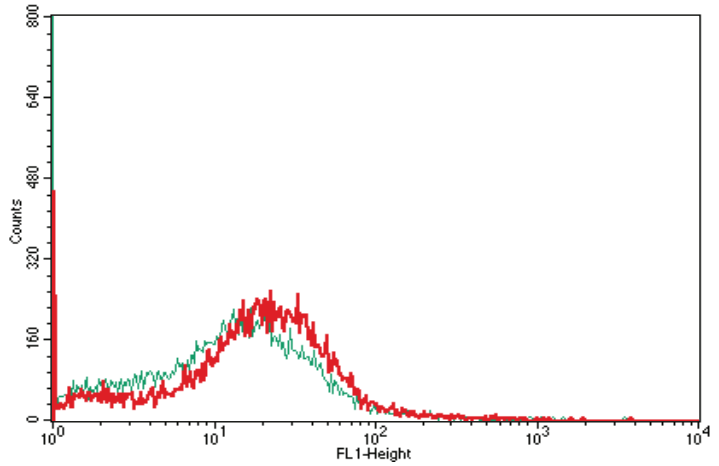

Figure 5.42: Proliferation of endothelial cells following **36** hours of 7-17% cyclic strain

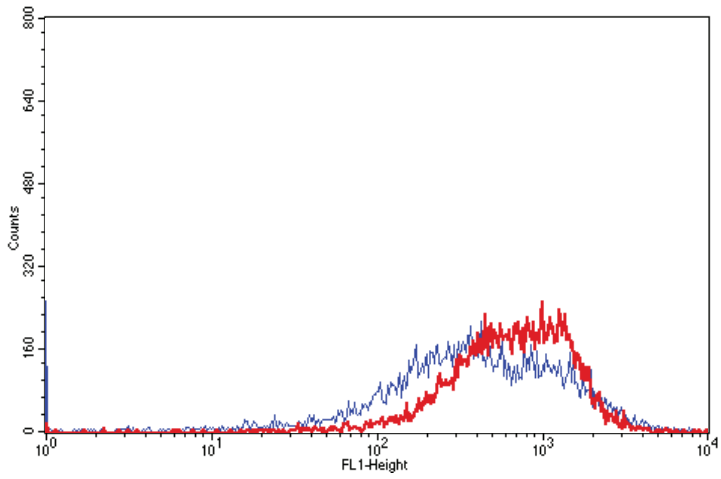

Figure 5.43: Proliferation of endothelial cells following **12** hours of physiological shear

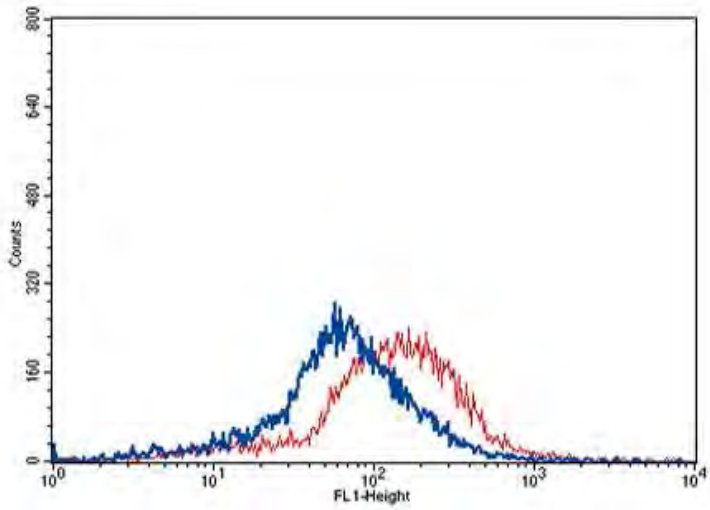

Figure 5.44: Proliferation of endothelial cells following **24** hours of physiological shear

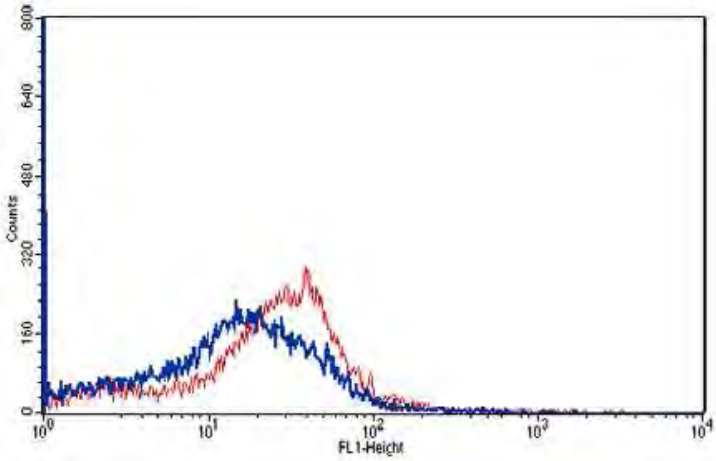

Figure 5.45: Proliferation of endothelial cells following **36** hours of physiological shear

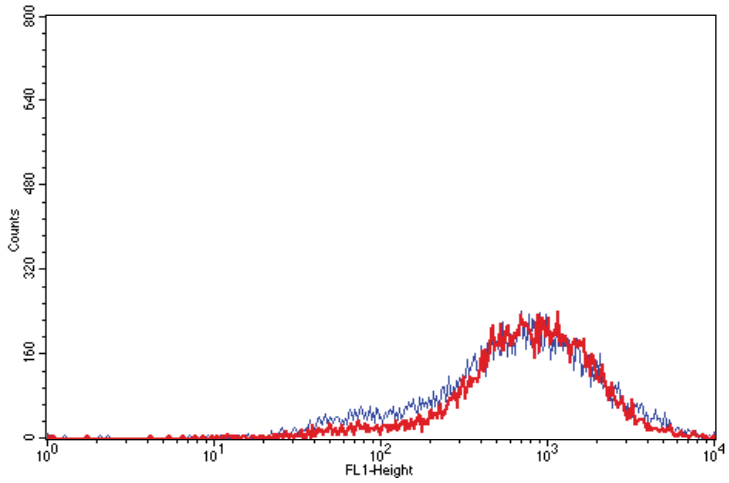

Figure 5.46: Proliferation of endothelial cells following **12** hours of low shear

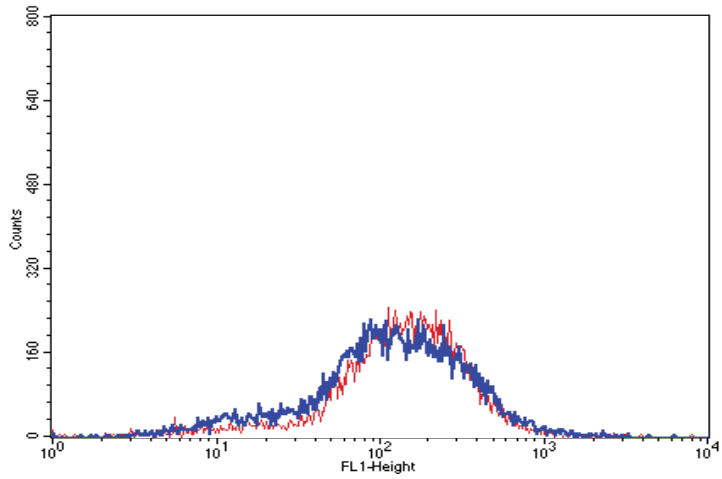

Figure 5.47: Proliferation of endothelial cells following **24** hours of low shear

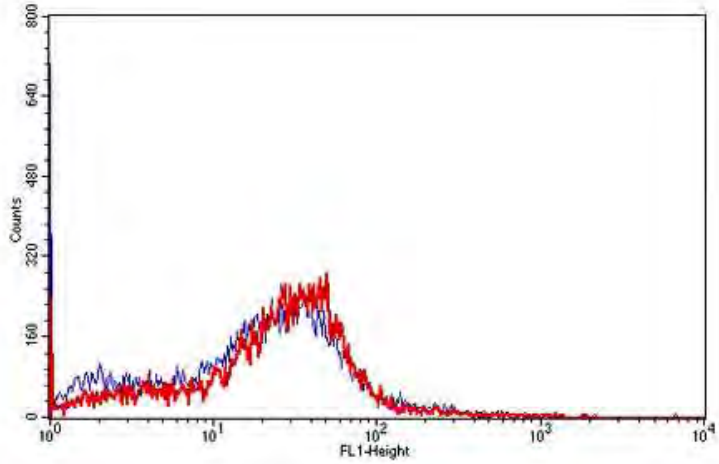

Figure 5.48: Proliferation of endothelial cells following **36** hours of low shear

At the highest strain rate, Figures 5.40 to 5.42, negligible differences were noted between controlled and strained samples thus implying that proliferation was neither promoted nor inhibited. Consequently it is believed that the cells respond quickly to the initial introduction of strain but ultimately are affected by the constantly changing amplitude. Amplitudes of strain within $\pm 2\%$ of the average strain promote proliferation but increasing this variation to $\pm 5\%$ appears to negate the positive promotion of cell proliferation by cyclic strain.

Physiological laminar shear certainly promotes the division of endothelial cells, Figures 5.43 to 5.45 however the low shear examined in Figures Figures 5.46 to 5.48 had negligible effects on either promoting or discouraging proliferation.

The insignificant difference between the proliferation of the control and low shear samples and the control and high strain samples provide little information. However it can be concluded that as proliferation is neither promoted nor prohibited at theses ranges of high strain and low shear, analysing endothelial cell proliferation at above or below these values would not induce any beneficial proliferative effects. In contrast the results of the strain analysis at the two lower average strains provide valuable data on the amplitudes of cyclic strain required to promote cell division.

5.6 Summary

The above section of the study transfers the measurements recorded *in vivo* and utilises them *in vitro*, accurately assessing the apoptotic, necrotic, proliferative and membrane permeability reactions of human endothelial cells when subjected to shear stresses and strains.

In summary endothelial cell cultures exposed to both low and physiological laminar shear stress responded with significant remodeling, seen by elongation and alignment of the cells with the direction of flow, and, to a certain extent, with the formation of actin stress fibers which aligned themselves with the long axis of the cell. It is believed that the threshold level of shear stress is between 5 and 10 dynes/cm^2 as when the changes in membrane permeability of the cells are examined under shear conditions it was found that the endothelial cells adapt to reduce the transendothelial permeability at the higher rate of physiological shear. It has also been demonstrated that physiological levels of cyclic strain act to promote a healthy and functioning tight junction in endothelial cells.

This study has established that the behaviour of the endothelial cells is greatly altered

when subjected to high cyclic strain and that the threshold levels of cyclic strain for endothelial cell remodeling is dependent on magnitude and amplitude. In order to accurately assess the apoptotic and necrotic responses of endothelial cells in the area surrounding an artificial bifurcation, it was found that cyclic strains of 7% to 17% should be monitored. It is also suggested that all cyclic strain tests to evaluate necrosis should be allowed to run for a minimum of 36 hours.

The proliferation of endothelial cells is promoted under physiological levels of shear and strain however increased levels of strain and reduced shear appear to neither promote nor prohibit proliferation thus concluding that proliferation is not favourable above or below these thresholds. It is believed that the low shear of 5 dynes must still provide enough flow to support the protective functions associated with laminar shear and endothelial cells as the permeability was not altered however it does not promote cell proliferation thus preventing homeostasis from being preserved.

Hypertension is closely associated with an increase in the extent and the severity of atherosclerosis. Thus the conclusion is drawn that as hypertension increases the magnitude of the strain experienced by endothelial cells, it induces an increase in cell turnover and an associated enhancement of permeability. The enhancement in permeability and altered proliferation experienced by cells at the higher strain rate reflects not only the occurrence at a distal bypass graft junction but also the effects that would be experienced by hypertensive patients. The results from the present *in vivo* study and *in vitro* model may provide some clarification on which strain rates should be explored when examining the responses of endothelial cells.

As detailed in the literature review, previous studies have shown that mechanical strain can regulate morphological and phenotypical responses in endothelial cells. However the majority of previous studies were conducted on strains varying from 0% to various magnitudes when in fact specific ranges should be monitored as arteries are never at 0% strain (Zhao et al., 1995; Cheng et al., 1996; Cotter et al., 2004; Von Offenberg Sweeney et al., 2005; Collins et al., 2006a; Lehoux et al., 2005). This study introduces new parameters for the examination of endothelial cell reactions *in vitro*.

Chapter 6

Conclusions and Recommendations for Further Work

6.1 Conclusions

This thesis focused on the measurement of cyclic strains at the distal femoral bypass graft junction following the introduction of both vein and ePTFE grafts. It validated the techniques employed by using finite element analysis for caparison and it examined the effects that pressure induced strain has on endothelial cells.

6.1.1 Silicon and Finite Element Models

The laboratory models showed that:

- The videoextensometer proved accurate in the measurement of deflections when applying static pressures of 10KPa to 20KPa to silicon models.
- The 45° silicon/graft model produced strains of magnitude of at least twice those experienced by the homogenous silicon model and up to 5 to 6 times those experienced by the straight silicon model. Similar results were found using finite element analysis.
- The location of the greatest displacement was along the suture line however this location did not experience the greatest strain. The greatest strain occurred at the inner surface of the heel.

- The bed of the junction is pulled up towards the junction when the internal pressure is applied and experiences a compressive strain.

6.1.2 Surgical Measurements and Finite Element Models

The normal responses to altered biomechanical and haemodynamic conditions result in compensatory changes in artery wall thickness and/or lumen diameter, whereas abnormal or pathologic conditions may result in alterations in wall thickness and lumen diameter that advance to lumen stenosis. It is possible that intimal thickening may be a response to conditions of chronically reduced blood flow. However the author postulates that this increased wall thickness is a response to chronically increased wall tensile stress caused principally by pressure. Measurement of arterial deflections following femoral bypass surgery were successfully completed and the following concluded:

- Patients with an artificial graft experience higher strain in both radial and longitudinal directions.
- Finite element analysis predicted that upon the introduction of a bypass graft strains of up to seven times greater than those usually experienced by the artery were produced. Measurement of deflections during elective femoral bypass surgery showed approximately a five fold increase.
- The locations of pressure induced high stress values predicted by FEA coincide with areas that have a predilection for the pathogenesis of atherosclerosis after invasive surgery.

6.1.3 Endothelial Cell Responses

The response to injury hypothesis postulates that endothelial cell dysfunction is the precursor in the events leading to the formation of an atherosclerotic plaque hence a number of endothelial cell responses were examined *in vitro* under the same conditions of strain that exists *in vivo* following bypass surgery.

- Endothelial cell cultures exposed to both low and physiological laminar shear stress responded with significant remodeling, seen by elongation and alignment of the cells with the direction of flow, and, to a certain extent, with the formation of actin stress

fibers which aligned themselves with the long axis of the cell. It is believed that the threshold level of shear stress is between 5 and 10 dynes/cm^2.

- ZO-1 exhibits a discontinuous and jagged localisation pattern at the cell to cell border in unstrained cells and becomes considerably more continuous and well defined following strain and shear experiments.
- This study demonstrates that the behaviour of the endothelial cells is greatly altered when subjected to high cyclic strain and that the threshold levels of cyclic strain for endothelial cell remodeling is dependent on magnitude and amplitude.
- Physiological shear stress and physiological cyclic strain significantly reduce transendothelial cell premeability.
- To induce necrotic responses in endothelial cells in the area surrounding an artificial bifurcation a cyclic strain of 12$\pm$5% should be employed for a minimum of 36 hours.
- Physiological laminar shear encourages cell proliferation. However low shear did not have any beneficial effects.
- The strain analysis defines the amplitudes of cyclic strain required to promote cell division.
- The results from this *in vivo* study and *in vitro* model provide some clarification on which shear and strain parameters should be explored when examining the responses of endothelial cells to bypass grafts.

6.2 Recommendations for Further Work

Finite Element Analysis is an important tool for predicting the effects of pressure on specific materials under various conditions. However

- imaging techniques could be employing in order to provide realistic geometries for finite element models.
- Advanced finite element models could incorporate the location of the blockage in relation to the distal junction and provide information on the fluid structure interaction surrounding the bypass graft junction.

- Sutures could be incorporated into the models and the stress concentrations caused by them examined.

As the conclusions have shown, endothelial cells undoubtedly exist in a dynamic state and respond to alterations in their environment, namely changes in the level of shear stress and alterations in pressure causing mechanical stretch and strain. It is the authors belief that both shear and strain play a role in plaque initiation and growth as a number of genes relevant to the development of atherosclerosis expressed by endothelial cells have shear response elements and strain response elements that facilitate their initiation.

- One of the primary factors associated with atherosclerosis is the build up of low-density lipoprotein within the arterial wall. Despite the correlation between low shear stress and vascular lesion formation, there is little research on the effects of pressure induced mechanical forces on the molecular regulators of endothelial cell permeability. Thus it is suggested that the expression of various genes associated with permeability and proliferation, such as the expression of intercellular adhesion molecule-1 (ICAM-1) and of monocyte chemotactic protein-1 (MCP-1) , be examined under the similar conditions of strain.

- As smooth muscle cells are arranged circumferentially at right angles to the long axis of the artery, the structure is such that it can resist longitudinal and especially circumferential loads. It is proposed that smooth muscle cells be examined under the same conditions of strain in order to examine any altered responses that may invoke atherosclerotic lesion formation or growth.

An alternative hypothesis known as the 'monoclonal hypothesis' suggests that atherosclerosis begins as a mutation or viral hit, which transforms an individual, isolated smooth muscle cell into the progenitor of a proliferative clone in a similar manner as to a begin tumor. In accordance with this hypothesis, plaques and tumors may share important pathogenic features including the occurrence of one or more mutational events. In other words plaque may be a result of a clonal growth of smooth muscle cells, in response to a mutational event. Elevated levels of aneuploidy cells have been found to exist in aortic endothelial cells of elderly subjects in addition to those suffering from atherosclerosis. The results imply that coronary artery disease in humans is a condition typified by an increase of DNA damage, positively correlated with the severity of the atherosclerotic disease (Botto et al., 2001). Recent studies suggest that alterations in DNA which are present in atherosclerotic

tissues can play a fundamental role in the pathogenesis of this disease. It has been shown that DNA samples extracted from smooth muscle cells of atherosclerotic lesions possess transforming capabilities (Penn et al., 1986). This evidence puts forward the hypothesis that genomic destabilization can result in the misregulation of the cells harboring specific mutations and this may in fact play a crucial role in the formation of the atherosclerotic plaque. It is suggest that this theory be investigated further under the conditions of strain recorded during the present study.

References

B. Ablad, et al. (1988). 'The role of sympathetic activity in atherogenesis: effects of ß-blockade'. *Am Heart Journal* **166**:322–327.

J. Archie (2001). 'Presidential address: A brief history of arterial blood flow–from Harvey and Newton to computational analysis.'. *J Vasc Surg* **34**(3):398–404.

L. Badimon, et al. (1992). 'Endothelium and atherosclerosis.'. *J Hypertens Suppl* **10**(2):S43–50.

P. Ballyk, et al. (1998). 'Compliance mismatch may promote graft-artery intimal hyperplasia by altering suture-line stresses.'. *J Biomech* **31**(3):229–37.

A. Banes, et al. (1985). 'A new vacuum-operated stress-providing instrument that applies static or variable duration cyclic tension or compression to cells in vitro'.

A. Benetos, et al. (2002). 'Influence of age, risk factors, and cardiovascular and renal disease on arterial stiffness: clinical applications.'. *Am J Hypertens* **15**(12):1101–8.

B. Blackman, et al. (2002). 'A new in vitro model to evaluate differtial responses of endothelial cells to simulated arterial shear stress waveforms'. *J of Biomedical Engineering* **124**:397–407.

A. Blann & G. Lip (1998). 'The endothelium in atherothrombotic disease: assessment of function, mechanisms and clinical implications.'. *Blood Coagul Fibrinolysis* **9**(4):297–306.

R. Botnar, et al. (2000). 'Hemodynamics in the carotid artery bifurcation: a comparison between numerical simulations and in vitro MRI measurements'. *Journal of Biomechanics* **33**(2):137–144.

N. Botto, et al. (2001). 'Evidence for DNA damage in patients with coronary artery disease'. *Mutat Res* **493**(1-2):23–30.

F. Boudi (2006). *http://www.emedicine.com/med/topic182.htm* .

D. Brewster (1995). 'Prosthetic grafts'. *Rutferford RB. Vascular surgery. Philadelphia: WB Saunder* pp. 429–51.

a. British Heart Foundation (2004). 'Operations for CHD 1977 to 2003'. *http://www.heartstats.org/datapage.asp?id=836* **British Heart Foundation**.

T. Brown (2000). 'Techniques for mechanical stimulation of cells in vitro: a review'. *Journal of Biomechanics* **33**(1):3–14.

T. Brown, et al. (1998). 'Loading paradigms-intentional and unintentional-for cell culture mechanostimulus.'. *The American journal of the medical sciences* **316**(3):162.

A. Burton (1972). 'Transmural pressures, pressure gradients and resistance flow in the vascular bed'. *Physiology and Biophysics of Circulation* **2nd Edition Year Book Medical Publishers**:88–91.

T. Campbell, et al. (2007). 'Pressure Induced Strain at Femoral Artery Bypass Graft Junctions'. *Proceedings of ASME SBC, Colorado, USA* .

W. C. Cardiovascular (2009). 'Cardiovascular Treatments'.

A. Carrel & C. Guthrie (1905). 'The transplantation of veins and organs'. *Am Med* **10**:1101–1102.

K. Cassar, et al. (2005). 'The role of platelets in peripheral vascular disease.'. *Eur J Vasc Endovasc Surg* **25**(1):6–15.

H. Chaudhry, et al. (1997). 'Residual stresses in oscillating thoracic arteries reduce circumferential stresses and stress gradients.'. *J Biomech* **30**(1):57–62.

J. Cheng, et al. (1996). 'Cyclic strain enhances adhesion of monocytes to endothelial cells by increasing intercellular adhesion molecule-1 expression'. *Hypertension* **28**(3):386–391.

S. Chien, et al. (1998). 'Effects of mechanical forces on signal transduction and gene expression in endothelial cells'.

A. Clowes (1995). 'Pathologic intimal hyperplasia as a response to vascular injury and reconstruction'. *Vascular Surgery* **1**:285–295.

J. Cockcroft & I. Wilkinson (2002). 'Arterial stiffness and pulse contour analysis: an age old concept revisited'. *Clinical Science* **103**(4):379–380.

J. Cole, et al. (2002a). 'Is there a haemodynamic advantage associated with cuffed arterial anastomoses?'. *Journal of biomechanics* **35**(10):1337–1346.

J. Cole, et al. (2002b). 'Numerical investigation of the haemodynamics at a patched arterial bypass anastomosis'. *Medical Engineering and Physics* **24**(6):393–401.

N. Collins, et al. (2006a). 'Cyclic Strain-Mediated Regulation of Vascular Endothelial Occludin and ZO-1 Influence on Intercellular Tight Junction Assembly and Function'.

N. Collins, et al. (2006b). 'Cyclic Strain-Mediated Regulation of Vascular Endothelial Occludin and ZO-1 Influence on Intercellular Tight Junction Assembly and Function'.

E. Cotter, et al. (2004). 'Regulation of endopeptidases EC3. 4.24. 15 and EC3. 4.24. 16 in vascular endothelial cells by cyclic strain: role of Gi protein signaling'.

R. Cox (1977). 'Effects of age on the mechanical properties of rat carotid artery'. *American Journal of Physiology- Heart and Circulatory Physiology* **233**(2):256–263.

D. Crawford & D. Blankenhorn (1991). 'Arterial wall oxygenation, oxyradicals, and atherosclerosis.'. *Atherosclerosis* **89**(2-3):97–108.

R. De Caterina & P. Libby (2007). *Endothelial dysfunctions and vascular disease*. Blackwell Publishing.

G. Denecker, et al. (2001). 'Death receptor-induced apoptotic and necrotic cell death: differential role of caspases and mitochondria'. *Cell Death and Differentiation* **8**(8):2001–08.

a. Deptartment of Health (2004). *Hospital Episode Statistics (2002/03) NHS Hospitals in England*. Department of Health, London.

C. Dewey Jr (1984). 'Effects of fluid flow on living vascular cells.'. *Journal of biomechanical engineering* **106**(1):31.

P. Dobrin (1978). 'Mechanical properties of arteries'. *J of Physiological Reviews* **58**:397–460.

P. Dobrin (1992). 'On the roles of deformation, tension, and wall stress as critical stimuli eliciting myointimal/medial hyperplasia.'. *J Vasc Surg* **15**(3):581–2.

P. Dobrin & T. Canfield (1984). 'Elastase, collagenase, and the biaxial elastic properties of dog carotid artery'. *American Journal of Physiology- Heart and Circulatory Physiology* **247**(1):124–131.

E. Ducasse, et al. (2004). 'Interposition vein cuff and intimal hyperplasia: an experimental study.'. *Eur J Vasc Endovasc Surg* **27**(6):617–21.

G. Dunn Labortechnik (2009). 'BioFlex Culture System'.

V. Echave, et al. (1979). 'Intimal hyperplasia as a complication of the use of the polytetra fluoroethylene graft for femoral-popliteal bypass'. *Surgery* **86**:791–798.

C. Ethier (2002). 'Computational Modeling of Mass Transfer and Links to Atherosclerosis'. *Annals of Biomedical Engineering* **30**(4):461–471.

A. Fanning, et al. (1998). 'The tight junction protein ZO-1 establishes a link between the transmembrane protein occludin and the actin cytoskeleton'. *Journal of Biological Chemistry* **273**(45):29745–29753.

M. Fillinger, et al. (2003). 'Prediction of rupture risk in abdominal aortic aneurysm during observation: wall stress versus diameter.'. *J Vasc Surg* **37**(4):724–32.

A. Fisher, et al. (2001). 'Endothelial cellular response to altered shear stress'.

R. Fisher, et al. (2003). 'The distaflo graft: a valid alternative to interposition vein?'. *Eur J Vasc Endovasc Surg* **25**(3):235–9.

F. Fowkes, et al. (1991). 'Edinburgh Artery Study: prevalence of asymptomatic and symptomatic peripheral arterial disease in the general population'. *International journal of epidemiology* **20**(2):384–392.

S. Fox (1992). *Human Physiology*. William C. Brown.

S. Frangos, et al. (2001). 'The integrin-mediated cyclic strain-induced signaling pathway in vascular endothelial cells'. *Endothelium* **8**(1):1–10.

M. Friedman, et al. (1992). 'Effects of arterial compliance and non-Newtonian rheology on correlations between intimal thickness and wall shear.'. *J Biomech Eng* **114**(3):317–20.

D. Fry (1968). 'Acute Vascular Endothelial Changes Associated with Increased Blood Velocity Gradients'. *Circulation Research* **22**(2):165–197.

D. Fry (1987). 'Mass transport, atherogenesis, and risk'. *Arteriosclerosis, Thrombosis, and Vascular Biology* **7**(1):88–100.

Y. Fung (1993). *Biomechanics: mechanical properties of living tissues*. Springer.

Y. Fung & S. Liu (1991). 'Changes of zero-stress state of rat pulmonary arteries in hypoxic hypertension'. *Journal of Applied Physiology* **70**(6):2455–2470.

A. Gentile, et al. (1998). 'Vein patching reduces neointimal thickening associated with prosthetic graft implantation.'. *Am J Surg* **176**(6):601–7.

J. Gilbert, et al. (1994). 'Strain profiles for circular cell culture plates containing flexible surfaces employed to mechanically deform cells in vitro.'. *Journal of biomechanics* **27**(9):1169.

M. Gimbrone, et al. (2000). 'Endothelial Dysfunction, Hemodynamic Forces, and Atherogenesis a'. *Annals of the New York Academy of Sciences* **902**(1 Atherosclerosis V the 5th Saratoga International conference):230–240.

M. Gimbrone Jr (1995). 'Vascular endothelium: an integrator of pathophysiologic stimuli in atherosclerosis.'. *The American journal of cardiology* **75**(6):67B.

R. Gore (1976). 'Process for producing porous products'. US Patent 3,953,566.

D. Groarke, et al. (2001). 'Analysis of the C-terminal tail of the rat thyrotropin-releasing hormone receptor-1 in interactions and cointernalization with β-arrestin 1-green fluorescent protein'. *Molecular Pharmacology* **59**(2):375–385.

R. Gross, et al. (1949). 'Methods for preservation and transplantation of arterial grafts: observations on arterial grafts in dogs. Report of transplantation of preserved arterial grafts in nine human cases'. *Surg Gynecol Obstet* **88**:689–701.

M. Haga, et al. (2003). 'Shear stress and cyclic strain may suppress apoptosis in endothelial cells by different pathways'. *Endothelium* **10**(3):149–157.

N. Harhaj & D. Antonetti (2004). 'Regulation of tight junctions and loss of barrier function in pathophysiology'. *International Journal of Biochemistry and Cell Biology* **36**(7):1206–1237.

M. Heise, et al. (2004). 'Flow pattern and shear stress distribution of distal end-to-side anastomoses. A comparison of the instantaneous velocity fields obtained by particle image velocimetry'. *Journal of Biomechanics* **37**(7):1043–1051.

G. Helmlinger, et al. (1991). 'Effects of pulsatile flow on cultured vascular endothelial cell morphology'. *Journal of biomechanical engineering* **113**:123.

R. Hendrickson, et al. (1999). 'Ethanol enhances basal and flow-stimulated nitric oxide synthase activity in vitro by activating an inhibitory guanine nucleotide binding protein'. *Journal of Pharmacology and Experimental Therapeutics* **289**(3):1293–1300.

C. Hermann, et al. (1997). 'Shear stress inhibits H2O2-induced apoptosis of human endothelial cells by modulation of the glutathione redox cycle and nitric oxide synthase'. *Arteriosclerosis, thrombosis, and vascular biology* **17**(12):3588–3592.

K. Hironaka, et al. (1997). 'In vivo aortic wall characteristics at the early stage of atherosclerosis in rabbits'. *American Journal of Physiology- Heart and Circulatory Physiology* **273**(3):1142–1147.

N. Hunter (2009). 'Stroke-how we could save 500 lives a year'. *http://www.irishhealth.com/article.html?id=7486* **13th October**.

T. Iba & B. Sumpio (1991). 'Morphological response of human endothelial cells subjected to cyclic strain in vitro.'. *Microvascular research* **42**(3):245.

M. Juonala, et al. (2004). 'Endothelial dysfunction linked with early signs of atherosclerosis in young adults'. *Circulation, Journal of the America Heart Association, www.americanheart.org/ presenter.jhtml?identifier=3025948* .

M. Kaazempur-Mofrad, et al. (2004). 'Characterization of the Atherosclerotic Carotid Bifurcation Using MRI, Finite Element Modeling, and Histology'. *Annals of Biomedical Engineering* **32**(7):932–946.

T. Katsuno, et al. (2008). 'Deficiency of zonula occludens-1 causes embryonic lethal phenotype associated with defected yolk sac angiogenesis and apoptosis of embryonic cells'. *Molecular Biology of the Cell* **19**(6):2465.

T. Kawasaki, et al. (1987). 'Non-invasive assessment of the age related changes in stiffness of major branches of the human arteries'. *Cardiovascular Research* **21**(9):678.

F. Kempczinski (2000). 'Vascular conduits: An overview'. *Vascular Surgery. Philadelphia: WB Saunders Company* pp. 527–31.

P. Kreienberg, et al. (2000). 'Adjunctive techniques to improve patency of distal prosthetic bypass grafts: polytetrafluoroethylene with remote arteriovenous fistulae versus vein cuffs.'. *J Vasc Surg* **31**(4):696–701.

G. Kroemer, et al. (2005). 'Classification of cell death: recommendations of the Nomenclature Committee on Cell Death'. *Cell Death and Differentiation* **12**:1463–1467.

P. Kuijper, et al. (1996). 'Platelet-dependent primary hemostasis promotes selectin-and integrin-mediated neutrophil adhesion to damaged endothelium under flow conditions'. *Blood* **87**(8):3271.

J. Kunlin (1949). 'Venous grafts in the therapy of endarteries obliterans'. *Arch J Med Cocur* **42**:371–374.

D. Labanyi (2006). *Irish Times Health Supplement* **7th March**.

B. Langille & S. Adamson (1981). 'Relationship between blood flow direction and endothelial cell orientation at arterial branch sites in rabbits and mice'. *Circulation Research* **48**(4):481–488.

M. LaPlaca & L. Thibault (1997). 'An in vitro traumatic injury model to examine the response of neurons to a hydrodynamically-induced deformation'. *Annals of biomedical engineering* **25**(4):665–677.

K. Lee & X. Xu (2002). 'Modelling of flow and wall behaviour in a mildly stenosed tube.'. *Med Eng Phys* **24**(9):575–86.

S. Lehoux, et al. (2005). 'Differential regulation of vascular focal adhesion kinase by steady stretch and pulsatility'.

M. Lei, et al. (1996). 'Geometric design improvements for femoral graft-artery junctions mitigating restenosis'. *Journal of biomechanics* **29**(12):1605–1614.

M. Lei, et al. (1997). 'Hemodynamic simulations and computer-aided designs of graft-artery junctions'. *Journal of biomechanical engineering* **119**:343.

M. Lei, et al. (1995). 'Numerical investigation and prediction of atherogenic sites in branching arteries.'. *J Biomech Eng* **117**(3):350–7.

M. Lemson, et al. (2000). 'Intimal hyperplasia in vascular grafts.'. *Eur J Vasc Endovasc Surg* **19**(4):336–50.

A. Leuprecht, et al. (2002). 'Numerical study of hemodynamics and wall mechanics in distal end-to-side anastomoses of bypass grafts'. *J. Biomech* **35**(2):225–236.

M. Levesque & R. Nerem (1985). 'The elongation and orientation of cultured endothelial cells in response to shear stress.'. *Journal of biomechanical engineering* **107**(4):341.

W. Li & B. Sumpio (2005). 'Strain-induced vascular endothelial cell proliferation requires PI3K-dependent mTOR-4E-BP1 signal pathway'. *American Journal of Physiology-Heart and Circulatory Physiology* **288**(4):1591–1597.

Y. Li, et al. (2005). 'Molecular basis of the effects of shear stress on vascular endothelial cells'. *J Biomech* **38**(10):1949–71.

P. Liddy (2004). 'Atherosclerosis, The new view'. *Scientific American* **Vol 6**:50–59.

S. Ling, et al. (1968). 'Application of heated film velocity and shear probes to haemodynamic studies'. *Circulation Research* **23**:789–801.

R. Linton & W. Wilde (1970). 'Modifications in the technique for femoropopiliteal saphenous vein bypass autografts'. *Surgery* **67**(1):234.

X. Liu, et al. (2003). 'Physiologic cyclic stretch inhibits apoptosis in vascular endothelium'. *FEBS letters* **541**(1-3):52–56.

F. LoGerfo, et al. (1983). 'Downstream anastomotic hyperplasia. A mechanism of failure of Dacron arterial grafts'. *Ann of Surgery* **197**:479.

P. Longest, et al. (2003). 'Particle hemodynamics analysis of Miller cuff arterial anastomosis'. *Journal of vascular surgery* **38**(6):1353–1362.

R. Lyon, et al. (1987). 'Protection from atherosclerotic lesion formation by reduction of arterial wall motion'. *J of Vascular Surgery* **5**:59–67.

F. Magarey, et al. (1965). 'Effects of experimental coarctation of the aorta on atheroma in sheep.'. *J Pathol Bacteriol* **90**(1):129–33.

A. Malek, et al. (1999). 'Hemodynamic Shear Stress and Its Role in Atherosclerosis'. *JAMA* **282**:2035–2042.

S. Marcovina, et al. (2003). 'Report of the National Heart, Lung, and Blood Institute Workshop on Lipoprotein (a) and Cardiovascular Disease: Recent Advances and Future Directions'. *Clinical Chemistry* **49**:1785–1796.

A. May, et al. (1963). 'Critical arterial stenosis'. *Surgery* **53**:513–524.

M. Mayr, et al. (2000). 'Biomechanical stress-induced apoptosis in vein grafts involves mitogen-activated protein kinases'. *FASEB Journal* **15**:261–270.

S. McCue, et al. (2004). 'Shear-induced reorganization of endothelial cell cytoskeleton and adhesion complexes'. *Trends in Cardiovascular Medicine* **14**(4):143–151.

J. Miller, et al. (1984). 'Interposition vein cuff for anastomosis of prosthesis to small artery'. *ANZ Journal of Surgery* **54**(3):283–285.

M. Moore, et al. (2001). 'Role of tensile stress and strain in the induction of cell death in experimental vein grafts.'. *J Biomech* **34**(3):289–97.

W. Moore & J. Malone (1979). 'Effect of flow rate and vessel caliber on critical arterial stenosis'. *J Surg Res* **26**:1–9.

K. Morinaga, et al. (1985). 'Effect of wall shear stress on intimal thickening of arterially transplanted autogenous veins in dogs.'. *Journal of vascular surgery: official publication, the Society for Vascular Surgery and International Society for Cardiovascular Surgery, North American Chapter* **2**(3):430.

L. Morris (2004). 'Numerical and Experimental Investigation of mechancical factors in the treatments of abdominal aortic aneurysms'. *University of Limerick PhD Thesis* .

N. National Cancer Institute (2001). 'SEER Cancer Statistics Review 1975-2000,'.

M. Nazemi, et al. (1990). 'Pulsatile Flow and Plaque Formation in Carotid Artery Bifurcations'. *J of Biomechanics* **23 (10)**:1031–1037.

W. Nichols & M. O'Rourke (1998). *McDonald's blood flow in arteries*. Oxford University Press New York.

T. Nielsen, et al. (2001). 'Intraoperative endothelial damage is associated with increased risk of stenoses in infrainguinal vein grafts'. *European Journal of Vascular and Endovascular Surgery* **21**(6):513–519.

N. Noori, et al. (1999). 'Blood flow in distal end-to-side anastomoses with PTFE and a venous patch: results of an in vitro flow visualisation study'. *European Journal of Vascular and Endovascular Surgery* **18**(3):191–200.

M. Okano & Y. Yoshida (1994). 'Junction complexes of endothelial cells in atherosclerosis-prone and atherosclerosis resistant regions on flow dividers of brachocephalic bifurcations in the rabbit aorta'. *Biorheology(Oxford)* **31**(2):155–161.

G. Papageorgiou & N. Jones (1988). 'Circumferential and longitudinal viscoelasticity of human iliac arterial segments in vitro.'. *Journal of biomedical engineering* **10**(1):82.

C. Patrick & L. McIntire (1995). 'Shear stress and cyclic strain modulation of gene expression in vascular endothelial cells'. *Blood purification* **13**(3-4):112–124.

M. Pearce, et al. (1996). 'Shear stress activates cytosolic phospholipase A2 (cPLA2) and MAP kinase in human endothelial cells'. *Biochemical and Biophysical Research Communications* **218**(2):500–504.

A. Penn, et al. (1986). 'Transforming gene in human atherosclerotic plague DNA'. *Proc. Natl. Acad. Sci. USA 83* pp. 7951–7955.

D. Piorko, et al. (2001). 'Compliance in anastomoses with and without vein cuff interposition.'. *Eur J Vasc Endovasc Surg* **21**(5):461–6.

S. Pradhan & B. Sumpio (2004). 'Molecular and biological effects of hemodynamics on vascular cells'. *Front Biosci* **9**:3276–3285.

A. Rachev & S. Greenwald (2003). 'Residual strains in conduit arteries'. *J Biomech* **36**(5):661–70.

M. Raghavan, et al. (2006). 'Regional distribution of wall thickness and failure properties of human abdominal aortic aneurysm'. *Journal of biomechanics* **39**(16):3010–3016.

M. Raghavan, et al. (2000). 'Wall stress distribution on three-dimensionally reconstructed models of human abdominal aortic aneurysm'. *Journal of vascular surgery* **31**(4):760–769.

M. Raghavan, et al. (1996). 'Ex vivo biomechanical behavior of abdominal aortic aneurysm: assessment using a new mathematical model'. *Annals of biomedical engineering* **24**(5):573–582.

N. Resnick, et al. (2003). 'Fluid shear stress and the vascular endothelium: for better and for worse'. *Progress in biophysics and molecular biology* **81**(3):177–199.

W. Roberts (1975). 'The hypertensive diseases. Evidence that systemic hypertension is a greater risk factor to the development of other cardiovascular diseases than previously suspected.'. *Am J Med* **59**(4):523–32.

R. Ross et al. (1993). 'The pathogenesis of atherosclerosis: a perspective for the 1990 s'. *Nature* **362**(6423):801–809.

C. Rowe, et al. (1999). 'Local haemodynamics of arterial bypass graft anastomoses'. *Proceedings of the Institution of Mechanical Engineers, Part H: Journal of Engineering in Medicine* **213**(5):401–409.

R. Rutherford (2000). *Vascular surgery*. 5th Edition Saunders Philadelphia.

H. Salacinski, et al. (2001). 'Cellular engineering of vascular bypass grafts: Role of chemical coatings for enhancing endothelial cell attachment'. *Medical and Biological Engineering and Computing* **39**(6):609–618.

M. Sato, et al. (1996). 'Viscoelastic properties of cultured porcine aortic endothelial cells exposed to shear stress.'. *J Biomech* **29**(4):461–7.

G. Schultz, et al. (1986). 'A five-to seven-year experience with externally-supported Dacron prostheses in axillofemoral and femoropopliteal bypass.'. *Ann Vasc Surg* **1**(2):214–24.

H. Shin, et al. (2004). ' Adaptive responses of endothelial cells to cyclic pressure'. *Proceedings of IMECE 2004, ASME International Mechanical Engineering Congress and Exposition, Ahaheim, California.* .

P. Sipkema, et al. (2003). 'Effect of cyclic axial stretch of rat arteries on endothelial cytoskeletal morphology and vascular reactivity'. *Journal of biomechanics* **36**(5):653–659.

H. Sorensen, et al. (2003). 'Haemodynamic properties of PTFE femoropopliteal bypass grafts as determined by a new magnetic resonance technique.'. *Eur J Vasc Endovasc Surg* **26**(5):544–9.

V. Sottiurai, et al. (1989). 'Distal anastomotic intimal hyperplasia: histopathologic character and biogenesis.'. *Annals of vascular surgery* **3**(1):26.

J. Spence, et al. (1984). 'Haemodynamic modification of aortic atherosclerosis. Effects of propranolol vs. hydralazine in hypertensive hyperlipidemic rabbits'. *Atherosclerosis* **50**:325–333.

P. Stonebridge, et al. (1997). 'Randomized trial comparing infrainguinal polytetrafluoroethylene bypass grafting with and without vein interposition cuff at the distal anastomosis'. *Journal of Vascular Surgery* **26**(4):543–550.

D. Sumners, et al. (2000). *Vascular surgery - Chapter 3 Essential Haemodynamic Principles*. 5th Edition Saunders Philadelphia.

B. Sumpio, et al. (1997). 'Regulation of tPA in endothelial cells exposed to cyclic strain: role of CRE, AP-2, and SSRE binding sites'. *American Journal of Physiology- Cell Physiology* **273**(5):1441–1448.

B. Sumpio, et al. (1998). 'Regulation of PDGF-B in endothelial cells exposed to cyclic strain'.

M. W. N. L. Sydorak, G.R. (1972). 'Effect of increasing flow rates and arterial caliber on critical arterial stenosis'. *Surgery Forum* **23**:243.

M. Taylor, et al. (1992). 'Improved technique for polytetrafluoroethylene bypass grafting: long-term results using anastomotic vein patches'. *British Journal of Surgery* **79**(4).

M. Thubrikar & F. Robicsek (1995). 'Pressure-Induced Arterial Wall Stress and Atherosclerosis'. *The Annals of Thoracic Surgery* **59**(6):1594–1603.

M. Thubrikar, et al. (1990). 'Study of stress concentration in the walls of the bovine coronary arterial branch'. *Journal of Biomechanics 23 (1)* pp. 15–26.

J. Tinsley, et al. (2004). 'Isoform-specific knockout of endothelial myosin light chain kinase: closing the gap on inflammatory lung disease'. *Trends in pharmacological sciences* **25**(2):64–66.

A. Tiwari, et al. (2002). 'Development of a hybrid cardiovascular graft using a tissue engineering approach'. *The FASEB journal* **16**(8):791–796.

U. Trahtemberg, et al. (2007). 'Calcium, leukocyte cell death and the use of annexin V: fatal encounters'. *Apoptosis* **12**(10):1769–1780.

O. Traub & B. Berk (1998). 'Laminar shear stress mechanisms by which endothelial cells transduce an atheroprotective force'.

B. Tropea, et al. (2000). 'Reduction of Aortic Wall Motion Inhibits Hypertension-Mediated Experimental Atherosclerosis'. *Arteriosclerosis, Thrombosis, and Vascular Biology* **20**(9):2127–2133.

W. Trubel, et al. (1994). 'Compliance and formation of distal anastomotic intimal hyperplasia in Dacron mesh tube constricted veins used as arterial bypass grafts.'. *ASAIO J* **40**(3):M273–8.

W. Trubel, et al. (2004). 'Experimental comparison of four methods of end-to-side anastomosis with expanded polytetrafluoroethylene'. *British Journal of Surgery* **91**(2).

H. Tseng, et al. (1995). 'Fluid shear stress stimulates mitogen-activated protein kinase in endothelial cells'. *Circulation research* **77**(5):869–878.

E. Tzima, et al. (2005). 'A mechanosensory complex that mediates the endothelial cell response to fluid shear stress'. *Nature* **437**(7057):426–431.

M. Ulrich, et al. (1999). 'In vivo analysis of dynamic tensile stresses at arterial end-to-end anastomoses. Influence of suture-line and graft on anastomotic biomechanics'. *European Journal of Vascular and Endovascular Surgery* **18**(6):515–522.

S. Vallabhaneni, et al. (2004). 'Heterogeneity of tensile strength and matrix metalloproteinase activity in the wall of abdominal aortic aneurysms'. *Journal of Endovascular Therapy* **11**(4):494–502.

K. Van de Graaff & S. Fox (1995). 'Human Concepts of Anatomy and Physiology' **4th Edition Wm C Brown**:607–607.

J. Van der Heijden-Spek, et al. (2000). 'Effect of age on brachial artery wall properties differs from the aorta and is gender dependent a population study'.

G. van Nieuw Amerongen & V. van Hinsbergh (2002). 'Targets for pharmacological intervention of endothelial hyperpermeability and barrier function'. *Vascular pharmacology* **39**(4-5):257–272.

L. VanDeBerg, et al. (1964). 'The effect of arterial stenosis and sympathectomy on blood flow and the erogram'. *Ann Surg* **159**:623–35.

H. Vogel (1980). 'Influence of maturation and aging on mechanical and biochemical properties of connective tissue in rats.'. *Mechanisms of ageing and development* **14**(3-4):283.

N. Von Offenberg Sweeney, et al. (2005). 'Cyclic strain-mediated regulation of vascular endothelial cell migration and tube formation'. *Biochemical and Biophysical Research Communications* **329**(2):573–582.

A. Voorhees, et al. (1952). 'The use of tubes constructed from vinyon" N" cloth in bridging arterial defects.'. *Ann Surg* **135**(3):332–6.

M. Walsh, et al. (2003). 'On the existence of an optimum end-to-side junctional geometry in peripheral bypass surgery–a computer generated study.'. *Eur J Vasc Endovasc Surg* **26**(6):649–56.

S. Weinbaum & S. Chien (1993). 'Lipid transport in aspects of atherogensis'. *Journal of Biomechanical Engineering* **115**:602–610.

J. Wentzel, et al. (2003). 'Shear stress, vascular remodeling and neointimal formation.'. *J Biomech* **36**(5):681–8.

J. Wikstrand, et al. (1988). 'Primary prevention with metoprolol in patients with hypertension. Mortality results from the MAPHY study'. *JAMA* **259**(13):1976–1982.

S. Yamaguchi, et al. (2002). 'Cyclic Strain Stimulates Early Growth Response Gene Product 1–Mediated Expression of Membrane Type 1 Matrix Metalloproteinase in Endothelium'. *Laboratory Investigation* **82**(7):949–956.

Q. Yu, et al. (1993). 'Neutral axis location in bending and Young's modulus of different layers of arterial wall'. *American Journal of Physiology- Heart and Circulatory Physiology* **265**(1):52–60.

C. Zairns, et al. (1983). 'Carotid bifurcation atherosclerosis. Quantitative correlation of plaque locationwith flow velocity profiles and wall shear stress'. *Circ Res* **53**(502):1.

S. Zhao, et al. (1995). 'Synergistic effects of fluid shear stress and cyclic circumferential stretch on vascular endothelial cell morphology and cytoskeleton'. *Arteriosclerosis, thrombosis, and vascular biology* **15**(10):1781–1786.

W. Zheng, et al. (2001). 'Mechanisms of coronary angiogenesis in response to stretch: role of VEGF and TGF-β'. *American Journal of Physiology- Heart and Circulatory Physiology* **280**(2):909–917.

Appendices

Appendix A

Publications

Cole, R., Campbell, T., Davies, M., and Grace, P., (2003) 'Experiments to Investigate Intramural Stress and Strain at the Distal Anastomosis of the Femoral Artery Bypass Graft', Proceedings of Bioengineering in Ireland, 9th Annual Conference, Cavan, Ireland.

Campbell, T., Cole, R. and Davies, M., (2003) 'The Effects of Intramural Pressure on the Arterial Wall at the Distal Anastomosis', Proceedings of IRCSET Symposium, Dublin, Ireland.

Cole, R., Campbell, T. and Davies, M. (2003) 'Pressure Induced Stresses and Strains in a Simulated Femoral Artery Bypass Graft Junction', Proceedings of IMECE, ASME International Mechanical Engineering Congress and Exposition, Washington D.C., USA

Campbell, T., Cole, R. and Davies, M., (2004) 'The Influence of Intramural Pressure on Restenosis at the Distal Anastomosis of a Femoral Artery Bypass', Proceedings of Bioengineering in Ireland, 10th Annual Conference, Limerick, Ireland.

Campbell, T., Cole, R. and Davies, M., (2004) 'Measurement and Prediction of the Tensile Stress and Strain in the Femoral Artery and Bypass Graft - Stress Induced Physiological Responses of an Arterial Wall', Proceedings of IRCSET Symposium, Dublin, Ireland.

Campbell, T., Cole, R., Davies, M. and O'Donnell, M., (2004) 'Stress Distributions along

the Inner Wall of the Femoropopliteal Bypass Graft Anastomoses', Proceedings of IMECE, ASME International Mechanical Engineering Congress and Exposition, Annaheim, USA

Campbell, T., Cole, R. and Davies, M., (2004) 'The Effects of Intramural Pressure on the Arterial Wall at the Distal Anastomosis', 7th Annual Sir Bernard Crossland Symposium, Dublin, Ireland - Poster, awarded 2nd prize.

Campbell, T., Cole, R. and Davies, M., (2005) 'Plaque Growth in a Femoral Artery Bypass Graft: How is it Instigated and how does it Propagate?', Proceedings of Bioengineering in Ireland, 11th Annual Conference, Dublin, Ireland.

Campbell, T., Cole, R. and Davies, M., (2005) 'Measurement and Prediction of the Tensile Stress and Strain in the Femoral Artery and Bypass Graft - Why are Arterial Bypasses Necessary and why do they Fail?', Proceedings of IRCSET Symposium, Dublin, Ireland.

Campbell, T., Cole, R., O'Donnell, M. and Davies, M., (2006) 'Measurement and Prediction of Arterial Stresses and Strains Resulting in Plaque Growth at Femoral Artery Bypass Graft Junctions', Proceedings of Bioengineering in Ireland, 12th Annual Conference, Galway, Ireland.

O'Donnell, M., Cole, R., Campbell, T. and Davies, M., (2006) 'Arterial Tissue Remodelling Induced by Hypertension', Proceedings of Bioengineering in Ireland, 12th Annual Conference, Galway, Ireland.

Campbell, T., Cole, R. and Davies, M., (2006) 'Pressure Induced Restenosis of Femoral Artery Bypass Grafts', Journal of Biomechanics, Vol.39 Suppl 1, page S328

Campbell, T., Cole, R. and O'Donnell, M., (2007) 'Pressure Induced Strain at Femoral Artery Bypass Graft Junctions', Proceedings of ASME SBC, Colorado, USA

Appendix B

Silicon Models

In order to ensure repeatability in the manufacturing of the silicon models a number of curing methods and materials were attempted.

- Initially white wax was used to cast the wax mould however this proved to be ineffective as it had a tendency to sag almost immediately.
- A reinforcement bar was placed in the die before the wax was cast in order to support the wax. This did improve the strength of the wax but it was then necessary to heat the dies to prevent the wax from losing its' viscosity as the cross-sectional area for it to flow was reduced.
- Tex-wax was then employed but had a tendency to have an uneven surface. To prevent this happening, the side of the die was tapped when filling which encouraged the wax to fill all cavities. Furthermore the dies were heated to prevent the wax from solidifying too quickly.
- Initially silicon with a hardener was used, however it was found that this created large bubbles even though no signs of the bubble appeared upon removal from the vacuum chamber. This was possibly due to the fact that it was cured in an oven at an elevated temperature which caused the air to expand in the silicon but had no exit to escape from.
- It was also attempted to stand up the die as this prevented the wax mould from sagging however this proved very difficult as it was almost impossible to contain the silicon in the die due to the air hole and the injection hole.

- The most efficient method and that used in this study was to let the silicon cure in the atmosphere as the oven encouraged the sagging of the wax mould when the silicon was curing around it as the heat caused the wax to lose it's stiffness.

B.1 Wax Mould and Silicon Model Procedure

1. The mould were thoroughly degreased with acetone and cotton buds prior to use in each procedure.

2. Texwax was placed in a pot and heated until completely melted. Fresh wax was used on each occasion as reusing wax diminishes its strength.

3. The aluminium dies used for casting were heated to 55°C in order to prevent the was from solidifying on contact with the mould walls.

4. Reinforcement bars were placed into the dies after being tightly bolted together. The moulds were held at an optimal angle and the melted wax was slowly poured into them. During the cooling of the wax the moulds were tapped gently using a mallet to allow any air bubble that may have been in the cast to rise into the waste material at the top of the cast.

5. As the wax solidified and contracted additional was was continually poured into the mould to ensure no voids occurred during the cooling process.

6. The moulds were left to cool in the atmosphere for six to eight hours ensuring the wax had hardened sufficiently.

7. Once the wax had completely solidified the mould was carefully opened and the casting removed. The excess material from the top of the cast was removed along with the flash in order to ensure that the cast fit correctly into the second mould.

8. The wax mould was then dipped into a Wacker Schutzfilm SF 18 in order to prevent adhesion to the wax by the silicon. The wax moulds were then placed in the silicon injection dies which had been degreased with acetone and cleaned with isopropyl alcohol.

9. As the placement of the wax cores dictate the distribution of wall thickness it was vital that they fit exactly into the moulds. Hence each wax mould was securely

fastened at each end with an additional drop of wax to prevent movement by the mould ensuring no alterations in the thickness of the wall.

10. The inner surfaces of the dies were sprayed with a silicon release agent (Ambersil formula 8) which assists in the removal of the silicon models when complete.

11. Silicon was mixed in a transparent beaker. 9 parts of Elastosil RT 601 A and 1 part of Elastosil RT 601 B were slowly mixed using a pin.

12. The beaker was then placed in a vacuum oven at a pressure of 0.2bar to remove air bubbles. The pressure was dropped and normalised on a continuous basis ensuring the solution is free of air bubbles, thus negating erroneous regions of stress concentrations. (Note it was also found that placing the mixture in the freezer temporarily allowed any bubbles to rise naturally from the mixture.)

13. A syringe was used to slowly draw the silicon from the beaker, ensuring no air intake, and inject it into the dies containing the wax moulds through the injection holes. Silicon was injected until it was seen to spurt from the air hole at the opposite end of the die. A further small amount was added thereby expelling any air which may be trapped in the die.

14. The die was placed in a level surface and left to cure in the atmosphere.

15. Once cured the wax was removed from the interior of the model. This was done by hanging the model from a support within an oven at $90°C$. The melted wax and reinforcement bars were collected from below the model and disposed of.

16. Finally when the majority of the wax had been removed the silicon model was carefully rinsed with hot water in order to remove any residue and set aside to dry. The models were examined for any defects such as air bubbles.

Figure B.1: Straight section mould with slots for guide pins.

Figure B.2: Straight Section Mould for wax core

Appendix C

Finite Element Analysis

The finite element method of analysis has established itself as a primary tool for the engineer in design analysis processes. ProMechanica is a design tool which enables parametric studies as well as design optimisation to be set up and assessed in an efficient manner. The application of this software in this project allows the analysis of the effects of intramural pressure on the walls of the artery. This appendix details numerous FEA results for the idealised models.

Figure C.1 and Figure C.2 clearly show how slices can be analysed through the finite element models. This allows a comparison of the deflections occurring on the inner and outer surfaces.

Figure C.3 and Figure C.4 display displacemnets following static pressure.

Figure C.5 and Figure C.6 show how changing the angle of attaching a bypass graft can influence both the magnitude and location of the deflections.

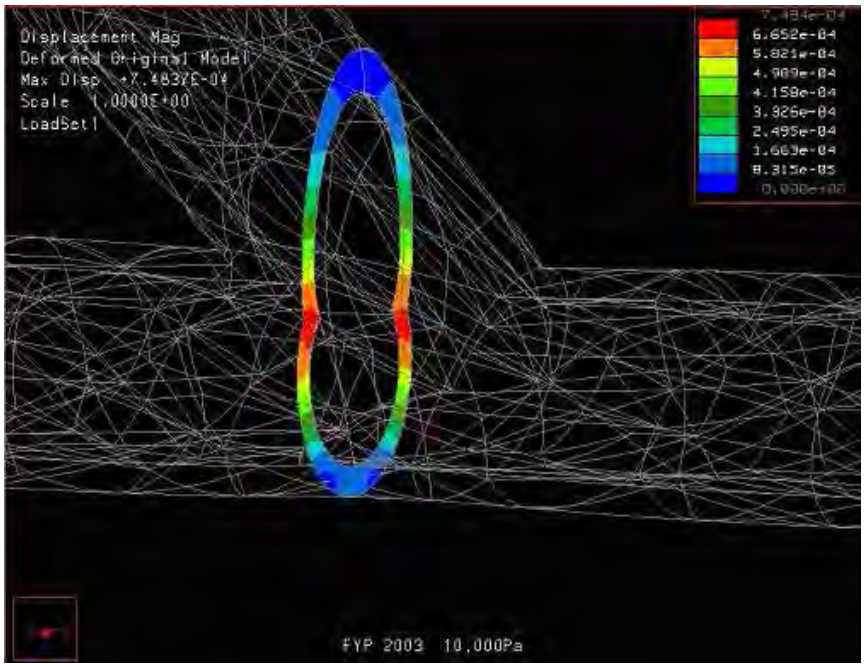

Figure C.1: Displacements at specific points surrounding the bifurcation

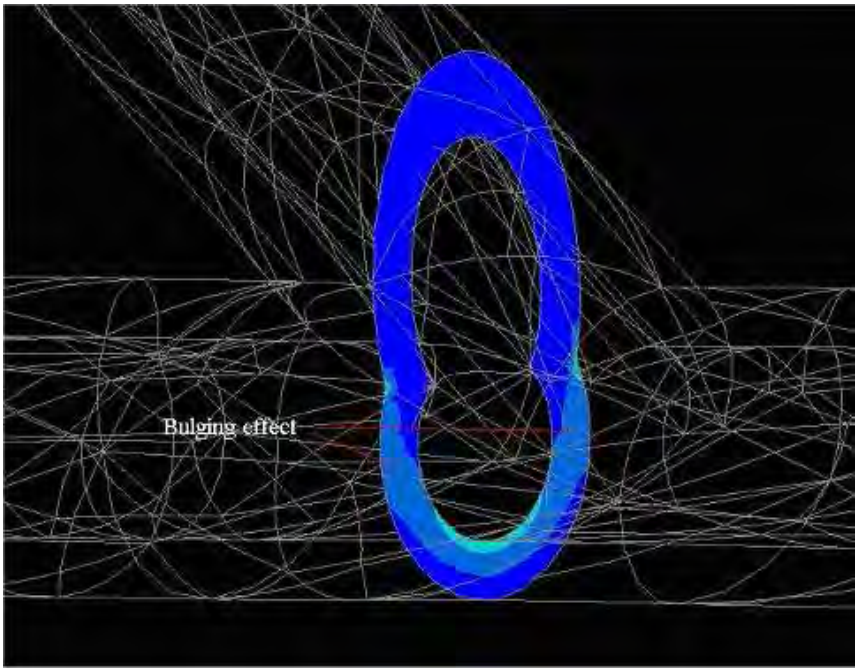

Figure C.2: Bulging effect

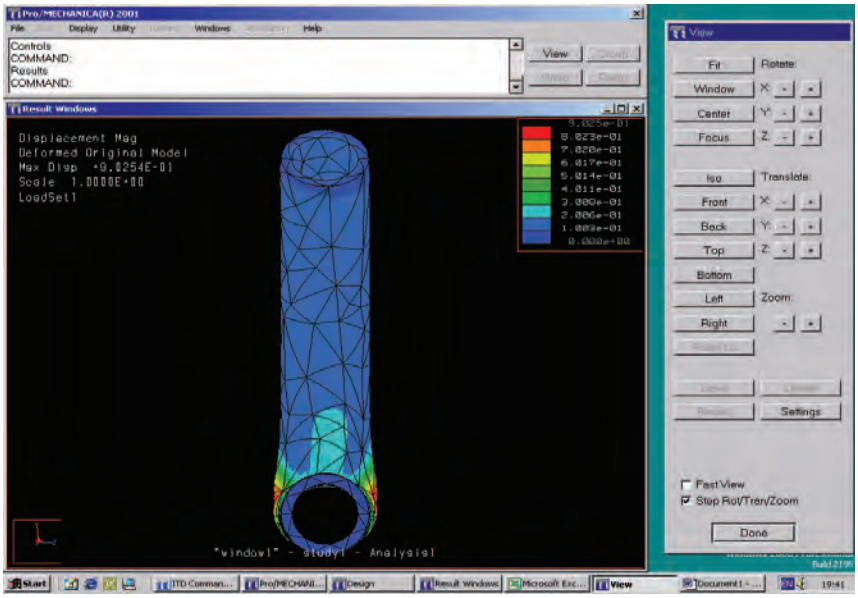

Figure C.3: Displacements surrounding the bifurcation

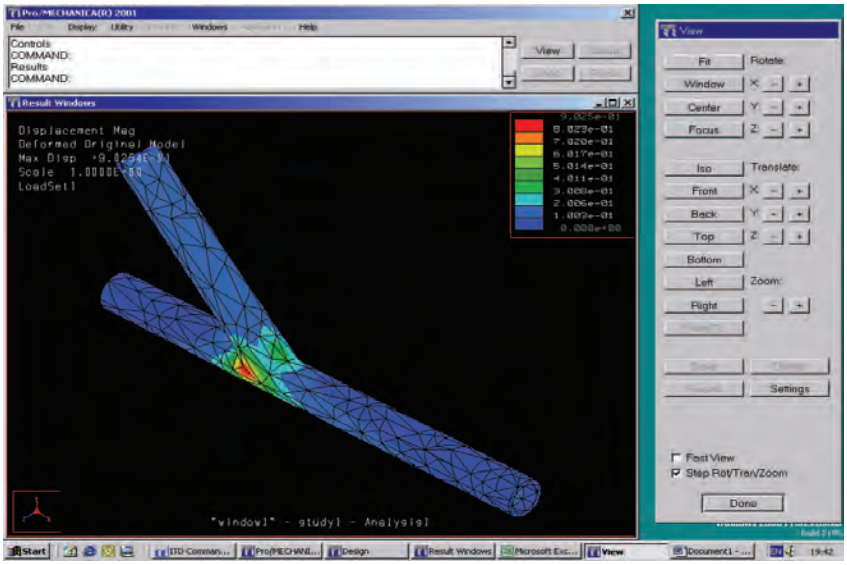

Figure C.4: Displacements surrounding the bifurcation

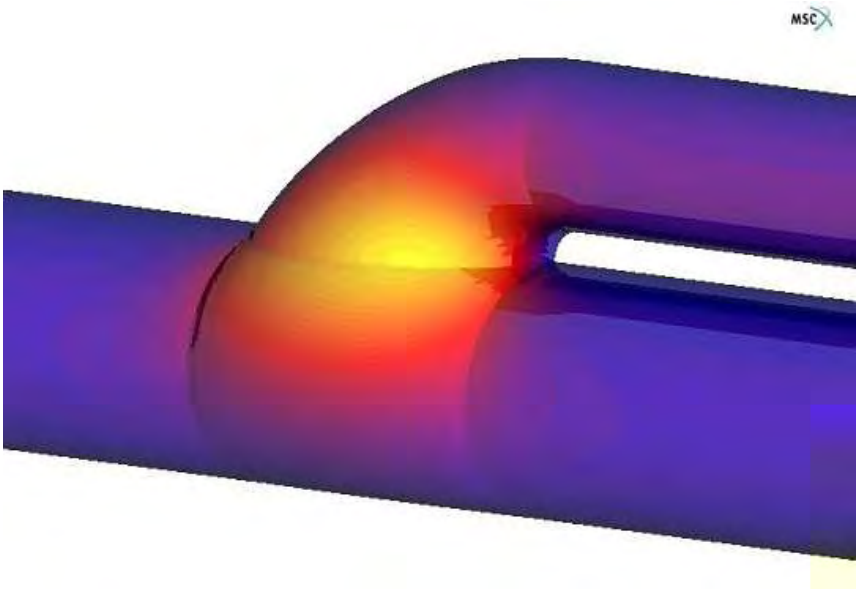

Figure C.5: Displacements surrounding the bifurcation

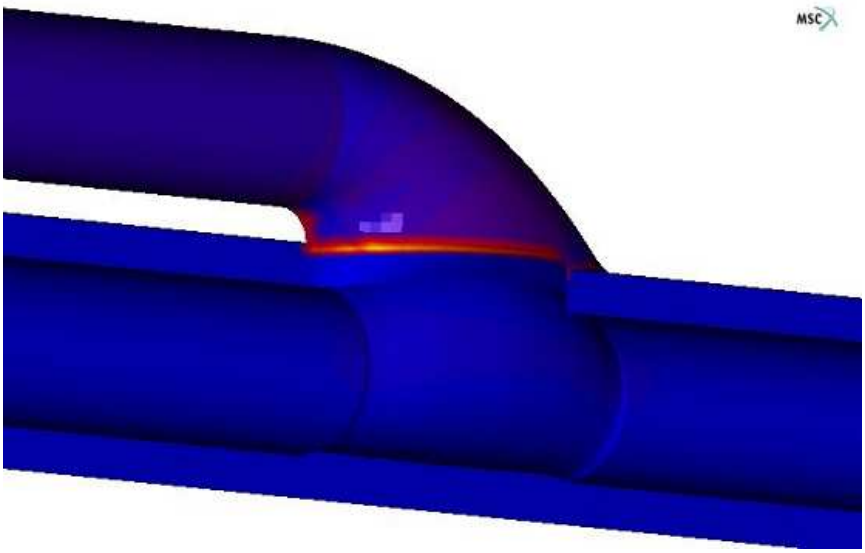

Figure C.6: Displacements surrounding the bifurcation

Appendix D

Surgical Consent Forms

Prior to undertaking the videoextensometer experiments in surgery or to performing duplex ultrasound on participants, each patient was consulted and supplied with the following information. All participants willingly signed the attached consent forms.

Full approval for the surgical experiments was obtained from the University of Limericks Ethics Board and also the Mid-Western Region Health Boards' Ethics Committee.

Project Title: Stress and Strain Measurement of the Femoral Artery and Bypass Graft

Investigators: Triona Campbell, Dr. Reena Cole, Prof. Mark Davies, Prof. Pierce Grace

I have read the information sheet, and I freely agree to participate in this study.

Name: _____
(BLOCK CAPITALS PLEASE)

Signed: _____ Date: _____

Investigator:
Signed: _____ Date: _____

Please return to:

Triona Campbell
Dr. Reena Cole,
Mechanical & Aeronautical Engineering Department,
University of Limerick, Limerick

Phone: 061 202471
Phone: 061 213069
Fax: 061 202393
Email: reena.cole@ul.ie

or

Prof. Pierce Grace
Department of Vascular Surgery,
Mid West Regional Hospital, Limerick

Phone: 061 482121

Figure D.1: Surgical Consent Form for Videoextensometer Experiments

Project Title: Stress and Strain Measurement of the Femoral Artery and Bypass graft

Researchers: Triona Campbell, Dr. Reena Cole, Prof. Mark Davies, Prof. Pierce Grace

What is the study about?
Blockages, or occlusions, in the femoral artery in the leg, result in reduced blood flow to the lower leg, which can cause ulcers and gangrene. Elective femoro-popliteal bypass surgery involves using a graft to bypass the blocked section of artery to return blood flow to lower leg.

There can be a tendency for these grafts to re-block, and the cause of this is still fully unknown. It is our hypothesis that it is strain in the arteries that causes the hardening. Two methods will be used to investigate this hypothesis. The first involves duplex ultrasound scanning of the femoral artery, which takes less than one hour. This is non-invasive, and there are no side effects. The second method is the imaging of the artery during an elective femoro-popliteal procedure. The imaging will be performed with a charge coupled device (CCD) camera connected to a personal computer. This is non-invasive, and will not disrupt the surgery.

What will I have to do?
You are being asked to participate in this study, as you have elected to undertake femoro-popliteal bypass surgery. You will have to do nothing. Images will be taken during the procedure, in order to calculate the strain in the artery. The procedure will not be disrupted, and you will not be touched in anyway during this study. While the operation is in progress, the artery in your leg will be photographed. You will not be identified from the photographs.

You will also be asked to undergo Duplex Ultrasound Scanning of leg. The scan works rather like sonar does in detecting submarines under the water. A device rather like a microphone is pressed against the area being scanned, often using some jelly to improve the contact. This device sends out very high frequency sound waves, which go into area being examined, and bounce back when they hit an organ (like an echo bounces back when you shout across a valley). This is all processed by a computer, which produces a map of the area being scanned (e.g. your femoral artery), like on a radar screen. The technique allows us to see static structures, but also to observe moving parts (e.g. the artery pulsing).

What are the risks/benefits?
There are no added risks from this study over the risks normally associated with the surgical operation. The benefits are long-term, in that the study is to help in the understanding of why grafts can re-block a few years after the elective surgery.

What if I do not want to take part?
You are under no obligation to take part. Participation is entirely voluntary.

Figure D.2: Patient Videoextensometer Experiment Information

What happens to the information?
The information will be used to further the research. No direct connection between volunteers and the data will be kept. All information will be anonymous (i.e. Patient A, B etc.)

Who else is taking part?
Other people also electing to undergo femoro-popliteal bypass surgery are being approached to volunteer.

What if something goes wrong?
Nothing can go wrong with regard to this study, as the study does not include any contact with you during the surgery. There is no risk associated with the ultrasound scanning.

What happens at the end of the study?
At the end of the study, the findings of the research will be published. There will be no reference to any particular person, and no connection between results and patients.

What if I have more questions or do not understand something?
If you have any more questions, or require clarification, please do not hesitate to contact us, (details below).

What happens if I change my mind during the study?
You can change your mind at any time before the end of the study, and you will be omitted from the study.

Contact details

Triona Campbell — Phone: 061 202471
Dr. Reena Cole, — Phone: 061 213069
Mechanical & Aeronautical Engineering Department, — Fax: 061 202393
University of Limerick, Limerick — Email: reena.cole@ul.ie

Prof. Pierce Grace
Department of Vascular Surgery, — Phone: 061 482121
Mid West Regional Hospital, Limerick

If you have concerns about this study and wish to contact someone independent, you may contact
The Chairman of the University of Limerick Research Ethics Committee
c/o Registrar & Corporate Secretary's Office
University of Limerick
Limerick
Tel: (061) 202022

Figure D.3: Patient Videoextensometer Experiment Information

Project Title: Stress and Strain Measurement of the Femoral Artery and Bypass Graft – Follow up measurements

Investigators: Triona Campbell, Dr. Reena Cole, Prof. Mark Davies, Prof. Pierce Grace

I have read the information sheet, and I freely agree to participate in this study.

Name: _____
(BLOCK CAPITALS PLEASE)

Signed: _____ Date: _____

Investigator:

Signed: _____ Date: _____

Please return to:

Triona Campbell
Dr. Reena Cole,
Mechanical & Aeronautical Engineering Department,
University of Limerick, Limerick

Phone: 061 202471
Phone: 061 213069
Fax: 061 202393
Email: reena.cole@ul.ie

or

Prof. Pierce Grace
Department of Vascular Surgery,
Mid West Regional Hospital, Limerick

Phone: 061 482121

Figure D.4: Surgical Consent Form for Duplex Ultrasound

Project Title: Stress and Strain Measurement of the Femoral Artery and Bypass Graft – Follow up measurements

Researchers: Triona Campbell, Dr. Reena Cole, Prof. Mark Davies, Prof. Pierce Grace

What is the study about?
Blockages, or occlusions, in the femoral artery in the leg, result in reduced blood flow to the lower leg, which can cause ulcers and gangrene. Elective femoro-popliteal bypass surgery involves using a graft to bypass the blocked section of artery to return blood flow to lower leg.

There can be a tendency for these grafts to re-block, and the cause of this is still fully unknown. It is our hypothesis that it is strain in the arteries that causes the hardening.

Previously you agreed to allow us to take measurements at the time of your bypass surgery.
Two methods were used to take these measurements. The first involved imaging of the artery during an elective femoro-popliteal procedure. The imaging was performed with a charge coupled device (CCD) camera connected to a personal computer, and was non-invasive and did not disrupt the surgery. The second method was duplex ultrasound scanning of the femoral artery, which again is non-invasive, and there are no side effects.

To further that study we wish to take measurements using Duplex Ultrasound scanning, at periods approximately 12, 24 and 36 months after your original bypass surgery.

What will I have to do?
You will return at periods approximately 12, 24 and 36 months from your bypass surgery to undergo Duplex Ultrasound Scanning of leg. The scan works rather like sonar does in detecting submarines under the water. A device rather like a microphone is pressed against the area being scanned, often using some jelly to improve the contact. This device sends out very high frequency sound waves, which go into area being examined, and bounce back when they hit an organ (like an echo bounces back when you shout across a valley). This is all processed by a computer, which produces a map of the area being scanned (e.g. your femoral artery), like on a radar screen. The technique allows us to see static structures, but also to observe moving parts (e.g. the artery pulsing).

What are the risks/benefits?
There are no risks associated with this study. The benefits are long-term, in that the study is to help in the understanding of why grafts can re-block a few years after the elective surgery.

What if I do not want to take part?
You are under no obligation to take part. Participation is entirely voluntary.

Figure D.5: Patient Duplex Ultrasound Experiment Information

What happens to the information?
The information will be used to further the research. No direct connection between volunteers and the data will be kept. All information will be anonymous (i.e. Patient A, B etc.)

Who else is taking part?
Other people who volunteered for the original study are being approached to volunteer for this follow up study.

What if something goes wrong?
Nothing can go wrong with regard to this study, as there is no risk associated with the ultrasound scanning.

What happens at the end of the study?
At the end of the study, the findings of the research will be published. There will be no reference to any particular person, and no connection between results and patients.

What if I have more questions or do not understand something?
If you have any more questions, or require clarification, please do not hesitate to contact us, (details below).

What happens if I change my mind during the study?
You can change your mind at any time before the end of the study, and you will be omitted from the study.

Contact details

Triona Campbell
Dr. Reena Cole,
Mechanical & Aeronautical Engineering Department,
University of Limerick, Limerick

Phone: 061 202471
Phone: 061 213069
Fax: 061 202393
Email: reena.cole@ul.ie

Prof. Pierce Grace
Department of Vascular Surgery,
Mid West Regional Hospital, Limerick

Phone: 061 482121

If you have concerns about this study and wish to contact someone independent, you may contact
The Chairman of the University of Limerick Research Ethics Committee
c/o Registrar & Corporate Secretary's Office

Figure D.6: Patient Duplex Ultrasound Experiment Information

Appendix E

Cell Culturing Procedures and Assays

E.1 Materials

All reagents used in this study were of the highest purity commercially available and were of cell culture standard when applicable.

Acros Organics (New Jersey, USA)

- Formaldehyde (37%)

AGB Scientific (Dublin, Ireland)

- White bottomed 96 well plates

Amersham Pharmacia Biotech (Buckinghamshire, UK)

- Anti-mouse 20 antibody, HRP conjugated
- Anti-rabbit 20antibody, HRP conjugated

Bio Sciences Ltd (Dun Laoghaire, Ireland)

- FACS Flow Fluid
- FACS Rinse Solution
- FACS Clean Solution
- 5ml Polysterene Round Bottom Tube
- V12883 - Vybrant CFDA SE Cell Tracer Kit
- V13241 - Vybrant Apoptosis Assay

Cambrex BioScience Wokingham Ltd (Wokingham, UK)

- EGM2 Bullet Kit
- HAEC Cells, CC-2535
- Reagent Pack, CC-5033

Cruinn (Dublin, Ireland)

- Greiner 5ml, 10ml, 25ml and 50ml pipettes
- Greiner 610mm x 810mm Hi-Temp Autoclave Bags
- Greiner 2ml Cryovial
- T-175 tissue culture flasks
- T-75 tissue culture flasks
- T-25 tissue culture flasks
- 10, 100, 200 and 1000 mL pipette tips
- 15ml and 50ml centrifuge tubes

DAKO Cytomation, Cambridgeshire UK

- DAKO Mounting Media

Dunn Labortechnik GmbH (Asbach, Germany)

- BF-3001P Bioflex® Culture plates - Pronectin coated

Lennox (Dublin, Ireland)

- Ethanol 2.5L
- Latex power free gloves

Millipore (Cork, Ireland)

- Transwell®-Clear Polyester (PET) Membrane inserts

Molecular Probes (Oregon, USA)

- Alexa Fluor 488 F(ab')2 fragment of goat anti-mouse IgG (H+L)

- Rhodamine Phaloidin
- Primary mouse anti-Occludin antibody

MWG Biotech (Milton Keynes, UK)

- GAPDH primer set
- Occludin primer set
- ZO-1 primer set

Sigma Aldrich (Tallaght, Dublin, Ireland)

- 1.5 mL micro tube with safety cap
- 6-well tissue culture plates
- BSA
- DAPI staining
- DMSO tissue culture grade
- Brightline Haemocytomoeter
- Hanks Balanced Salt Solution
- Fluorescein Isothiocyanate (FITC) FD40S (250mg)
- phosphate buffered saline (PBS)
- Penicillin-Streptomycin
- Triton X-100
- Trypsin-EDTA (10x)

E.2 Media for Culturing HAEC

Cells were cultured using the EGM media supplied by Cambrex BioSciences, details of which can be viewed in table E1.

Table E.1: HAEC Media

Media supplement	Volume
Media	479.8ml
FBS	10ml
Penicillin Streptomycin	5ml
rhEGF	0.5ml
Hydrocortisone	0.2ml
GA-1000 (Gentamicin, Amphotericin-B)	0.5ml
VEGF	0.5ml
rhFGF-B (with Heparin)	2ml
R^3-IGF-1	0.5ml
Ascorbic Acid	0.5ml
Heparin	0.5ml

E.2.1 Freezing Media for HAEC

Complete Media 50%, FBS 40%, DMSO 10%.

E.2.2 Function of Additives to the Media

- FBS: Fetal bovine serum is a blood component containing many undefined proteins, growth factors etc. Used to aid the growth of cells in vitro.
- Penicillin Streptomycin: Antibiotic that interferes with the final stage of syntheses if the bacterial cell wall.
- rhEGF: (human recombinant derived EGF) epidermal growth factor stimulating the growth of epithelial and endothelial cells.
- Hydrocortisone: Primary glucocorticoid secreted by the adrenal cortex used as an anti-inflammatory.
- GA-1000: (Gentamicin Sulfate, Amphotericin-B) - antibiotics.
- VEGF: Vascular Endothelial Growth Factor is an important protein associated with angiogenesis; a process necessary for tumour growth and vasculagenesis.
- rhFGF-B: Human recombinant Fibroblast Growth Factor is a Heparin binding growth factor which stimulates all cell types of the skin and endothelial cells.
- Heparin: A highly sulphated glycosaminoglycan used as an anticoagulant.

- R^3-IGF-1: Recombinant Insulin-like Growth Factor-1 is used to support growth of various cell types in low serum or serum-free culture. IGF1 Long R3 can be used as a substitute for insulin and its effectiveness at low concentrations facilitates downstream protein purification.
- Ascorbic Acid: An organic acid used due to its antioxidant properties.
- DMSO: Protects against the deleterious effects of freezing i.e. a cryoprotective agent which protects the cells from rupture by the formation of ice crystals.

E.3 Initial Culturing Process

The culturing processes detailed in sections E2 and E3 were obtained from the suppliers Cambrex BioScience Wokingham Ltd., UK.

1. The external surfaces of all vials and the medium bottle were decontaminated with ethanol.
2. Ensure cryovial was wiped with ethanol before opening. In a sterile field the cap was briefly opened a quarter turn to relieve pressure and then retightened. The cryovial was quickly thawed in a 37$°C$ waterbath ensuring the entire vial was not submerged.
3. 12-15ml of room temperature growth medium (x no of T75 flasks) was placed in each T75 cell culture vessel.
4. The cells in the cryovial were resuspended and using a micropipette, the cells were dispensed into the culture vessel(s). The culture vessel were gently rocked to evenly distribute the cells and returned to the incubator at 37$°C$ humidified with 5% CO_2.

E.4 Subculturing Process

1. 2ml (x no of T75 flasks) of Trypsin/EDTA, 7ml (x no of T75 flasks) of HEPES-BSS and 4ml (x no of T75 flasks) of Trypsin Neutralising Solution was were thawed and allowed to come to room temperature.
2. The growth medium was removed from 4$°C$ storage and allow to start warming to room temperature.

3. The external surfaces of all vials and the medium bottle were decontaminated with ethanol prior to placing in the LAF unit.

4. One flask at a time was subcultured.

5. The media was aspirated from the culture vessel and the cells were washed with 5ml of room temperature HBSS.

6. The HBSS was aspirated from the flask.

7. The cells were covered with 2ml of Trypsin. Prior to using the trypsin it was heated in a waterbath for 2 to 3 minutes as the enzyme works better when warmed. Trypsinisation was allowed to continue until approximately 90% of the cells were rounded up. This entire process takes about 2 to 6 minutes.

8. The flask was rapped against the palm of ones hand to release the majority of the cells from the culture surface. If only a few cells detach they were allowed to trypsinise for a further 30 seconds and the flask was rapped again. After the cells have released, the trypsin in the flask was neutralised with 4ml of room temperature Trypsin Neutralising Solution (TNS).

9. If the cells did not detach within 7 minutes the trypsin was either not warm enough or not activated enough. If this occurred either the cells were re-trypsinised with fresh warm Trypsin/EDTA or rinsed with TNS and then warm fresh medium was added to the culture flask.

10. The supernatant containing the detached cells was then transferred to a sterile 15ml centrifuge tube.

11. The flask was rinsed with 2ml of HBSS to collect all residual cells and this rinse was added to the centrifuge tube.

12. The tube was centrifuged at 1000rpm for 5 minutes. (The centrifuge was always balanced with a second centrifuge tube containing the same amount of liquid as the cell sample)

13. The supernatant was aspirated off ensuring to leave the pellet of cells in the base of the centrifuge tube. The pellet was loosened by flicking the tube with ones finger.

14. The cells were diluted in 4-5ml of media and counted using a hemacytometer or cell counter and the total number of cells calculated.

15. Cell viability was assessed using Trypan Blue.

16. New culture flasks were prepared by labeling each with the passage number, cell type and date and adding 12 to 15ml of new growth media.

17. A specific volume of uniformly suspended cells was dispensed into each culture flask and the flasks returned to the incubator at 37°C humidified with 5% CO_2.

E.5 Freezing Process

1. After step 15 above

2. Cells were diluted in 1ml of freezing media per vial and each vial labeled with the passage number, cell type and date.

3. The cells were frozen at a slow steady pace using an isopropanol cooler in a -80°C freezer which brought down the temperature of the cells at a constant rate of approximately 1°C per minute. Once the cell temperature had reduced to -80°C the cells were transferred to Liquid Nitrogen for storage. (Note: cells must be stored in liquid nitrogen to reduced risk of microbial contamination, or of cross contamination with other cell lines or of genetic drift and morphological changes).

E.6 Permeability Assay

1. 5 x 10^5 cm^2 HAEC's were seeded to each well of the 6 well BioFlex plate.

2. The cells were grown to confluency over 48 hours.

3. The cells were strained for 36 hours at various ranges on a Flexercell TensionPlusT FX-4000TT.

4. The cells were then washed with HBSS or PBS.

5. 0.5ml trypsin was then added to each well and incubated for 5 to 7 minutes until all the cells had rounded up.

6. A cell count was performed and the cells were then plated at a high density (1x 10^5 cells per insert) suspended in 2ml growth medium into the Transwell abluminal chamber.

7. 4ml of growth medium was placed in the Transwell sub luminal compartment.

8. Once the cells had reached confluency (within 48 hours) they were monitored for transendothelial permeability.

9. 5mg/ml of FITC Dextran was made up and the eppendorf protected with a layer of tinfoil to avoid exposure to light.

10. At T = 0, FITC (40KDa) dextran was added to the abluminal chamber at a concentration of 250μg/ml (2ml of media with dextran was placed in the abluminal compartment and 4ml of pure media in the sub luminal compartment).

11. FITC Dextran was added to the first 6 wells and media to the following 6 wells, of a 96 well plate, in order to provide information on the maximum and minimum concentrations of dextran present.

12. Diffusion of FITC dextran across the monolayer of HAEC's was allowed to continue for 3 hours.

13. Samples of 28μl media were gathered every 30 minutes from the sub luminal compartment and diluted with 372μl of pure media. Following each sample being taken the 6 well plate was returned to the incubator at 37$^{\circ}C$ humidified with 5% CO_2.

14. Each sample was monitored in triplicate (100μl per well of a 96 well plate). The microplate was covered with tinfoil following each time point to preventing any exposure to light.

15. The plate was then assessed for FITC dextran florescence at excitation and emission wavelengths of 490nm and 520nm respectively.

16. The results were expressed as a total subluminal flouresence at a given time point (0-180min) expressed as a percentage of the total abluminal florescence.

E.7 Apoptosis/Necrosis Assay

1. 5 x 10^5 cm^2 Human Aortic Endothelial cells (HAEC's) were seeded to each well of the 6 well BioFlex plate.
2. The cells were grown to confluency over 48 hours.
3. The cells were then thoroughly washed with 1ml HBSS.
4. This was aspirated off and 2mls of serum free media was added to each well and the plates were allowed to quiesce for 48 hours.
5. The relevant strain test was run for 12, 24 or 36 hours on a Flexercell TensionPlusT FX-4000TT.
6. Each well was washed with 0.5ml HBSS.
7. 0.5ml trypsin was then added to each well and incubated for 1-2 minutes until all the cells had rounded up.
8. The trypsin was neutralised with 0.5ml TNS or Media and transferred to a 1.5ml eppendorf.
9. The cells were spun at 1500rpm for 5 minutes and the supernatant removed from each eppendorf.
10. 0.5ml of HBSS:0.1% BSA was added to each and the eppendorfs were again spun at 1500rpm for 5 minutes.
11. The supernatant was removed and 1ml of HBSS:0.1% BSA added. The cells were spun a final time.
12. 200μl of Annexin binding buffer(ABB) (200μl ABB + 800μl HBSS) followed by 1μl of Annexin V and finally 0.4μl of red-flourescent propidium iodide (PI) (5μl PI + 45μl 1X ABB) were added to each sample.
13. The solution was mixed and transferred to a falcon tube for Fluorescent-activated cell sorting (FACS). Each sample was monitored in triplicate.
14. Finial analysis was performed by the FACS system.

* *note from step 9 all cell samples were kept on ice.*

E.8 Proliferation Assay

1. 5 x 10^5 cm^2 HAEC's were seeded to each well of the 6 well BioFlex plate.
2. The cells were grown to confluency over 48 hours.
3. The cells were then thoroughly washed with 1ml HBSS or PBS.
4. 90μl of DMSO were added to the carboxyfluorescein diacetate, succinimidyl ester (500μg CDFA-SE) to bring it to solution.
5. 12.5μl CFDA-SE cell tracer were added to 25mls HBSS (dilution of 1:2000). 1ml of this solution was then added to each well and the plate was incubated for 5 to 10 minutes.
6. The supernatant was aspirated off and media added to the cells to allow them recover for a few hours.
7. This was aspirated off and 2mls of serum free media was added to each well and the plates were allowed to quiesce for 48 hours.
8. The relevant strain test was run for 12, 24 or 36 hours on a Flexercell TensionPlusT FX-4000TT.
9. Each well was washed with 0.5ml HBSS or PBS.
10. 0.5ml trypsin was then added to each well and incubated for 5 minutes until all the cells had rounded up.
11. The trypsin was neutralised with 0.5ml TNS or Media and transferred to a 1.5ml eppendorf.
12. The cells were spun at 1500rpm for 5 minutes and the supernatant removed from each eppendorf.
13. 0.5ml of HBSS:0.1% BSA was added and the eppendorfs were again spun at 1500rpm for 5 minutes.
14. The supernatant was removed and 1ml of HBSS:0.1% BSA added. The cells were spun a final time.

15. The supernatant was removed and 200μl of HBSS:0.1% BSA was added to the pellet and the mix was transferred to a FACS tube. Each sample was monitored in triplicate.

16. Finial analysis was performed by the FACS system.

** note from step 12 all cell samples were kept on ice.*

E.9 Zonula Occluden-1 Immunocytochemistry

1. The cells were washed twice with PBS (0.1% BSA).

2. The cells were fixed with 3% formaldehyde and dH_2O (samples were maintained in ice during this step).

3. The cells were again washed twice with PBS (0.1% BSA).

4. The cells were then permeabilised with 0.2% Triton X-100 and dH_2O for 15 minutes.

5. 5% BSA was added for 30 minutes to block the cells.

6. The cells were again washed twice with PBS (0.1% BSA).

7. 5% BSA and the primary mouse anti ZO-1(0.25μg/ml BBMvEC/1μg/ml BAEC) were added and the samples incubated for 2 hours.

8. The cells were again washed twice with PBS (0.1% BSA).

9. 5% BSA and the secondary Alexa Flour 488 conjugated goat, anti mouse (1:400) were added and the samples incubated for 1 hour.

10. The cells were again washed twice with PBS (0.1% BSA).

11. The cells were stained for 3 minutes with Dapi staining (1:2000 with dH_2O)

12. The cells were again washed twice with PBS (0.1% BSA).

13. The cells were mounted and sealed in Dako for 15 minutes prior to imaging by standard fluorescent microscopy (Olympus BX50).

E.10 Rhodamine Phaloidin Immunocytochemistry

1. The cells were washed twice with PBS (0.1% BSA)
2. The cells were fixed with 3% formaldehyde and dH_2O (samples were maintained in ice during this step)
3. The cells were again washed twice with PBS (0.1% BSA)
4. The cells were then permeabilised with 0.2% Triton X-100 and dH_2O for 15 minutes
5. The cells were again washed twice with PBS (0.1% BSA).
6. Rhodamine Phaloidin (1:80 with PBS) was added to the cells for 10 minutes.
7. The cells were again washed twice with PBS (0.1% BSA).
8. The cells were stained for 3 minutes with Dapi staining (1:2000 with dH_2O)
9. The cells were again washed twice with PBS (0.1% BSA).
10. The cells were mounted and sealed in Dako for 15 minutes prior to imaging by standard fluorescent microscopy (Olympus BX50).

E.11 Fixing of cells

1. Wash the cells twice with PBS (0.1% BSA).
2. Fix the cells with 3% Formaldehyde (dH_20) for 15 minutes whilst keeping the samples on ice.
3. Remove the supernatant. Cover the cells in PBS (0.1% BSA)
4. Wrap the samples in tin foil and keep in the refridgerator.

Appendix F

FACSCalibur™ Apoptosis Analysis

The FACSCalibur™ system (BD Bio Sciences Ltd, Dun Laoghaire, Ireland) is a four-colour, dual laser flow cytometer, which is capable of both cell sorting and cell analysis. This system was employed in order to analyse cell proliferation, apoptosis and necrosis.

Figures F.1 and F.2 represent a sample of the output from the FACSCalibur™ system following the testing of samples for 36 hours at a strain rate of 7% to 17%. In the output table the regions are defined as follows

- R1 refers to the selection group of cells,
- R2 are health cells,
- R3 are early stage apoptotic cells,
- R4 are late stage apoptotic cells and
- R5 are necrotic cells.

The horizontal axis, labelled Alexa Fluor, is recombinant annexin V conjugated to fluorophore Alex Flour® 488 dye. Alexa Fluor 488 annexin V[95] is a green-fluorescent conjugate (excitation/emission wavelengths, ∼495/519nm) which has spectral characteristics similar to fluorescein conjugates, but exhibits fluorescence that is brighter, much more photostable and less pH dependent (Molecular Probes Guidelines, www.probes.com)

The vertical axis is labeled PI for propidium iodide, which is a red fluorescent nucleic acid biding dye. PI is impermeant to live cells and apoptotic cells however it will stain necrotic cells.

The axes abbreviations are defined as follows

- FL refers to fluorochrome

- FSC refers to forward scatter
- SSC refers to side scatter

The raw data for every test is available on CD as including all raw data in this report would prove an over consumption of paper!

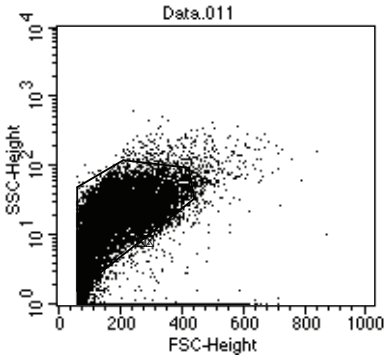

Region Statistics

File: Data.011 Sample ID: Control

Acquisition Date: 04-Mar-08 Total Events: 15415

Region	Events	% Gated	% Total
R1	12746	100.00	82.69
R2	12190	95.64	79.08
R3	2	0.02	0.01
R4	1	0.01	0.01
R5	568	4.46	3.68

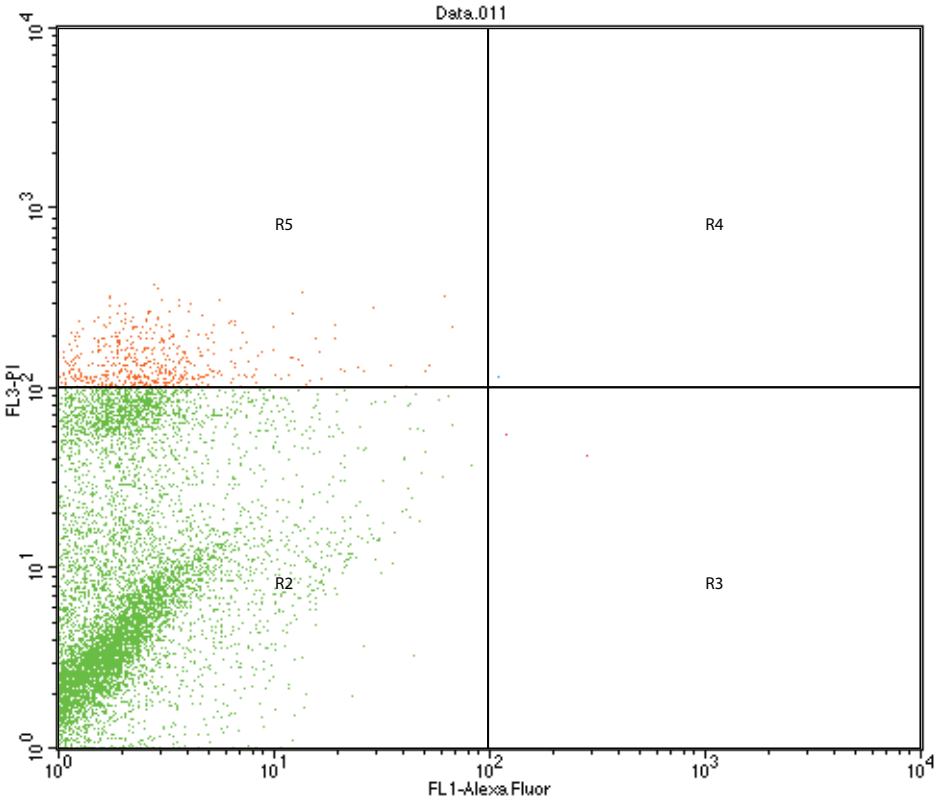

Figure F.1: FACSCalibur™ system raw data for apoptotic and necrotic analysis

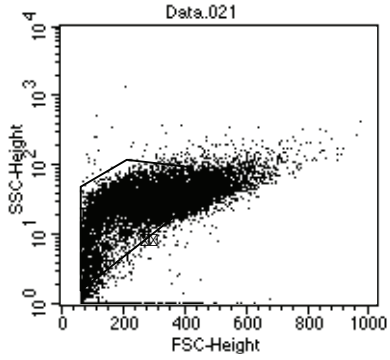

Region Statistics

File: Data.021 Sample ID: Strain

Acquisition Date: 04-Mar-08 Total Events: 11846

Region	Events	% Gated	% Total
R1	8784	100.00	74.15
R2	6682	76.07	56.41
R3	12	0.14	0.10
R4	15	0.17	0.13
R5	2078	23.66	17.54

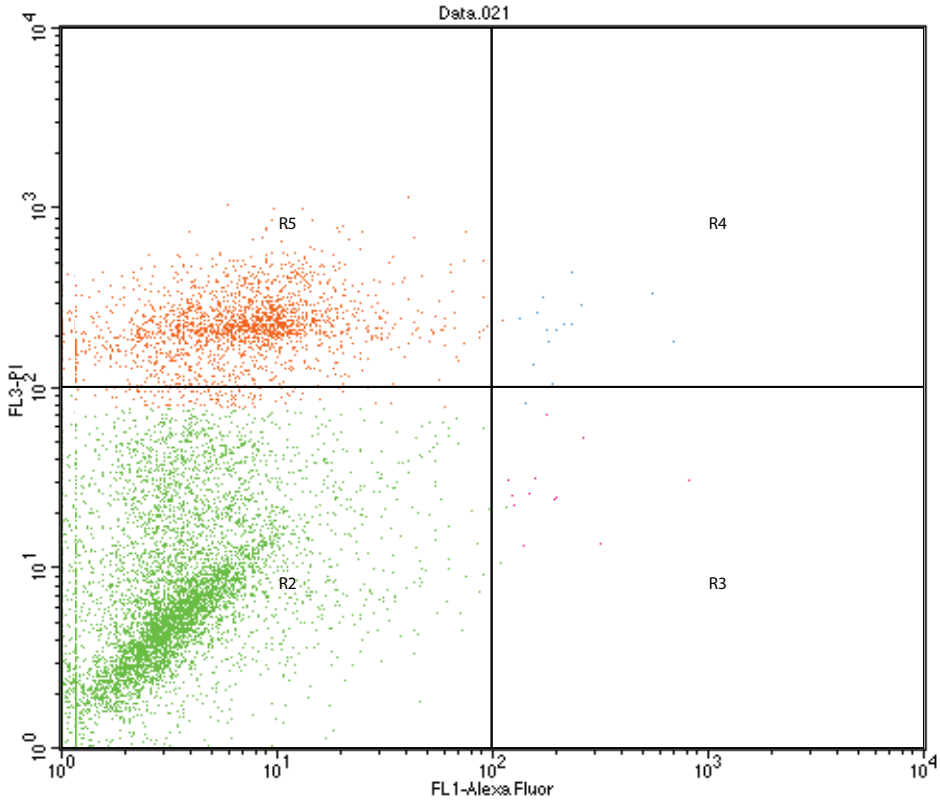

Figure F.2: FACSCalibur™ system raw data for apoptotic and necrotic analysis

Appendix G

Cell Experimental Results - Set 2

Each experiment was repeated during the course of this study in order to ensure the accuracy of every procedure employed. The graphs in Figures G.1 through Figure G.15 are the transendothelial permeability results of the second cell culture tests performed *in-vitro*. Each condition of shear and strain was again examined.

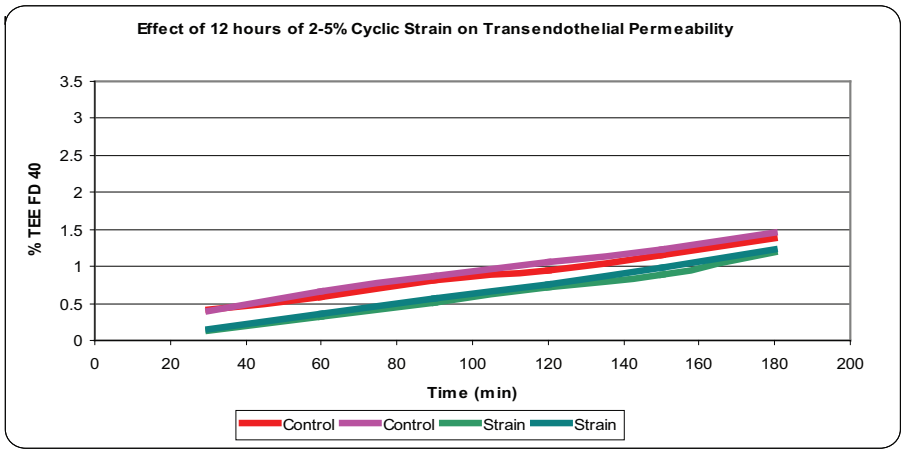

Figure G.1: Trans Endothelial Exchange following 12 hours of 2-5% strain

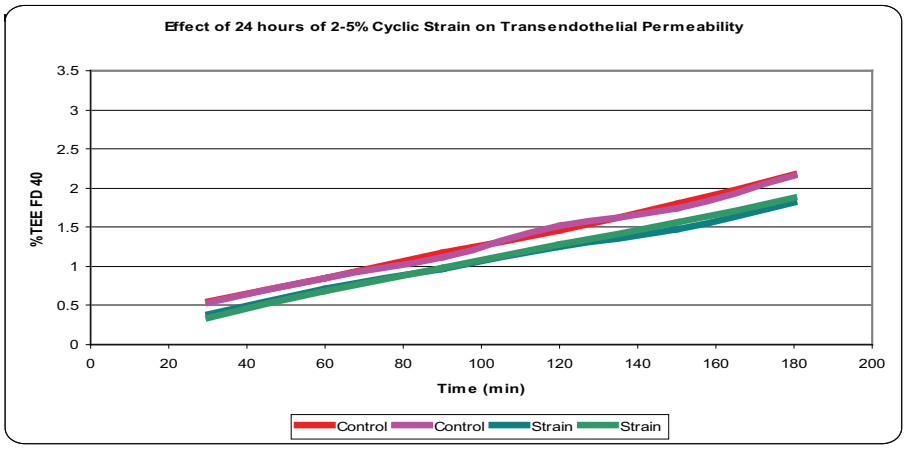

Figure G.2: Trans Endothelial Exchange following 24 hours of 2-5% strain

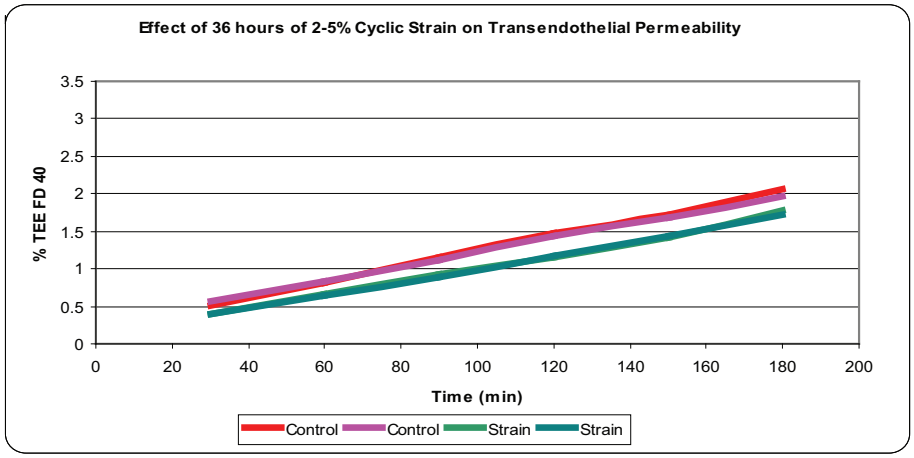

Figure G.3: Trans Endothelial Exchange following 36 hours of 2-5% strain

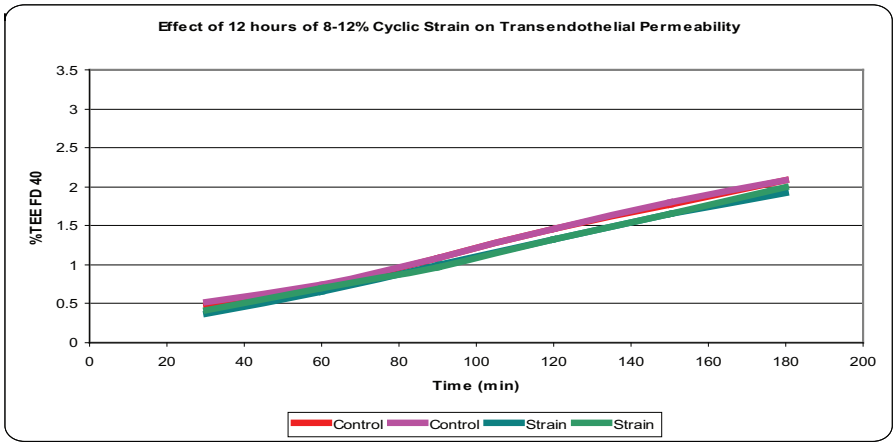

Figure G.4: Trans Endothelial Exchange following 12 hours of 8-12% strain

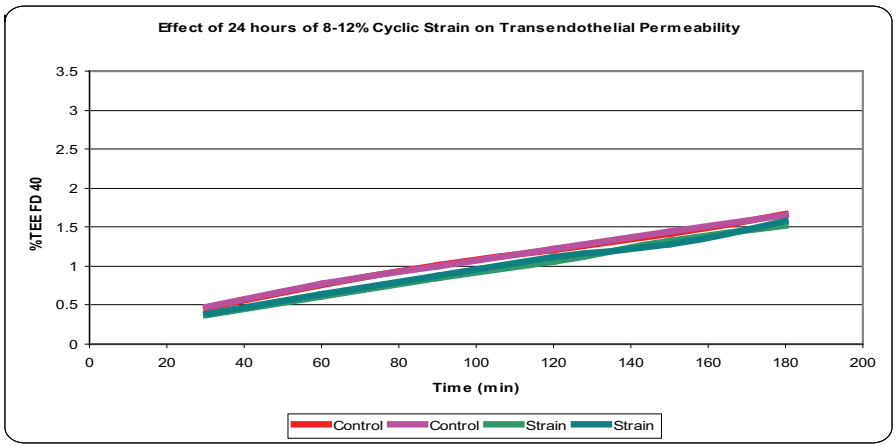

Figure G.5: Trans Endothelial Exchange following 24 hours of 8-12% strain

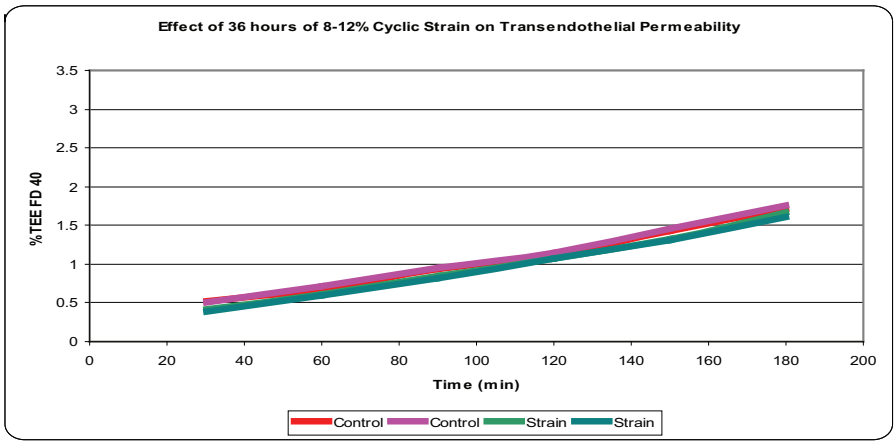

Figure G.6: Trans Endothelial Exchange following 36 hours of 8-12% strain

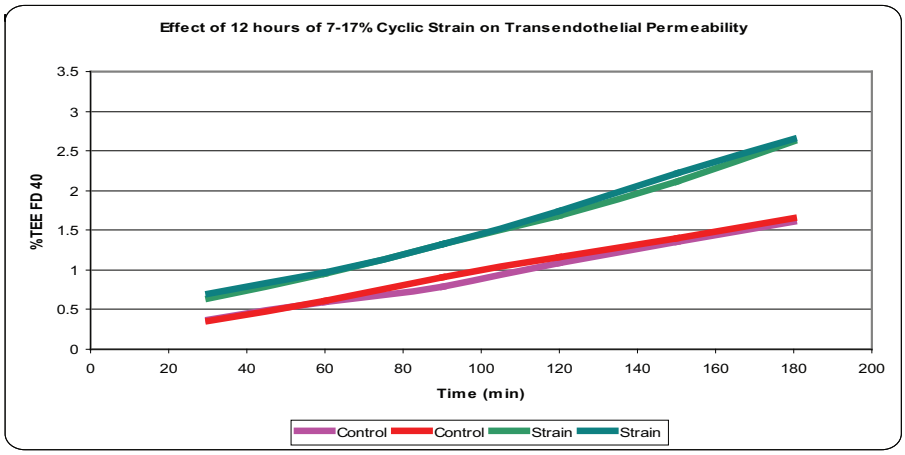

Figure G.7: Trans Endothelial Exchange following 12 hours of 7-17% strain

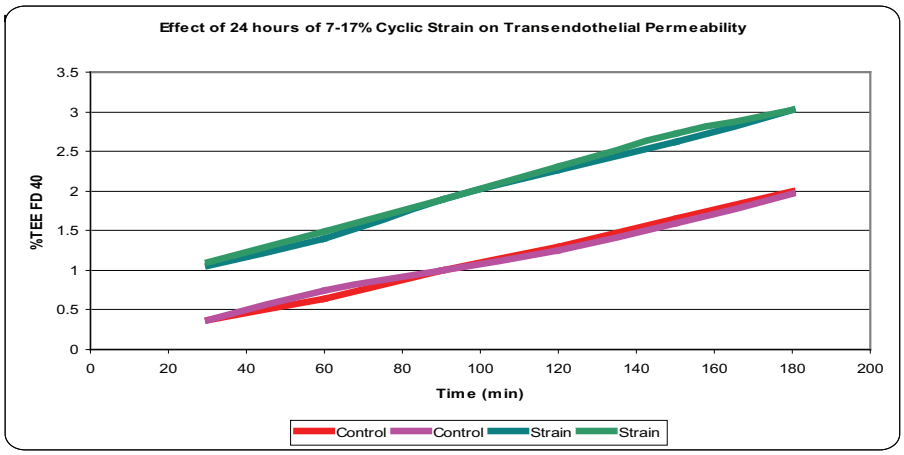

Figure G.8: Trans Endothelial Exchange following 24 hours of 7-17% strain

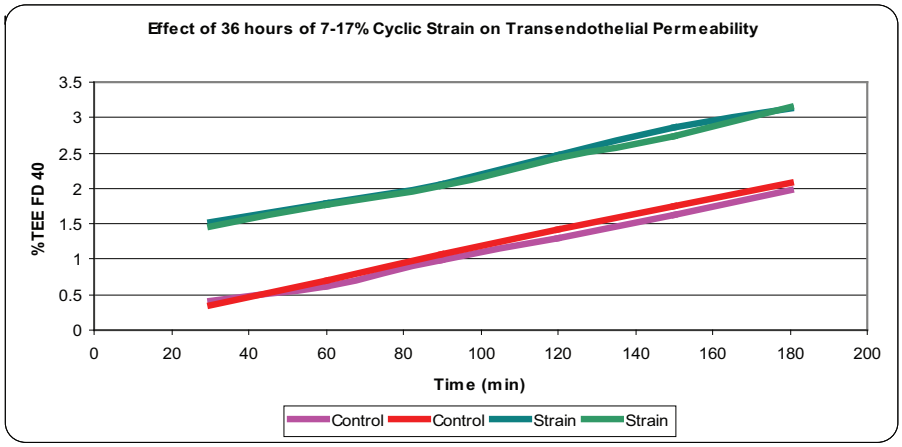

Figure G.9: Trans Endothelial Exchange following 36 hours of 7-17% strain

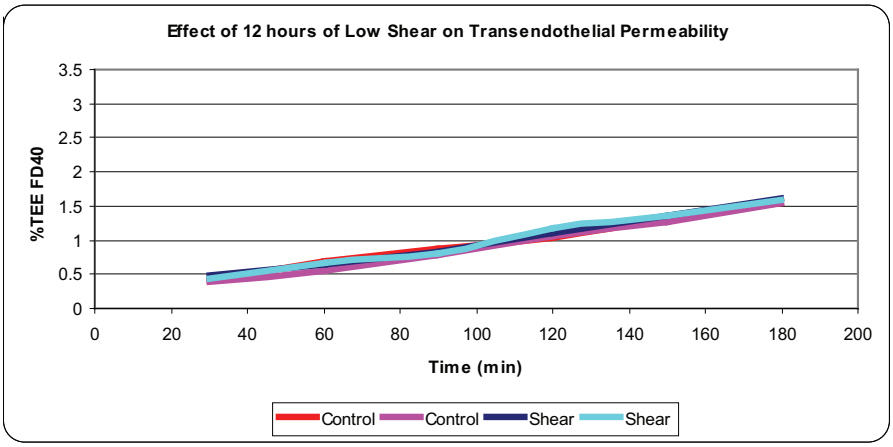

Figure G.10: Trans Endothelial Exchange following 12 hours of low shear

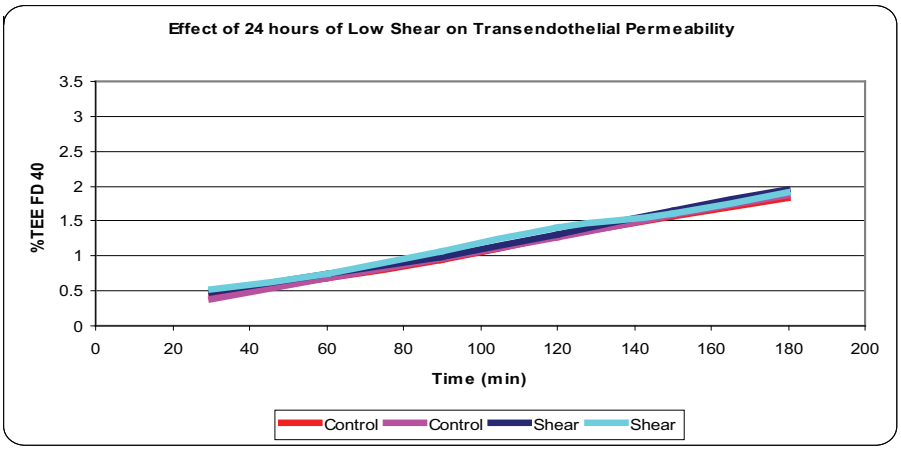

Figure G.11: Trans Endothelial Exchange following 24 hours of low shear

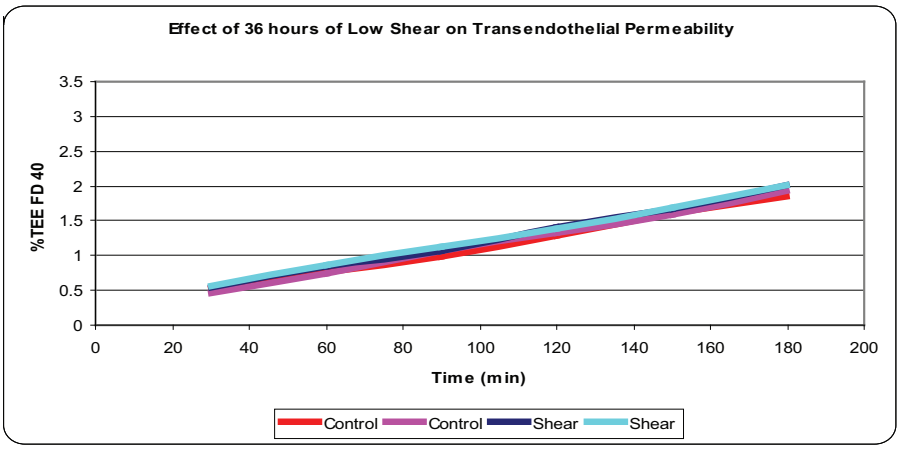

Figure G.12: Trans Endothelial Exchange following 36 hours of low shear

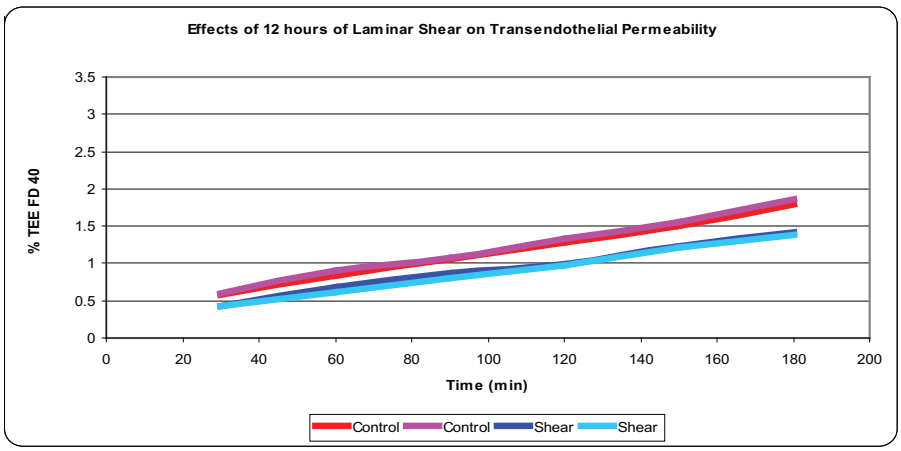

Figure G.13: Trans Endothelial Exchange following 12 hours of physiological shear

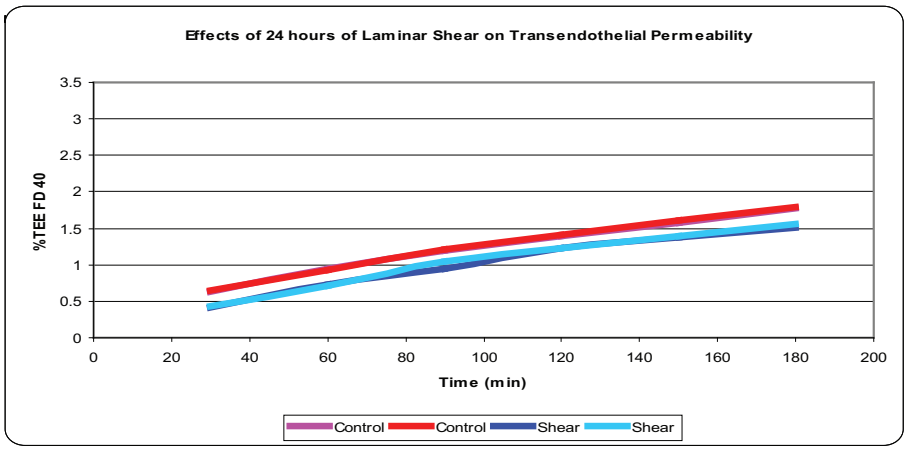

Figure G.14: Trans Endothelial Exchange following 24 hours of physiological shear

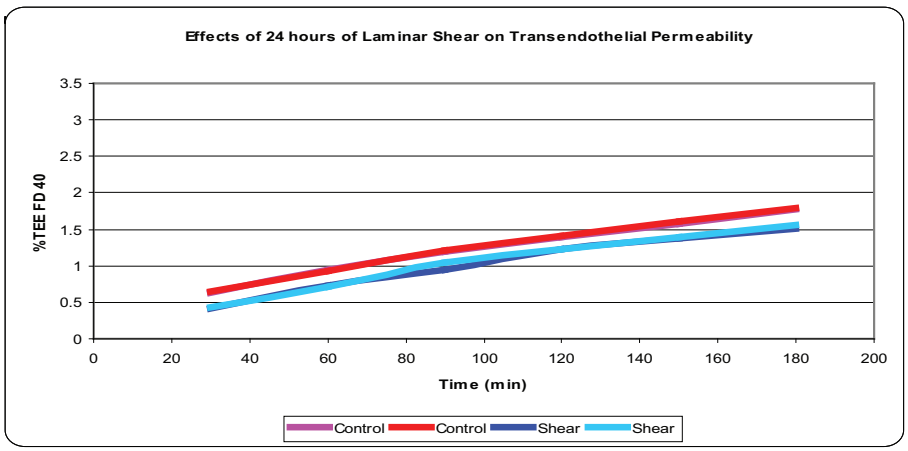

Figure G.15: Trans Endothelial Exchange following 24 hours of physiological shear

The graphs represented in G.16 through G.21 display the second set of results for the apoptotic and necrotic reactions of endothelial cells when exposed to the various magnitudes of strain or shear.

All results are similar to those presented in Chapter 5, thus showing the reproducibility, repeatability and the accuracy of the testing methods employed during all experiments carried out during the course of this study.

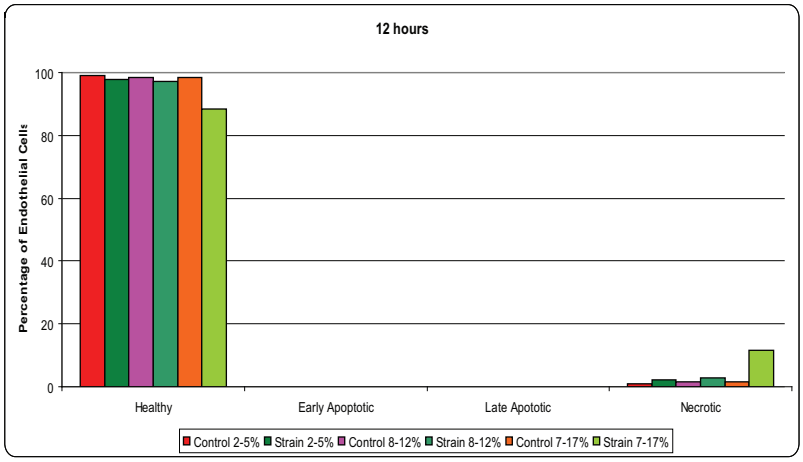

Figure G.16: Apoptotic and Necrotic reactions of endothelial cells following 12 hours of each strain range

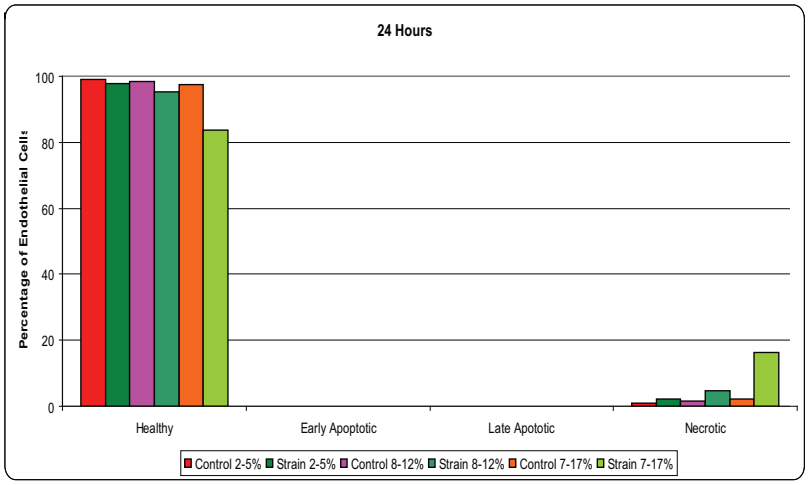

Figure G.17: Apoptotic and Necrotic reactions of endothelial cells following 24 hours of each strain range

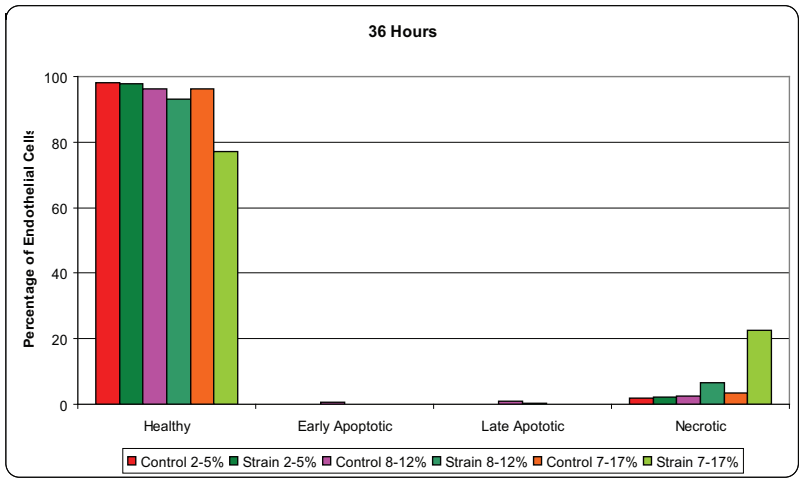

Figure G.18: Apoptotic and Necrotic reactions of endothelial cells following 36 hours of each strain range

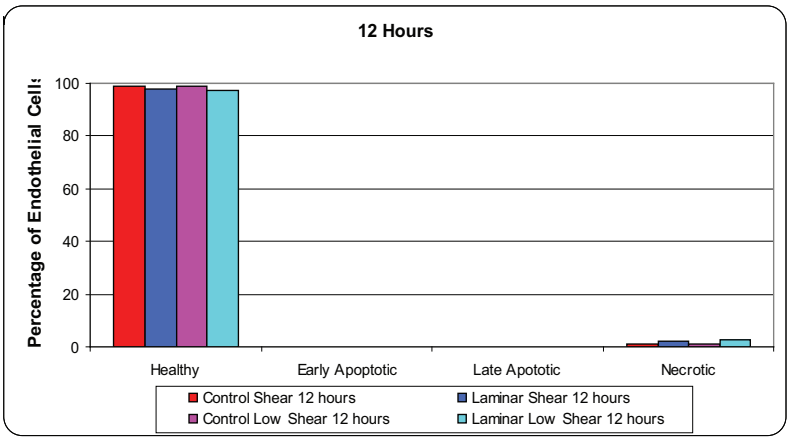

Figure G.19: Apoptotic and Necrotic reactions of endothelial cells following 12 hours of low or physiological shear

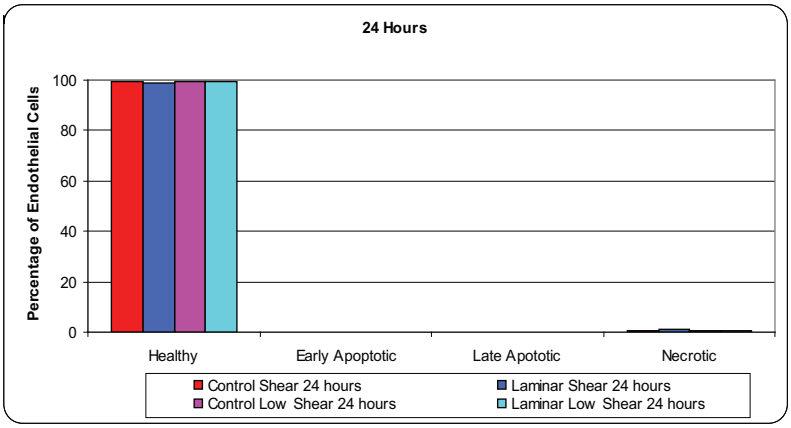

Figure G.20: Apoptotic and Necrotic reactions of endothelial cells following 24 hours of low or physiological shear

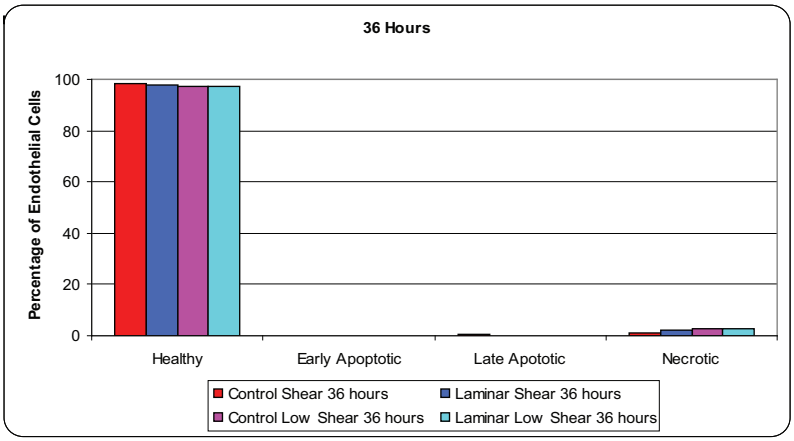

Figure G.21: Apoptotic and Necrotic reactions of endothelial cells following 36 hours of low or physiological shear